

Nora Jansson

# Carbon Nanostructures as Lubricant Additives

Mechanisms, Functionalization  
and Future Outlook

Master's thesis in Chemistry

Supervisor: Solon Oikonomopoulos

Co-supervisor: Nuria Espallargas

April 2021



Nora Jansson

# **Carbon Nanostructures as Lubricant Additives**

Mechanisms, Functionalization  
and Future Outlook

Master's thesis in Chemistry  
Supervisor: Solon Oikonomopoulos  
Co-supervisor: Nuria Espallargas  
April 2021

Norwegian University of Science and Technology  
Faculty of Natural Sciences  
Department of Chemistry



Norwegian University of  
Science and Technology



# ABSTRACT

---

Friction and wear between contacting surfaces in relative motion are major sources of energy loss that can be mitigated through various lubrication strategies. Today, most liquid lubricants are complex chemical systems comprised of a base fluid, which provides the main performance properties, and several carefully selected functional additives, which provide the base fluid with the necessary functionalities for each targeted application. In recent years, increased environmental concern and regulations have fueled the search for new base fluids and lubricant additives with reduced environmental impact.

Owing to their attractive mechanical, thermal, and chemical properties, carbon nanostructures have been proposed as potential candidates for a new generation of friction-modifying and antiwear additives. However, despite much research on the lubrication performance of carbon nanostructures over the last couple of decades, a comprehensive understanding of the mechanisms by which carbon nanostructures reduce friction and wear is still lacking. Furthermore, surface functionalization is generally required to achieve stable dispersion of carbon nanostructures in the lubricant. Yet, few studies have attempted to discern how functionalization influences the lubrication performance of the nanoadditives beyond improving dispersibility.

This thesis aims to review and systematize the growing body of literature on the performance of carbon nanostructures as lubricant additives and contribute to the establishment of better guidelines for future research and development on the subject. This was achieved by identifying and categorizing the carbon nanostructures in question, critically evaluating their proposed lubrication mechanisms, and investigating the role of surface functionalization in lubrication.

It was found that carbon nanomaterials can exhibit a wide range of structural, mechanical, and chemical properties, and that this greatly influences the mechanisms by which they can reduce friction and wear when employed as additives. More specifically, dimensionality, structural integrity, and the nature of chemical interactions were identified as particularly important parameters governing the tribological behavior of carbon nanostructures. Evaluation of the theoretical basis for the proposed lubrication mechanisms revealed that several of the mechanisms are still quite poorly understood. However, despite certain ambiguities at the conceptual level, it was concluded that certain carbon nanostructures (carbon quantum dots and graphene-based nanostructures) are promising candidates for a new generation of lubricant additives due to their excellent properties as carrier materials and the well-established and rich chemistry of carbon. Together, these properties offer several routes for surface functionalization and endless opportunities for tailoring additive properties. As a result, surface functionalization has the potential to not only affect dispersibility but also enhance the inherent lubrication mechanisms of the nanostructure and potentially allow for development of multifunctional additives.

# SAMMENDRAG

---

Friksjon og slitasje mellom overflater i kontakt og relativ bevegelse er viktige kilder til energitap som kan reduseres gjennom bruk av smøremidler. Moderne, flytende smøremidler er komplekse kjemiske systemer som består av en hovedvæske, som gir smøremiddelet sine grunnegenskaper, samt en rekke funksjonelle tilsatzstoffer som tilpasser smøremiddelets egenskaper til spesifikke bruksområder. Økt miljøhensyn og strengere regulering av utslipp i senere år har forsterket behovet for nye tilsatzstoffer med redusert miljøpåvirkning.

På bakgrunn av attraktive mekaniske, termiske og kjemiske egenskaper har karbon nanostrukturer blitt foreslått som aktuelle kandidater til denne nye generasjonen av friksjon- og slitasjereduserende tilsatzstoffer. Men, til tross for mye forskning på karbon nanostrukturer de siste 20 årene har en helhetlig forståelse av mekanismene som står bak deres smørende egenskaper uteblitt. Og, selv om funksjonalisering av overflaten som regel er nødvendig for å kunne dispergere disse nanostrukturene i smøremidler, er det få studier som har undersøkt hvordan overflatefunksjonalisering påvirker ytelsen til smøremiddelet utover dispersjonsstabilitet.

Målet for denne masteroppgaven er å oppsummere og systematisere tilgjengelig litteratur på smøreegenskapene til karbon nanostrukturer, og bidra til framtidig etablering av retningslinjer for videre forskning på temaet. Dette ble gjort ved å identifisere og kategorisere de aktuelle nanostrukturene, kritisk evaluere de foreslåtte smøremekanismene og undersøke effekten av overflatefunksjonalisering under smøring.

Det ble funnet at karbon nanostrukturer kan ha svært varierende mekaniske og kjemiske egenskaper, samt ulik morfologi, og at dette påvirker hvordan de kan bidra til friksjon- og slitasjereduksjon under smøring. Dimensjonalitet, strukturell integritet og tilbøyelighet for kjemiske interaksjoner ble identifisert som spesielt innflytelsesrike parametere som påvirker smøreevne. Vurdering av det teoretiske grunnlaget for de foreslåtte smøremekanismene i litteraturen avslørte at vår forståelse av de underliggende fenomenene er begrenset. Til tross for disse konseptuelle tvetydighetene, ble det konkludert med at enkelte av karbon nanostrukturene (spesifikt carbon quantum dots og grafén-baserte strukturer) allikevel er lovende kandidater for fremtidige tilsatzstoffer fordi de er gode bærematerialer. Disse bæreegenskapene, kombinert med innholdsrik og veletablert karbonkjemi, tilrettelegger for funksjonalisering av karbon-baserte tilsatzstoffer med skreddersydde egenskaper. Muligheten for slik tilpasning åpner døren for utvikling av tilsatzstoffer med spesifikke smøremekanismer og muligens multifunksjonalitet.

# PREFACE

---

This master's thesis is the result of work carried out from February 2020 to April 2021 and concludes my attendance at the 2-year master's degree program in Chemistry (MSCHEM) at the Norwegian University of Science and Technology (NTNU) in Trondheim.

The work was performed at the Organic Chemistry group at the Department of Chemistry with Associate Professor Solon Oikonomopoulos as the main supervisor. Professor Nuria Espallargas from the Department of Mechanical and Industrial Engineering provided invaluable support as the co-supervisor.

Financial contributions made from The Research Council of Norway, (RCN) through the ACT programme (Accelerating CCS Technologies, Horizon2020 Project No 294766) are gratefully acknowledged.

With the onset of the COVID-19 pandemic and the resulting restriction of laboratory access, it was initially decided that the experimental work of the thesis should be supported by conducting a short literary review, intended for publication, while awaiting further development. Despite the eventual re-opening of laboratory facilities, it was jointly decided with my supervisors that a shift from an experimental to a theoretical master's thesis was necessary due to sustained restricted access necessary resources and the general uncertainty of the situation. As a result, the scope and length of the literature review was expanded and adapted into this thesis. The pursuit of publishing an adapted version of this literature review in a peer-reviewed journal will recommence upon completion of my master's degree.

01.04.21

Nora Jansson



## ACKNOWLEDGEMENTS

---

The work with this thesis over the last year has been a challenging endeavor, especially with the emergence of the COVID-19 pandemic. Yet, I look back at the past year with a sense of accomplishment and fulfilment. Despite several setbacks and days of frustration, I have really enjoyed delving deeper into the field of tribology, and I am eager to continue this academic journey. I have also learned a lot about myself throughout this process. The combination of home office and an independent project of this scale has taught me valuable lessons about time management, independency, and perseverance. All in all, I believe I have emerged from this project as a better and more resilient scientist-in-training. However, I could not have done it with the help of some very important people.

First, I would like to thank my main supervisor Solon Oikonomopoulos for taking me on as a master student and for guiding me through this process. Your availability and support have been greatly appreciated, and your relaxed and chill vibe has calmed my nerves more than once.

I would also like to extend my gratitude to Nuria Espallargas who introduced me to the field of tribology and provided invaluable insights throughout the project. Thank for you for believing in me and taking the time out of your busy schedule to help me whenever I needed it. This project would not have been possible without you. You have been an endless source of inspiration and I sincerely look forward to working with you for the next three years.

I also wish to acknowledge the Department of Chemistry at NTNU for allowing me to explore fields of my own interest.

On a more personal note, I would like to thank my friends and family for showing genuine interest in my project and providing much needed support throughout these trying times. In particular, I would like to thank Maja Olava Lindmo Ryan, Tonje Skaalvik and Sigrid Bergseng Lakså for allowing me to vent my frustration in times of need and providing delightful distractions when that was required. I would also like to thank my parents for their unwavering confidence in me and my abilities.

Last, but certainly not least, I would like to thank my best friend and the love of my life, Henrik Nyholm, for always being by my side and cheering me on. The time you have dedicated to discussing the topic of this thesis with me has been greatly appreciated, and I believe you will be a fully-fledged tribologists in no time. Thank you – I really could not have done this without you.



# TABLE OF CONTENTS

---

Abstract	v
Sammendrag	vi
Preface	vii
Acknowledgements	ix
List of figures	xiii
List of tables	xv
1 Introduction and Background	1
2 Introduction to Carbon Nanostructures and Their Tribological Performance	9
2.1 0D Carbon Nanostructures	11
2.1.1 Fullerenes	11
2.1.2 Carbon Nano-onions (CNOs)	12
2.1.3 Carbon Quantum Dots (CQDs)	12
2.1.4 Graphene Quantum Dots (GQDs)	13
2.1.5 Nanodiamonds (NDs)	14
2.2 1D Carbon Nanostructures	15
2.2.1 Carbon Nanotubes (CNTs)	15
2.3 2D Carbon Nanostructures	17
2.3.1 Graphene and Its Derivatives	17
3 Evaluation of Lubrication Mechanisms	21
3.1 Entering the Contact Area	22
3.2 The Interlaminar Shearing Mechanism	25
3.2.1 0D Carbon Nanostructures	26
3.2.2 1D carbon nanostructures	26
3.2.3 2D carbon nanostructures	27
3.3 The Ball- and Roller Bearing Mechanisms	31
3.3.1 0D Carbon Nanostructures	32
3.3.2 1D Carbon Nanostructures	38

3.3.3	2D Carbon Nanostructures	40
3.4	Protective Film Formation	41
3.4.1	0D Carbon Nanostructures	46
3.4.2	1D Carbon Nanostructures	54
3.4.3	2D Carbon Nanostructures	57
3.5	Corrosion Inhibition Effect	61
3.5.1	0D Carbon Nanostructures	62
3.5.2	1D Carbon Nanostructures	64
3.5.3	2D Carbon Nanostructures	64
3.6	Filling and Mending Effect	65
3.6.1	0D Carbon Nanostructures	66
3.6.2	1D Carbon Nanostructures	66
3.6.3	2D Carbon Nanostructures	67
3.7	Polishing Effect	67
3.8	Work Hardening Effect	68
3.9	Rheological Effects	69
3.9.1	0D Carbon Nanostructures	69
3.9.2	1D Carbon Nanostructures	72
3.9.3	2D Carbon Nanostructures	74
3.10	Chapter Summary and Comparison	76
4	Functionalization of Carbon Nanostructures	81
4.1	Achieving Dispersibility and Enhancing Adsorptivity	82
4.2	Enhancing Wettability	88
4.3	Exploiting Tribochemical Interactions	91
4.4	Nanocomposites of Mixed Dimensionality	94
4.5	Introducing Additional Additive Functionality	98
5	Interactions With Other Lubricant Additives	101
6	Summary and Outlook	107
7	Concluding Remarks	115

## LIST OF FIGURES

---

Figure 1.1: Lubrication regimes in liquid lubrication.	4
Figure 1.2: Low friction mono-molecular layer of adsorbed polar organic friction modifiers on metallic surfaces.	5
Figure 1.3: The number of yearly publications with the keywords nanoparticle and lubricant. Source: ISI Web of Science (March 2021).	6
Figure 2.1: Classification of carbon allotropes according to their dimensionality <sup>28</sup> .	10
Figure 3.1 Typical flow velocity pattern and pressure distribution of a rolling EHD contact <sup>4</sup> .	23
Figure 3.2: Comparison of average friction and specific wear rate of steel disks lubricated by urea-functionalized fluorinated MWCNTs at different concentrations <sup>118</sup> .	25
Figure 3.3: Interlayer shear mechanism of lamellar solids <sup>177</sup> .	25
Figure 3.4: (A) An illustration showing the proposed puckering effect, where adhesion to the sliding top creates out-of-plane deformation of the graphene sheet, leading to increased contact area and friction. (B) The variation in friction as a function of sheet thickness based on finite element modelling (FEM) simulation.	28
Figure 3.5: The egg box model used to illustrate (a) the low-mobility commensurate state and (b) the high-mobility incommensurate state of graphene.	29
Figure 3.6: (a) TEM picture of the tribofilm in the contact area on the Si <sub>3</sub> N <sub>4</sub> ball, and high-resolution TEM pictures of typical regions (b) near the Si <sub>3</sub> N <sub>4</sub> substrate, (c) inside the tribofilm and (d) around the Cr/tribofilm interface. (e-j) Elemental mapping of the tribofilm on the Si <sub>3</sub> N <sub>4</sub> ball lubricated by water with NDs <sup>100</sup> .	50
Figure 3.7: Cross-sectional TEM image of the wear scar on 316 steel lubricated by CQDs dispersed in water <sup>156</sup> .	51
Figure 3.8: Effect of adhesion strength of lamellar additives and the underlying substrate on friction. Although adhesion between lamellae is highly undesirable, adhesion of lamellae to the worn surface is essential. In general, material that is weakly adhered is quickly removed by the sweeping action of the sliding surfaces <sup>177</sup> .	58
Figure 3.9: TEM micromorphological images of the three types of graphene sheets: (d) for r-rGO; (e) for ir-rGO; (f) for ir-W-rGO <sup>144</sup> .	59
Figure 3.10: Working principle of organic and inorganic corrosion inhibitors <sup>279</sup> .	62
Figure 3.11: Schematic illustration of the filling effect.	65
Figure 3.12: The (a) apparent viscosity curves and (b) shear stress curves of deionized water, CDs solution (0.1 wt%), and GO dispersion (0.1 wt%) with increased shear rate <sup>77</sup> .	70

Figure 3.13: Lubrication mechanism of a steel-steel contact lubricated by (a) pure PEG, (b) 0.2 mg/mL rGO in PEG, and (c) 1.0 mg/mL rGO in PEG <sup>145</sup> .	75
Figure 3.14: Snapshots from simulations that examine the sliding of the topmost diamond surface on horizontally arranged nanotubes at different at different compressional loads: (a) and (b) are at a pressure of 0 GPa; the arrows act as markers showing how the positions of two of the nanotubes changes as they slide; (c) and (d) are with a pressure of 13.7 GPa <sup>240</sup> .	79
Figure 4.1: Comparison of wear rates on 52100 bearingchemi steel with pure hexadecane oil (16C) and hexadecane oil containing 10 mg/L oleylamine-functionalized graphene oxide (GO-16C) under various loads <sup>173</sup> .	84
Figure 4.2: Schematic illustration of the synthesis procedures of IL-functionalized GO <sup>153</sup> .	85
Figure 4.3: (a) Representative structure for GO. (b) APTMS was grafted onto GO targeting oxygen functionalities. Simultaneously several oxygen functionalities are eliminated during reflux reaction. (c) The DtBHBA was covalently grafted on amino sites of APTMS-functionalized graphene <sup>283</sup> .	86
Figure 4.4: Friction curves from nitrogen-doped CQDs in (a) PEG <sup>79</sup> and (b) castor oil <sup>211</sup> at various concentrations.	87
Figure 4.5: Contact angles of pure water, GO, rGO and BLG-rGO dispersion on the 316 stainless steel <sup>200</sup> .	89
Figure 4.6: Contact angles of pure water and PEI-RGO dispersion on the 201 stainless steel <sup>146</sup> .	91
Figure 4.7: Proposed lubrication model for aqueous dispersions of (a) pure CQDs and (b) 2D nanosheets decorated by CQD <sup>212</sup> .	95
Figure 4.8: SEM micrographs of the rGO/MoS <sub>2</sub> composite structure: (a)(b) cross-sectional and (c) top view <sup>324</sup> .	97
Figure 4.9: Possible antioxidant mechanism of DPA- functionalized and nitrogen-doped CQDs in PEG <sup>79</sup> .	98
Figure 4.10: Synthetic schematic of rGO-HBPE <sup>311</sup> .	99
Figure 4.11: Illustrative representation of formation and entrapment of CQDs within PMMA structure <sup>210</sup> .	100
Figure 5.1: The schematic illustration of the synthesis procedure of GNS/MoS <sub>2</sub> -NFs and GNS/MoS <sub>2</sub> -NPs <sup>330</sup> .	105

## LIST OF TABLES

---

Table 1: Common classes of functional additives and their purpose <sup>7</sup> .	2
Table 2: Technology readiness levels (TRLs) adopted by the EU Horizon 2020 program in 2014 <sup>333</sup> .	110

---



# 1 INTRODUCTION AND BACKGROUND

---

Ensuring smooth, reliable and long-lasting operation for the numerous moving parts in mechanical systems has been an important aspect for mechanical and industrial engineers for centuries <sup>1</sup>. Achieving this goal is highly dependent on the friction and wear characteristics of the contacting surfaces as they move relative to one another <sup>2</sup>. *Tribology* is the science of contacting surfaces in relative motion and encompasses the study and application of important engineering phenomena and practices such as friction, wear, lubrication and related design aspects. In this master's thesis, the prefix *tribo* will be used to denote the special nature of a mechanical, physical, and chemical process occurring during tribological contact <sup>3</sup>.

The frictional force arising between two surfaces as they move relative to one another provides resistance to sliding, which is not only associated with a higher overall energy demand to maintain movement, but it is also accompanied by a significant release of thermal energy. In addition to being a source of highly undesirable energy loss, the friction-generated heat may also damage the components through processes like thermal degradation and thermally induced oxidation. In addition to friction, the occurrence of material contact is inherently accompanied by wear in the form of material loss from the surfaces in contact (i.e. tribosurfaces). Wear is an unfortunate waste of material that can irreversibly compromise the performance and operational lifetime of a component. Therefore, significant economic savings and reduced carbon emissions from mechanical systems can be achieved by efficiently controlling and managing friction and wear. In mechanical systems, this is typically achieved through the use of lubricants and lubricating strategies. Holmberg and Erdemir <sup>2</sup> have estimated that tribological contacts account for approximately 23% of the world's total energy consumption, of which 20% is used to overcome friction and 3% is used to remanufacture worn parts and spare equipment due to wear and wear-related failures. They also estimated that improved friction control and wear protection through tribological research and development could reduce global energy losses due to friction and wear by as much as 40% in the long term (15 years), and the associated savings could amount to 1.4% of the annual global GDP and 8.7% of the total global energy consumption. Therefore, given this context and the environmental challenges the world will be facing in the upcoming years, lubricants, lubricating systems, and related strategies will become an even more relevant aspect of tribosystems.

Lubrication is an effective way of reducing friction and controlling wear that involves the introduction of a low shear strength lubricating film between the tribosurfaces. The study of such lubricating films to determine their effectiveness, enhance their ability to prevent damage, and reduce friction is an important and very central field of research within tribology <sup>1</sup>. The term *lubricant* is used to refer to any substance that reduces friction and wear as well as ensuring smooth movement and satisfactory operational lifetime of a tribosystem <sup>4</sup>. Although lubricants can be solid, semi-solid or even gaseous

depending on the system and application, most lubricants are liquid. One of the earliest documented uses of liquid lubricants was found in the grave of ancient Egyptian king Tehut-Hetep from the 15<sup>th</sup> century B.C., and describes how olive oil was used to lubricate wooden planks to aid the movement of large stones <sup>5</sup>. Animal fats and vegetable oils remained the primary source of lubricants until the dawn of the modern petroleum industry, after which petroleum-based lubricants became the standard for several emerging industries including manufacturing, transportation, and power generation. In 2017, the global lubricant consumption (excluding marine oils) exceeded 36 million tons, with the automotive industry accounting for as much as 57% <sup>6</sup>. Due to this high lubricant demand, the automotive industry has had a prominent role in the development of high-performance lubricants in the last decades, resulting in a market dominated by hydrocarbon-based lubricants originating from fossil fuel sources.

In the last century, the development of high-quality synthetic oils with higher purity and superior thermal stability has further advanced the lubricant industry. Today, tribologists and industrial engineers have a wide range of lubricant base oils, or more precisely, base fluids, with varying properties at their disposal. Yet, lubricant base fluids are rarely used on their own as their performance can be significantly improved by the addition of functional additives. Modern lubricant formulations generally consist of a base fluid, which provides the main performance properties, and a so-called additive package. This additive package is comprised of carefully selected functional additives that can either modify the inherent properties of the lubricant base fluid, like its viscosity and oxidative stability, or impart new properties, like resistance to emulsification, corrosion, or foaming. Lubricant additives can be classified according to their purpose, as shown in Table 1, which contains some common classes of functional additives along with their intended purpose and some frequently used compounds.

*Table 1: Common classes of functional additives and their purpose <sup>7</sup>.*

<b>Additive</b>	<b>Purpose</b>	<b>Chemical compounds</b>
Antioxidants	Prolong lubricant lifetime by delaying aging process caused by oxidation of the base fluid molecules.	Phenolic antioxidants, aromatic amines, organosulfur and organophosphorus compounds
Viscosity modifiers	Influence the viscosity-temperature relationship of the lubricant and reduce changes in lubricant viscosity caused by changes in temperature. This is typically done by introducing polymeric additives whose solubility and associated spatial extension is temperature dependent.	Polymers of suitable solubility which is dependent on chain length, structure and chemical composition. Olefin copolymers, polyalkyl(meth)acrylates, polyisobutylene, hydrogenated styrene-isoprene copolymers, hydrogenated styrene-butadiene
Pour point depressants	Alter the morphology of wax crystals formed at low temperatures to inhibit lateral crystal growth and allow the lubricant to remain pourable at lower temperatures. They may also provide an additional thickening effect.	Alkylated naphthalenes Polyalkyl(meth)acrylates, polyacrylates, acrylate-styrene copolymers, esterified olefin- or styrene maleic anhydride copolymers and alkylated polystyrene

Antiwear (AW) and extreme pressure (EP) additives	Protect the mated surfaces from direct contact and wear by forming tribochemical surface layers. AW additives are designed to reduce wear at moderate loads and temperatures whereas EP additives are used under highly loaded conditions to prevent scuffing or galling (i.e., welding). The latter are generally much more reactive and may lead to corrosive or tribocorrosive effects.	AW additives: phosphates supplemented with sulfur or molybdenum-containing compounds, zinc dialkyl dithiophosphates (ZDDP) EP additives: sulfurized olefins, dithiocarbamates, dithiophosphates, DMTD derivatives and chloride compounds
Friction modifiers (FMs)	Reduce friction at the interface of the rubbing surfaces by adsorbing to form thin monomolecular layers that limit surface asperity contact.	Long chain carboxylic acids, fatty acid esters, ethers, alcohols, amines, amides, imides. Functionalized polymers, dispersed nanoparticles and organo-molybdenum compounds
Corrosion inhibitors	Protect the metal surfaces from attack by corrosive species such as oxygen, moisture or acidic products formed by thermal or oxidative decomposition.	Sulfonates, carboxylic acid derivatives and mine neutralized alkylphosphoric acid partial esters
Antifoam agents	Hinder the formation of foam in the lubricant or to break up foam that is already formed.	Linear or cyclic liquid silicon defoamers or silicon-free alternatives such as various glycols, alcohols, stearates, and miscellaneous organic copolymers
Detergents and dispersants	Disperse and suspend particulate matter to prevent deposition on metal surfaces and formation of larger particles by agglomeration. Detergents and dispersants are amphiphilic surfactant molecules that are usually divided into metal-containing detergents and so-called ashless dispersants. The alkaline reserve of metal-containing compounds may also neutralize acids and oxidation products.	Metal-containing detergents: phenates, salicylates, sulfonates, thiophosphonates Ashless dispersants: polymeric molecules such as succinimides, esters, oxazoline and Mannich bases
Demulsifiers and emulsifiers	Demulsifiers are surfactants that separate water contamination from lubricating oils. The same class of chemical substances can be used as emulsifiers to stabilize intentional lubricant emulsions, like water-based metalworking fluids.	Alkaline-earth metal salts of organic sulfonic acids, polyethylene glycols and other ethoxylated substances
Dyes	Some lubricants contain dyes for marketing, identification, or leak detection purposes.	Oil-soluble azo dyes or fluorescent dyes

Ideally, the lubricant film should be sufficiently thick to maintain full separation of the tribosurfaces. However, depending on the system and operating conditions, this is not always attainable. Lubricants can be formulated to be operative in three different lubrication regimes: (1) the boundary lubrication regime, (2) the mixed lubrication regime, or (3) the hydrodynamic lubrication regime. In the hydrodynamic lubrication regime, the tribosurfaces are fully separated by the lubricant with the most important physical characteristic being its viscosity. In this case, typical additives for achieving effective lubrication are polymers with high molecular weight, among others. In the boundary and mixed lubrication regimes, there is true contact between the tribosurfaces, as shown in Figure 1.1. In this case, the so-called friction modifiers and antiwear additives become especially important<sup>8</sup>. These are surface active additives that reduce friction and wear on the interface by adsorbing or forming films on the surface that prevent direct metal-to-metal contact between the tribosurfaces.

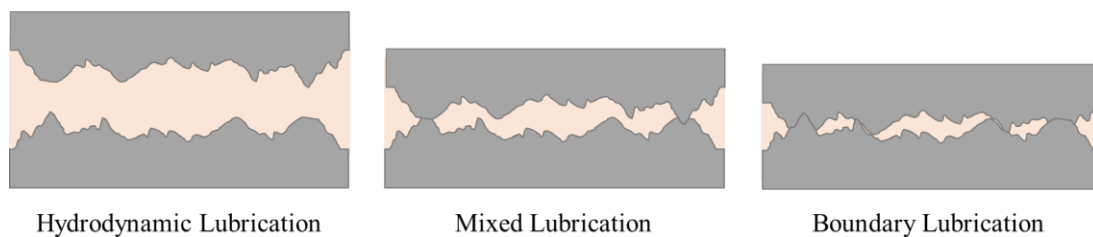


Figure 1.1: Lubrication regimes in liquid lubrication.

Conventional antiwear additives are effective at moderate loads and temperatures, and reduce wear on the tribosurface by forming durable films on the friction surfaces through tribochemical reactions<sup>8</sup>. While the precise nature of tribochemical reactions is still not fully understood, it is generally thought to be the result of either thermally induced chemistry at surface asperities due to flash temperatures, or mechanically induced chemistry due to the exposure of fresh nascent surface or electron emission from the surface<sup>9</sup>. In this regard antiwear additives are closely related to so-called extreme pressure additives that are active under high load and temperature conditions<sup>8</sup>. Most antiwear additives are phosphates modified with sulfuric, molybdenum or metallic moieties to tailor performance, resulting in protective surface films that are generally comprised of sulfates, sulfides, polyphosphates, zinc, iron, or other cation species<sup>8</sup>. Zinc dialkyl dithiophosphates (ZDDPs) were introduced in the late 1930s and are regarded as the most successful antiwear additives developed, though they were originally developed as antioxidants<sup>10</sup>. Its use is especially prevalent in the automobile industry. However, despite their superior antiwear capabilities and additional benefits as an antioxidant and corrosion inhibitor, numerous restrictions have been employed to limit the use of ZDDPs and other additives rich in zinc and phosphorous due to adverse impact on catalytic converters in emission control systems and diesel engine diagnostic systems, as well as environmental considerations. Hence, finding or developing effective and more benign antiwear additives is of great interest nowadays.

Friction modifiers reduce friction by forming an easily sheared physical or chemical boundary film between the tribosurfaces to minimize direct solid-solid interaction<sup>8</sup>. The first class of friction modifiers, known as *organic friction modifiers*, were introduced in the 1920s in the form of amphiphilic surfactant molecules, like fatty acids derived from fat or vegetable oils<sup>11</sup>. These polar molecules adsorb or self-assemble onto the tribosurface to form a vertically oriented monolayer whereby low-friction sliding is facilitated by the weak repulsion between opposing methyl groups, as illustrated in Figure 1.2. In the 1980s, a group of oil-soluble organo-molybdenum compounds that were originally developed as antiwear additives were found to also provide an appreciable reduction of boundary friction<sup>11</sup>. This class of tribochemically reactive friction modifiers are still used in many engine and gear oils where they reduce friction through *in situ* formation of lamellar molybdenum disulfide ( $\text{MoS}_2$ ) nanosheets with low shear strength on the rubbing surfaces. In the last couple of decades, polymers have been functionalized to preferentially adsorb onto polar tribosurfaces, resulting in a polymer-rich boundary

layer of higher viscosity, that reduce friction by separating the tribosurfaces by improved pressurized fluid film action, especially at low speeds.

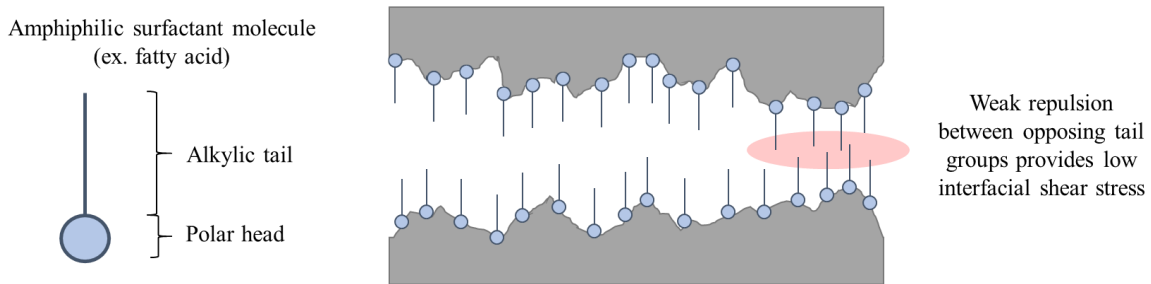
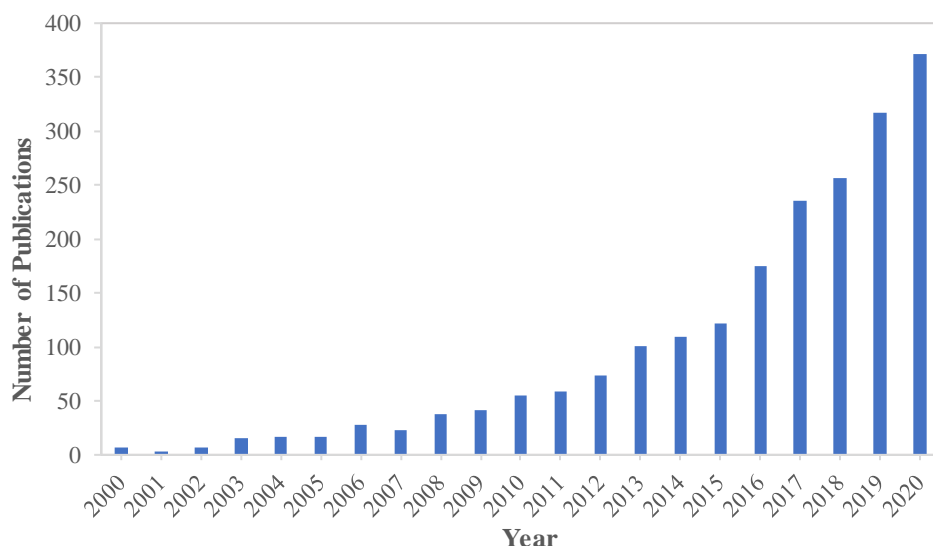


Figure 1.2: Low friction mono-molecular layer of adsorbed polar organic friction modifiers on metallic surfaces.

The most recent class of friction modifiers involve the use of dispersed nanostructures or solid colloidal particles. The term nanostructure refers to any material or structure that has at least one dimension on the nanometer scale <sup>12</sup>. Despite their small size, these nanostructures can significantly affect the properties of the fluid into which they are dispersed, even at extremely low concentrations <sup>13</sup>. For this reason, nanostructures have attracted a lot of attention across several fields of study, including tribology. In 2015, Spikes envisaged the following potential advantages of using nanoparticles as lubricant additives <sup>11</sup>:

- Particles in the size range 1 to 500 nm should be small enough to both remain dispersed in liquids by Brownian motion only and to pass undisturbed through filters that are often used in oil filters.
- The possibility to use chemistries that are insoluble in non-polar base fluids.
- Since their activity is limited to their surfaces, they should interact less with other additives present in the lubricant compared to conventional friction modifiers.
- Since their film formation is largely mechanical, nanostructures may form films on many different types of surfaces and in addition, they can be less chemically reactive than conventional additives, resulting in a more durable and less reactive film.
- They are likely to be highly non-volatile and thus not get lost in high temperature conditions.

A simple literature search on ISI Web of Science combining the keywords *nanoparticle* and *lubricant* served as the basis for the graph in Figure 1.3. It illustrates the growing interest in nanoparticles in the field of lubricants and the rapid exponential increase in the number of publications on the matter over the last couple of decades. Until now, the most widely researched and used nanostructures have been metals <sup>14,15</sup>, metal oxides <sup>16,17</sup>, or carbon-based nanostructures <sup>13,18,19</sup>.



*Figure 1.3: The number of yearly publications with the keywords nanoparticle and lubricant. Source: ISI Web of Science (March 2021).*

This search for new additives and the growing interest in nanoparticles is largely fueled by the growing emphasis on environmental considerations in later decades, and a desire for more environmentally acceptable lubricants (EALs). In 2005, the EU Commission decided in favor of implementing a European Ecolabel for lubricants with the aim of promoting the development and use of lubricating product with reduced environmental impact <sup>20</sup>. Products satisfying the requirements of the European Ecolabel must have reduced impact on the aquatic environment and soil, reduced CO<sub>2</sub> emissions, high percentages of renewable and raw materials, and limited use of hazardous substances <sup>21</sup>. In other words, lubricant systems will need to comply with increasingly stricter regulations and environmental criteria, which in some cases involve forcing replacement of current lubricant components with environmentally acceptable alternatives.

The 2020 report on Emerging Issues and Trends in Tribology and Lubrication Engineering by Society of Tribologists and Lubrication Engineers (STLE) predicted that the influential transportation sector, which represents 57% of the marked demand for lubricants, will remain a key contributor in the development of future lubricants <sup>22</sup>. The report further identified electrification of vehicles as an increasingly important strategy to comply with future vehicle emission standards. The transition from internal combustion engines (ICE) to electrical vehicles (EVs) is believed to be accompanied by a radical and fundamental shift in lubrication focus from hydrodynamic to elastohydrodynamic and boundary lubrication conditions, likely by switching to base fluids of lower viscosity <sup>23</sup>. Lowering the lubricant viscosity to reduce hydrodynamic friction is an approach that should ideally be combined with more efficient friction-reducing and antiwear additives <sup>24</sup>. Thus, a move towards environmentally acceptable lubricants involves finding new alternatives in terms of both base fluids and compatible lubricant additives.

Carbon nanostructures is a family of materials that is currently being considered as potential candidates for this new generation of friction- and wear-reducing lubricant additives. The growing interest in carbon nanomaterials in tribology over the last couple of decades can in large be attributed to their outstanding mechanical, thermal, and chemical properties. In particular, their excellent mechanical strength, thermal conductivity, thermal stability and chemical inertness are sought-after properties that should be highlighted. As they are comprised entirely out of carbon, they are believed to be a more environmentally friendly alternative to some of the current industry standards<sup>25-27</sup>. Moreover, the rich and well-established chemistry of carbon offers endless opportunities for chemical modification and tuning of properties. Another factor that has probably contributed to the research interest into carbon nanostructures in tribology is the success and prevalence of another carbon allotrope, namely graphite, which has been widely studied and used as a solid lubricant in the industry for centuries.

However, despite much research on the lubrication performance of carbon nanostructures over the last couple of decades, a comprehensive understanding of the mechanisms by which carbon nanostructures reduce friction and wear is still lacking. Moreover, despite the abovementioned notion that their nanoscale dimensions should allow dispersibility through Brownian motion, carbon nanoparticles are inherently hard to disperse and tend to agglomerate due to their high surface energy. For this reason, it has been recognized carbon nanostructures should be functionalized in order to achieve stable dispersion of the base fluid. Yet, few studies have attempted to discern how functionalization influences the lubrication performance of the nanoadditives beyond improving dispersibility.

This master's thesis aims to review and systematize the growing body of literature on the performance of carbon nanostructures as lubricant additives and contribute to the future establishment of guidelines for further research and development on the subject. This will be achieved by first identifying and categorizing the relevant carbon nanostructures in Chapter 2. In Chapter 3, the proposed lubrication mechanisms of carbon nanostructures will be investigated by critically evaluating their theoretical basis. To address the role of functionalization, Chapter 4 will attempt to summarize and systematize recent experimental literature in which surface functionalization provided other beneficial effects beyond improving dispersibility. Chapter 5 will present some general remarks relating to lubricant formulation with carbon nanostructures as well as potential interactions with other lubricant constituents. Lastly, a summary and outlook will be presented in Chapter 6, followed by concluding remarks in Chapter 7.



## 2 INTRODUCTION TO CARBON NANOSTRUCTURES AND THEIR TRIBOLOGICAL PERFORMANCE

---

Carbon has an extraordinary ability to form strong covalent bonds to both other carbon atoms and different non-metallic elements while in a variety of different hybridization states ( $sp$ ,  $sp^2$ ,  $sp^3$ ). This outstanding capability for bond formation is the basis for the wide range of carbon-based compounds and structures, ranging from small molecules to long chains. The naturally occurring carbon materials, i.e. amorphous carbon, diamond and graphite, have been known for centuries. Although both diamond and graphite are comprised exclusively of carbon atoms, their properties differ dramatically due to differences in how the carbon atoms are bonded. Graphite is an opaque black and soft material with remarkable electrical conductivity due to its layered structure of hexagonally ordered monolayers of  $sp^2$  hybridized carbon atoms, whereas diamond is a transparent electrical insulator of extraordinary hardness due to its tetrahedral crystal structure of  $sp^3$  hybridized carbon atoms. In the last decades, the gap between these natural carbon materials and organic molecules have been partially bridged by the discovery and identification of new carbon nanoallotropes with interesting properties and a wide range of potential applications <sup>28</sup>.

These carbon nanoallotropes can be classified in several different ways depending on which properties and characteristics are considered significant in a given field of study. For instance, a classification based on morphological characteristics, like the presence of internal structural voids in nanostructures such as fullerene and carbon nanohorns, may be useful for researchers in the field of catalysis as these empty spaces can accommodate catalytic particles or even provide nanoenvironments to facilitate specific reactions <sup>28</sup>. For a chemist, a classification based on the predominant type of covalent bond linking their carbon atoms may be more convenient. However, in tribology and the study of lubricant additives, where structural morphology is of great importance, a classification based on the dimensionality of the nanostructures is a more sensible approach. This scheme classifies nanostructures according to the number of dimensions in the material that are outside the nanometer size range. For instance, if all three dimensions of a material measures within the nanoscale, the material is said to be zero-dimensional (0D). This group encompasses structures such as fullerenes, carbon nano-onions (CNOs), nanodiamonds (NDs), carbon quantum dots (CQDs) and graphene quantum dots (GQDs). A one-dimensional (1D) nanomaterial has one dimension outside the nanoscale and includes nanoallotropes such as carbon nanotubes (CNTs), carbon nanofibers or nanowires, and carbon nanohorns (CNHs). Two-dimensional (2D) nanomaterials are sheet-like structures of nanoscale thickness, such as graphene, graphene nanoribbons and few-layer graphene. Figure 2.1 provides an overview of the established carbon nanoallotropes. For further elaboration on the classification, chemistry and application of carbon nanoallotropes, the reader is referred to extensive work by Georgakilas et al. <sup>28</sup>.

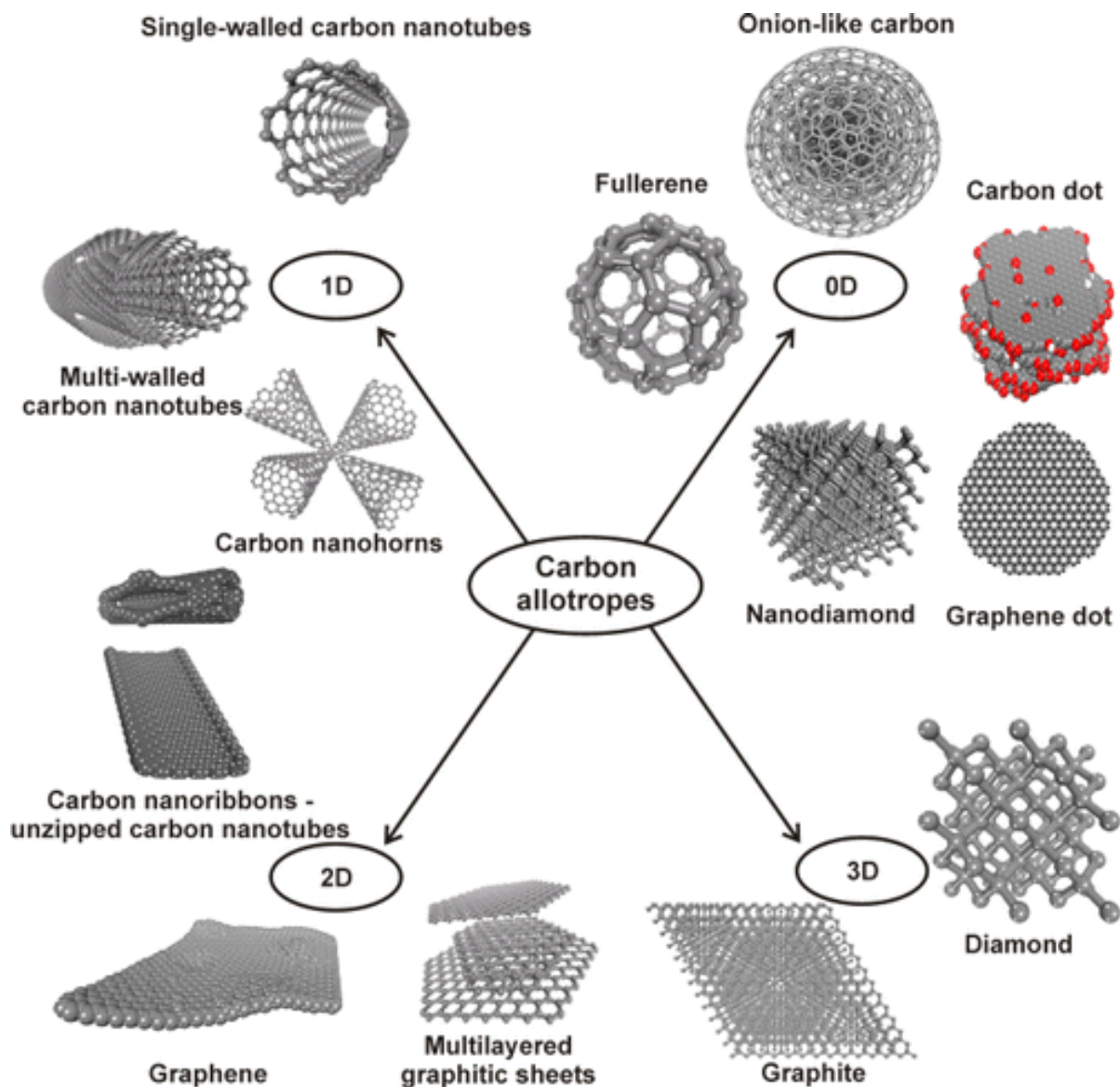


Figure 2.1: Classification of carbon allotropes according to their dimensionality<sup>28</sup>.

The following sections will use the framework of dimensionality to introduce the relevant carbon nanostructures that have been considered in this review. Some general properties and a brief overview of their tribological performance in experimental literature will be presented for each structure. Carbon nanohorns and carbon nanoribbons have been omitted from this review due to irrelevancy in the tribological field at present.

## 2.1 0D CARBON NANOSTRUCTURES

### 2.1.1 Fullerenes

The study of carbon nanostructures began with the discovery of fullerenes in 1985<sup>29</sup>. The first reported fullerene was comprised of 60 carbon atoms and labelled C<sub>60</sub>, however, several analogous structures with both higher and lower numbers of carbon atoms (e.g. C<sub>20</sub>, C<sub>70</sub>, C<sub>76</sub>) were subsequently discovered<sup>30</sup>. In general, fullerenes are hollow, close-caged, truncated icosahedral structures made up of sp<sup>2</sup>-hybridized carbon atoms arranged into 12 pentagons and  $n$  hexagons, given a total number of  $20+2n$  carbon atoms<sup>28</sup>. In addition to being the first discovered fullerene, C<sub>60</sub> is also by far the most abundant to date. With an external diameter of 0.71 nm, C<sub>60</sub> is the smallest known stable carbon nanostructure and can be regarded to lie on the boundary between molecules and nanomaterials<sup>28</sup>. For this reason, C<sub>60</sub> has chemical properties similar to a molecule and is soluble in several organic solvents including toluene (2.8 mg/mL) and carbon disulfide (7.9 mg/mL)<sup>31</sup>.

C<sub>60</sub> and other fullerenes are most often produced from graphite by vaporization using arc or plasma discharges, or laser irradiation<sup>28</sup>. An alternative method involving hydrocarbon combustion was developed for large-scale commercial production of fullerenes<sup>32</sup>. Common for all these methods is that they produce soot containing a small fraction of fullerenes which are subsequently isolated, typically using solvent extraction techniques<sup>33</sup>. The low yield and difficulty of isolating and purifying the desired products are two of the main disadvantages that greatly increases cost and environmental impact of fullerene production, despite using cheap and abundant raw materials<sup>28</sup>.

Fullerene (particularly C<sub>60</sub>) was one of the first carbon nanostructures to be studied as a potential lubricant additive. In 1994, Gupta and Bhushan<sup>18</sup> added C<sub>60</sub>-rich powder to liquid lubricants and greases and found that it greatly improved the friction and wear characteristics of a 52100 steel ball sliding against a hardened M50 steel disk. The addition of just 5 wt% C<sub>60</sub> to a paraffinic base oil reduced the wear scar on both surfaces while reducing the coefficient of friction by about 20% compared to using the pure base oil. The improvements in friction and wear of fullerenes were comparable to that of graphite or MoS<sub>2</sub> (5 wt%), and similar trends were observed in limited experiments with diester grease. Since then, a number of other studies have reported on the friction- and wear reducing effects from the addition of C<sub>60</sub> to various base fluids<sup>34-41</sup>. Lee et al.<sup>38</sup> studied the tribological properties of mineral oil with various concentrations (0.01, 0.05, 0.1, and 0.5 vol%) of fullerene C<sub>60</sub> in a disk-on-disk type tribometer and found that the concentration of fullerene nanoparticles was a key parameter controlling the friction coefficient and magnitude of wear on the rubbing surfaces. Ku et al.<sup>39</sup> studied the influence of 0.1 vol% C<sub>60</sub> on the tribological performance of various mineral oils with different viscosity grades and found that greater improvements in friction and wear properties were achieved in low-viscosity oils while the addition had little effect in more viscous oils. Moreover, the addition of C<sub>60</sub> not only reduced friction and wear on the rubbing surfaces, but also significantly increased the weld load.

### 2.1.2 Carbon Nano-onions (CNOs)

Carbon nano-onions (CNO), sometimes referred to as onion-like fullerenes (OLFs) or onion-like carbon (OLC), can be regarded as multi-shelled fullerenes as they comprise of concentric graphitic shells enclosing progressively smaller fullerenes<sup>28</sup>. They were first identified by Ugarte<sup>42</sup> in 1992 after intensely irradiating carbon nanotubes with electron beams. The mechanical properties, number of concentric shells and size of the resulting OLC particle depends on the method and conditions used for its synthesis. Most approaches for producing OLCs involve transforming some form of carbon into OLCs through activation by techniques such as arc discharge<sup>43-46</sup>, laser irradiation<sup>47</sup>, electron beams<sup>42,48</sup>, chemical vapor deposition<sup>49</sup>, or thermal annealing<sup>50,51</sup>. Herein, nanodiamonds are often used as precursors.

The tribological behavior of carbon nano-onions as lubricant additives (0.1 wt%) in PAO between AISI 52100 steel surfaces have been studied extensively by Joly-Pottuz and colleagues<sup>52-55</sup> by using a pin-on-flat setup with contact pressures in the range of 0.83-1.72 GPa. At low contact pressures (0.83 GPa) the friction is typically high (~0.1) and fluctuating during initial stages, before eventually stabilizing. At higher contact pressures (1.42 and 1.72 GPa), a very low steady state friction (~0.07) appears after only a short time (~100 cycles). Luo et al.<sup>56</sup> reported that the friction coefficient and wear scar diameter on 52100 steel ball after four-ball testing with 0.06 wt% CNOs was reduced by 43% and 19%, respectively, compared to pure SN150 base oil. Nunn et al.<sup>19</sup> dispersed 0.5 wt% CNO aggregates of 200 nm and 40 nm in PAO using proprietary dispersant before mixing with pure PAO in a 1:60 ratio and investigated its tribological behavior in a block-on-ring setup with SAE 01 tool steel. The friction of the CNO-enriched lubricants decreased over time and at the end of the test (after 5 hours) the obtained friction coefficient was ~8 times lower than that of pure PAO (0.12). However, in this case, the reduced friction was accompanied by increased wear.

### 2.1.3 Carbon Quantum Dots (CQDs)

Carbon Quantum Dots (CQDs), sometimes referred to as carbon nanodots, were first observed by Xu et al. while purifying single-walled carbon nanotubes (SWCNTs) prepared by arc discharge using an electrophoretic method<sup>57</sup>. The most striking feature of these 2-10 nm quasi-spherical nanoparticles is their tunable and relatively strong photoluminescence, which along with low toxicity and good biocompatibility has made CQDs attractive for applications such as biological labeling, bioimaging and drug delivery, as well as catalysis and optronics<sup>58</sup>. The particles themselves are typically amorphous in nature with varying volumetric ratios of graphitic and turbostratic carbon, in addition to a relatively high oxygen content<sup>28</sup>. Most of the carbon atoms are sp<sup>3</sup>-hybridized and the surface is easily functionalized.

Synthetic methods for preparing CQDs are generally classified as either physical or chemical<sup>58</sup>. The latter approach includes electrochemical synthesis<sup>59-61</sup>, various oxidation methods<sup>62-64</sup>, supported

synthetic routes<sup>65,66</sup>, microwave<sup>67,68</sup> or ultrasonic<sup>69</sup> techniques, and several synthetic routes in solution<sup>70,71</sup>. Physical methods include techniques such as arc discharge<sup>57</sup>, plasma treatments<sup>72,73</sup>, and laser ablation or passivation<sup>74–76</sup>.

The first studies investigating the potential of CQDs as lubricant additives began to emerge around 2017 and the preliminary results seem promising. Since as-prepared CQDs often have hydrophilic surface functional groups, they lend themselves perfectly to use as additives in water-based lubricants. Recently, Tang et al.<sup>77</sup> demonstrated that 0.1 wt% CQDs can reduce friction and wear of amorphous carbon (a-C) contacts by 33% and 80%, respectively, when used as lubricant additives in water. Using a ball-on-disk tribometer, Xiao et al.<sup>78</sup> found that the addition of 1.25 wt% CQDs to deionized water could reduce the friction of Si<sub>3</sub>N<sub>4</sub>-steel and Si<sub>3</sub>N<sub>4</sub>-Si<sub>3</sub>N<sub>4</sub> contacts by up to 30% and 14%, respectively. CQDs are also easily modified due to their chemically reactive surface functional groups. Ye et al.<sup>79</sup> synthesized CQDs with diphenylamine on the surface and investigated their performance as lubricant additives in polyethylene glycol (PEG) between AISI52100 steel balls in a four-ball tester. At the optimal concentration of 1 wt%, the mean coefficient of friction and wear scar diameter were reduced by 75% and 35%, respectively, without changes in viscosity. Even under high loads (588 N), there was still a considerable reduction in both friction (72%) and wear (42%). Ma et al.<sup>80</sup> modified CQDs with a mixture solution of choline chloride and ethylene glycol (molar ratio 1:2) and evaluated their tribological behavior in a rotating ball-on-disc tribometer. The additive demonstrated excellent tribological performance with a low friction coefficient of about 0.006 and a wear rate of about  $0.7 \times 10^{-14}$  m<sup>3</sup>/Nm at a CQD concentration of 3.6 at.%. Shang et al.<sup>81</sup> covalently grafted an imidazolium orthoborate ionic liquid to CQDs and studied its tribological properties in PEG. Under a load of 196 N, a concentration of 1.0 wt% functionalized CQDs reduced the friction and wear of the mated steel contact by 75% and 24%, respectively. Even when the applied load was 588 N, the friction and wear reduction was 70% and 92%, respectively, compared to pure PEG.

#### **2.1.4 Graphene Quantum Dots (GQDs)**

Graphene Quantum Dots (GQDs) were first fabricated by Ponomarenko et al.<sup>82</sup> in 2008 and can be regarded as small pieces of graphene that are less than 100 nm wide and less than 10 layers thick<sup>83</sup>. GQDs are similar to CQDs in that they also have a strong tunable photoluminescence, low toxicity and good biocompatibility. However, unlike CQDs, GQDs are crystalline and consist of mainly sp<sup>2</sup> hybridized carbon atoms<sup>28</sup>. The most interesting aspect of the zero-dimensional GQDs is arguably how their properties differ from those of two-dimensional graphene and other carbon nanomaterials due to quantum confinement and edge effects at sizes below 100 nm. For instance, while use of 2D graphene is limited in electronic and optoelectronics due to its lack of band gap, GQDs have a tunable and non-zero bandgap which provides them with interesting electronic and optical properties<sup>28</sup>. Moreover, GQDs have better solubility than carbon nanotubes (CNTs) since its large edge effects can be readily functionalized, whereas CNTs are limited by their dimensionality<sup>83</sup>. Quantum confinement and edge

effects typically increase with decreasing particle sizes and become particularly pronounced as the dimensions fall below 10 nm.

Approaches for preparing GQDs are often classified as top-down or bottom-up methods depending on the precursor material <sup>83</sup>. Top-down methods involve cutting up or reducing the size of graphitic structures such as carbon black <sup>84,85</sup>, coal <sup>86</sup>, graphene <sup>82</sup>, CNTs <sup>87,88</sup> or graphite <sup>89</sup>, whereas bottom-up synthesis involve stepwise chemical synthesis from smaller graphene-like polycyclic aromatic hydrocarbon precursors such as benzene <sup>90</sup> or glucose <sup>91</sup>.

As one of the most recently discovered carbon nanostructures, GQDs are still quite novel and research into their lubricating potential is still in its infancy. Still, He et al. <sup>92</sup> demonstrated that GQDs can act as excellent lubricant additives in 150NM mineral oil by using a four-ball tester and altering the concentration and type of GQDs. In particular, they reported that 0.8 wt% of an appropriate GQDs type could reduce the mean friction coefficient, wear scar diameter and depth lubricated by 150SN mineral oil under 392N by 65%, 44% and 91%, respectively. Qiang et al. <sup>93</sup> synthesized GQDs with abundant oxygen-rich surface functional groups and investigated its tribological performance as a water based lubricant additive in a steel-steel contact using a ball-on-disk reciprocal tribometer. An aqueous dispersion of 4 mg/mL GQDs exhibited a 43% reduction in friction and a 59% decrease in wear rate compared to pure water, and even outperformed corresponding dispersions of graphene oxide (GO).

However, since studies into their behavior as lubricant additives is severely limited it might be worth mentioning that GQDs have also been briefly studied as solid lubricants or coatings. For instance, Wolk et al. <sup>94</sup> synthesized dodecyl amine edge-functionalized few-layer graphene oxide quantum dots and spray deposited it onto steel surfaces. A thin film of the dodecyl amine functionalized graphene oxide quantum dots on steel lowered the friction and revealed a significant corrosion inhibition effect. Additionally, Yin et al. <sup>95</sup> obtained friction coefficients as low as 0.01 under heavy loads and high speeds in inert gaseous atmosphere by depositing GQDs onto three types of hydrogenated amorphous carbon coatings (graphite-like carbon, diamond-like carbon, and polymer-like carbon). The lubricating behavior was attributed to the formation of tribochemical films. Herein, the surface of the pin surface was covered by 2D-layered carbon and graphitic structures induced by structural transformation of GQDs. Meanwhile, the tribofilm on the disk surface was comprised of a silica-like SiO<sub>x</sub> boundary layer and a multicomponent layer induced by tribochemistry.

### **2.1.5 Nanodiamonds (NDs)**

Nanodiamonds (NDs) are comprised of mostly sp<sup>3</sup>-hybridized carbon atoms in crystal domains of diamondoid-like topology <sup>28,96</sup>. The properties of NDs are highly dependent on particle size, which is typically in the range 1-20 nm <sup>28</sup>. This is because the surface-bound sp<sup>3</sup>-hybridized carbon atoms are generally stabilized by bonding to hydrogen or other non-carbon elements. Thus, when the particle diameter is small and the percentage of surface atoms large, the properties of NDs resemble organic

molecules rather than bulk diamonds. Conversely, when the diameter increases, the percentage of surface-bound carbon atoms decreases and the bulk diamond character of the NDs becomes more predominant.

The archetypal NDs are synthesized using detonation methods with carbon-containing compounds such as trinitrotoluene (TNT) and hexogen<sup>96</sup>. NDs make up about 75% of the resulting soot and they have a relatively narrow size distribution centered around 4-5 nm. In particles of this size, about 15% of the carbon atoms are located on the surface and aid stabilization by bonding with hydrogen or other elements. The surface can be decorated by a variety of functional groups depending on the chemical conditions during purification.

Alongside fullerene, NDs were among the first carbon nanostructures to be studied for potential application as lubricant additives. Already in 1996, Tao et al.<sup>97</sup> reported that the addition of NDs could significantly improve the friction-reducing, antiwear and load-carrying capacity of paraffin oil under boundary lubrication conditions. Since then, the lubrication performance of ND additives have been studied extensively<sup>98</sup>. For example, Nunn et al.<sup>19</sup> found that the addition of 0.010-0.015 wt% to PAO led to a sharp reduction in friction after about 2 hours, after which the coefficient of friction remained stable at an extremely low value of ~0.002 (98.5% lower than that of pure PAO) for the remainder of the test. However, compared to pure PAO, the wear scar resulting from the addition of NDs was significantly increased by ~2.5 times. Chou and Lee<sup>99</sup> found that the addition of NDs could improve the tribological performance of ISO86 base oil on both carbon steels and aluminium alloy, however, the optimal concentration and extent of tribological enhancement varied among the different materials. Wu et al.<sup>100</sup> found that the addition of 0.5 wt% NDs to water reduced the friction between a Si<sub>3</sub>N<sub>4</sub> ball and Si wafer from ~0.4 to ~0.07.

## 2.2 1D CARBON NANOSTRUCTURES

### 2.2.1 Carbon Nanotubes (CNTs)

Carbon nanotubes (CNTs) are tubular nanostructures comprised of hexagonally arranged sp<sup>2</sup>-hybridized carbon atoms with high aspect ratios that are typically classified according to the number of graphitic layers in the walls<sup>28</sup>. Multi-walled carbon nanotubes (MWCNTs) can be described as several layers of concentrically arranged cylinders of graphenic carbon, and were first identified by Iijima in 1991 after using an arc discharge evaporation method similar to that used for fullerene synthesis<sup>101</sup>. A couple of years later, Iijima<sup>102</sup> and Bethune<sup>103</sup> independently reported on the discovery of single-walled carbon nanotubes (SWCNTs), which can be regarded as a single graphene sheet that is seamlessly rolled up to form a tube with ends capped by a hemisphere resembling a fullerene structure<sup>104</sup>. SWCNTs typically have a diameter around 0.4-2 nm, a length of several micrometers and an empty internal space<sup>28</sup>.

Because of this high length-to-diameter ratio, known as the aspect ratio, CNTs form highly entangled bundles that are held together through van der Waals interactions.

Another key parameter of CNTs is the chirality, which is given by the angle between the hexagonal lattice and the nanotube axis. Depending on the chirality and the resulting arrangement of carbon atoms along the nanotube circumference, SWCNTs can be either metallic or semiconducting, whereas MWCNTs can be regarded as metallic conductors<sup>104</sup>. Moreover, as a result of the one-dimensional nature of CNTs, electrons can be conducted without scattering or dissipating energy as heat, which is known as ballistic transport. Phonons also propagate easily along the tube, resulting in a room temperature thermal conductivity of about 3000 W/mK in an individual MWCNT<sup>105</sup>. All these properties, as well as exceptional tensile strength and elastic modulus, has made CNTs interesting for applications such as composite reinforcement<sup>106,107</sup>, electrochemical devices<sup>105</sup>, field effect transistors<sup>108,109</sup>, hydrogen storage<sup>110,111</sup>, catalyst support<sup>112,113</sup>, probe and sensor technology<sup>105,114,115</sup>.

Today, CNTs are mainly produced by three techniques, namely arc discharge, laser ablation and catalytic growth<sup>105,116</sup>. Some of the main challenges of CNT preparation is controlling chirality and the presence of metallic and amorphous carbon impurities<sup>28</sup>. Such impurities are often removed using an acid treatment, which in turn can introduce other impurities and degrade the nanotubes themselves<sup>105</sup>. Thus, purification is a challenge which adds to nanotube cost.

Owing to their large aspect ratio and high surface energy, CNTs are prone to aggregation and tend to form highly intermingled bundles with very poor lubricating properties. Thus, loosening these bundles and preventing aggregation is crucial to the lubrication performance of CNTs. This is typically done through chemical surface functionalization or use of surfactants. For example, Peng et al.<sup>117</sup> compared the lubrication performance of MWCNTs dispersed in water by the aid of sodium dodecyl sulfate (SDS) surfactant to that of unfunctionalized MWCNTs and confirmed that enhanced dispersion indeed yields better tribological properties. The SDS-dispersed MWCNTs exhibited good friction reducing and antiwear properties as well as enhanced load-carrying capacity. Particularly, the maximum non-seizure load was raised about 3–7 times when SDS-functionalized MWCNTs were added into water. Min et al.<sup>118</sup> functionalized fluorinated MWCNTs with urea and observed that the addition of only 0.15 wt% reduced the friction and wear rate of a water-lubricated steel contact by up to 81% and 97%, respectively. Joly-Pottuz et al.<sup>119,120</sup> asserted that after adding 0.1 wt% SWCNTs or MWCNTs to the polyalphaolefin (PAO) base oil, the friction coefficient could be reduced down to 0.08 and 0.06, respectively, depending on the contact pressure. Ye et al.<sup>121</sup> systematically studied the influence of length and diameter for MWCNT when used as lubricant additives and found that MWCNT samples with shorter lengths and smaller diameters performed better than long-length MWCNTs and larger diameters.

## 2.3 2D CARBON NANOSTRUCTURES

### 2.3.1 Graphene and Its Derivatives

Despite being theoretically predicted<sup>122</sup> and experimentally observed<sup>123</sup> several decades ago, graphene was not properly isolated and characterized until 2004<sup>124</sup>. Graphene is defined as a single carbon layer of graphitic structure, analogous to a polycyclic aromatic hydrocarbon of quasi-infinite size<sup>125</sup>. Herein, each carbon atom is  $sp^2$ -hybridized and covalently bonded to three neighboring carbon atoms to form a robust hexagonal lattice<sup>28</sup>. The remaining unhybridized p-orbital is oriented perpendicular to the graphene sheet and interact with each other to form a half full out-of-plane  $\pi$  band which acts to further strengthen the interatomic  $\sigma$  bonds<sup>126</sup>. As a result, graphene is one of the strongest currently known materials with a Young's modulus of 1 TPa and an intrinsic strength of 130 GPa<sup>127</sup>. Besides its impressive mechanical properties, graphene has been widely studied for its unique electrical characteristics. It is a zero-bandgap semiconductor with highly mobile charge carriers which are best described as massless Dirac fermions that can travel thousands of interatomic distances without scattering<sup>128</sup>. Graphene is also a great conductor of thermal energy<sup>129</sup>. Combined with optical transmittance of  $\sim 97.7\%$  pr. layer<sup>129</sup> and an ultrabroad optical adsorption spectrum<sup>130</sup>, these unique properties have made graphene an attractive material for numerous applications including flexible electronics, transistors, various photonics, composite materials, coatings, energy storage, sensor technology and various bioapplications<sup>129</sup>.

The potential applications of graphene are to a large extent dictated by the progress in graphene synthesis with respect to appropriate properties for specific applications and overall quality. The quality and properties of produced graphene is highly dependent on the method by which the graphene was produced and higher quality graphene is generally produced by more expensive methods<sup>28</sup>. Signs of lower quality graphene include poor mechanical strength and electrical conductivity due to the presence of defects or oxygen sites in the lattice structure, smaller nanosheets and the co-occurrence of multilayered structures. Graphene was first produced using the so-called scotch tape technique in which commercially available adhesive tape was used to mechanically exfoliate multiple layers of highly ordered pyrolytic graphite before depositing the peeled graphene onto the desired substrate<sup>27,124</sup>. Since then, several synthesis methods have been developed. Some top-down alternatives to dry mechanical exfoliation include liquid-phase exfoliation of graphite in specific organic solvents with surface tension around 40-50  $\text{mJ/m}^2$ <sup>131</sup>, and unzipping of carbon nanotubes by various physical, chemical or electrochemical techniques<sup>27,132</sup>. Bottom-up methods for graphene production generally aim to synthesize graphene from organic precursors or catalyze growth of graphene on a substrate<sup>133</sup>. Herein, some commonly used techniques are chemical vapor deposition (CVD)<sup>134,135</sup>, epitaxial growth<sup>136,137</sup> and arc discharge<sup>138,139</sup>.

Graphene oxide (GO) is a graphene derivative that can be described as a monomolecular layer of graphite decorated with various oxygen-containing functionalities such as epoxide, carbonyl, carboxyl and hydroxyl groups<sup>140</sup>. The presence of these polar functionalities enhances the hydrophilicity of the GO sheets and facilitates dispersibility in polar solvents. Through appropriate chemical or thermal treatments, GO can be partially reduced to form a structure known as reduced graphene oxide (rGO). Herein, the oxygen-containing groups have been removed and the conjugated structure recovered, resulting in a structure that resembles pristine graphene except for residual oxygen and other heteroatoms, as well as structural defects. Despite associated changes in mechanical strength and electronic properties compared to pristine graphene, GO and rGO have the added benefit of cheaper synthesis from inexpensive and abundant graphite.

Strictly speaking, graphene is defined as a single *monolayer* of conjugated  $sp^2$ -hybridized carbon atoms arranged in a hexagonal lattice structure. When several such layers are stacked and held together by van der Waals interactions, these two-dimensional graphene sheets make up the building blocks of three-dimensional bulk graphite. Unlike graphene, graphite shows semimetallic behavior and has a band overlap of about 41 meV<sup>141</sup>. According to Geim and Novoselov<sup>128</sup>, the electronic structure and many of the characteristic properties of graphene rapidly evolve with decreasing number of layers below 10 in graphite. For this reason, structures comprised of a few graphitic layers are often referred to as graphene in everyday practice despite not being monolayered. While monolayer graphene is a zero-gap semiconductor, the electronic spectrum of bilayer graphene shows a very small overlap and crossing of bands along one direction in the Brillouin zone<sup>141</sup>. For three or more layers, the electronic spectra become increasingly complicated as more charge carriers appear and the conduction and valence band begin to overlap. Beyond 10 layers, the structures should no longer be considered two-dimensional graphene but rather three-dimensional graphite. Thus, with respect to electronic properties, monolayered, bilayered and few-layered (3 to <10 layers) graphitic structures can be distinguished as three different 2D crystals<sup>128</sup>. In lubrication, the dimensionality of the friction-reducing and antiwear nanoadditive is of greater importance than electronic properties. Hence, in this review, the term *graphene* will henceforth be used as a collective term to describe these 2D carbon nanostructures. Yet, the reader is urged to keep in mind the true definition of terminology.

For use as lubricant additives, graphene-based nanostructures are probably the most extensively and systematically studied of all the carbon nanostructures, and the preliminary results are promising. Graphene is generally functionalized to enable dispersion in various base fluids. The hydrophilic surface functional groups of GO lend themselves perfectly to dispersion in water-based lubricants. For instance, Wu et al.<sup>100</sup> found that the friction coefficient observed in a water-lubricated  $Si_3N_4$ -Si contact with 0.1 wt% GO was about 5 times lower than that obtained using pure water. However, through use of an appropriate dispersant or additional surface functionalization, GO has also been used as a lubricant additive in non-polar lubricants. For example, Zhang et al.<sup>142</sup> covalently functionalized GO with 1-

dodecanethiol to enable dispersion in rapeseed oil and observed a 45% and 40% reduction of friction and wear at an additive concentration of 0.2 wt%. Wu et al.<sup>143</sup> demonstrated that the load-carrying capacity, friction, and wear of a Si<sub>3</sub>N<sub>4</sub>-52100 steel contact could be reduced by 18%, 15% and 35% by the addition of 0.5 wt% GO nanoplatelets to an 4010 aviation lubricant.

Reduced graphene oxide (rGO) also shows promising results as a lubricant additive. Using 1 wt% rGO in a hydraulic oil, Mao et al.<sup>144</sup> obtained a stable and low friction of approximately 0.0614, which was only ~62% lower than that of the pure base oil. Moreover, the low friction was accompanied by a wear reduction of 86%. Similarly, after the addition of 0.02 mg/mL rGO to PEG, Gupta et al.<sup>145</sup> observed a 70% and 50% reduction of friction and wear between sliding steel surfaces. Liu et al.<sup>146</sup> covalently functionalized rGO with polyethylenimine and demonstrated that a concentration of 0.05 wt% in water could reduce friction and wear by 55% and 45%, respectively, using a steel ball-on-plate tribotest.



### 3 EVALUATION OF LUBRICATION MECHANISMS

---

To date, carbon nanostructures have been added to lubricants primarily to reduce friction and wear in the boundary and mixed lubrication regimes. The main mechanism for doing so is generally ascribed to their small size allowing them to enter the narrow contact area where they can act as separators to limit direct contact between tribosurfaces in relative motion<sup>143,147–149</sup>. For a more comprehensive understanding of the friction- and wear-reducing capabilities of carbon nanostructures, researchers have proposed several additional lubrication mechanisms including the ball bearing mechanism<sup>56,97,100,150</sup>, interlaminar shearing<sup>151,152</sup>, tribofilm formation<sup>54,153–155</sup>, corrosion inhibiting effects<sup>78,94,156</sup>, work hardening effects<sup>157–159</sup>, polishing effects<sup>19,97</sup>, passivating effects<sup>160,161</sup>, rheological effects<sup>162,163</sup>, and filling or mending effects<sup>25,151,164,165</sup>. These mechanisms are often categorized into two main groups, the first of which encompasses effects arising directly from the nanoparticles, such as the ball bearing mechanism, interlayer shearing and tribofilm formation, whereas the mechanisms in the second group improve tribological performance through secondary effects that contribute to surface enhancement<sup>151,164</sup>. This category includes mechanisms like work hardening, polishing, smoothing, and mending of the tribosurfaces.

However, as seen in Chapter 2, carbon nanoallotropes make up a broad family of structures with a wide range of mechanical and chemical properties. This is reflected in the different ways they protect the tribosurfaces from friction and wear, and their working principle and lubrication mechanisms are usually specific to the type of carbon nanostructure and its inherent dimensionality. For instance, a two-dimensional graphene sheet would not be able to effectively roll between two tribosurfaces acting as a molecular ball bearing like a spherical zero-dimensional nanoparticle could. Nor would a nanodiamond be able to dissipate shear forces through interlaminar sliding in the way few-layer graphene structures do.

This chapter aims to elucidate which of the abovementioned lubrication mechanisms pertain to the various carbon nanostructures and how this differentiation relates to the dimensionality and properties of the different nanostructures. Additionally, the proposed lubrication mechanisms will be critically evaluated with respect to their theoretical basis. How carbon nanostructures can be delivered to the interfacial contact area will be presented in Section 3.1, while Sections 3.2 to 3.9 present the various ways in which they can enhance tribological performance once inside the contact area. At the beginning of each section, a brief introduction to the general principle or idea behind the lubrication mechanism will be presented before attempting to evaluate the extent to which 0D, 1D and 2D carbon nanostructures can reduce friction or wear by said mechanism, based on available literature. Finally, Section 3.10 will briefly summarize and compare the tribological behavior of 0D, 1D and 2D carbon nanostructures.

### 3.1 ENTERING THE CONTACT AREA

In order to partake in the improvement of boundary lubrication processes, the friction- and wear-reducing nanostructures must be present on the rubbing surfaces in the contact region. The requisite delivery of nanostructures to the contact interface can occur by two main mechanisms, namely adsorption and mechanical entrainment. In this context, mechanical entrainment refers to the process in which solid particles are caught between rubbing surfaces by purely mechanical action due to the relative motion of the surfaces and lubricant flow. Chiñas-Castillo and Spikes have published several articles on the mechanical behavior of solid colloidal and nanosized particles in liquid lubrication<sup>166-168</sup>. Even though their work focused mostly on spherical metallic nanoparticles rather than carbon nanostructures, the mechanical principles should still apply, at least in the case of 0D carbon nanostructures. As for carbon nanostructures of higher dimensionality (1D and 2D), the applicability of their findings should be carefully considered and evaluated.

In a purely rolling contact, Chiñas-Castillo and Spikes experimentally found that mechanical entrainment of nanoparticles only occurred when the fluid film thickness was less than the particle diameter (i.e., the entrainment process was controlled by the ratio of particle size to fluid film thickness)<sup>166</sup>. As the nanoparticles became entrained and passed through the narrow contact, they gradually formed a solid boundary film that enhanced the separation of the surfaces. This boundary film formation and the associated separation effect was lost if the base oil fluid film thickness was larger than the particle diameter at higher speeds, indicating that the colloidal particles only adhered to the solid if they were mechanically entrapped at the contact inlet. The particles that were not entrained when the fluid film was thick, may just have been rejected from the contact inlet by side or reverse flow, or simply passed through the contact without adhering to the surfaces or contributing to surface separation. These findings are consistent with the reported behavior of other types of nanoparticles<sup>167,169</sup> as well as larger micro-sized particles<sup>170</sup>.

The entrainment mechanism and its dependence on fluid film thickness is perhaps best understood by considering the flow pattern of an elastohydrodynamic (EHD) contact under purely rolling conditions. As seen in Figure 3.1, the flow at the EHD contact inlet can be divided into two main zones. Region A is characterized by reverse fluid flow that rejects particles away from the contact inlet, whereas fluid in region B passes through the contact. The stagnation point (S) is a neutral position on the velocity profile where the fluid forces acting on a particle will be balanced. When the mean entrainment speed of the contact is low and the particle diameter is large compared to the fluid film thickness, this stagnation point is located relatively close to the contact inlet, thus increasing the probability of large particles getting close enough to get pinched by the mating surfaces in the region where almost all flow passes through the contact. Using a simplistic approximation, Chiñas-Castillo and Spikes found that as long as the particle diameter is larger than the fluid film thickness, there are frictional forces acting to drag the pinched particles at the inlet into the contact, thus, entraining them<sup>166</sup>. When the speed is high, however,

the stagnation point and the reverse flow vortices move away from the contact inlet, making it harder for particles to reach the point where they can be entrained by the surfaces <sup>4</sup>. Also, when the fluid film thickness is larger than the particle diameter, there is no pinching action or frictional forces acting upon the particles that do indeed reach the contact inlet, making it more likely for these particles to end up in lines of reverse flow.

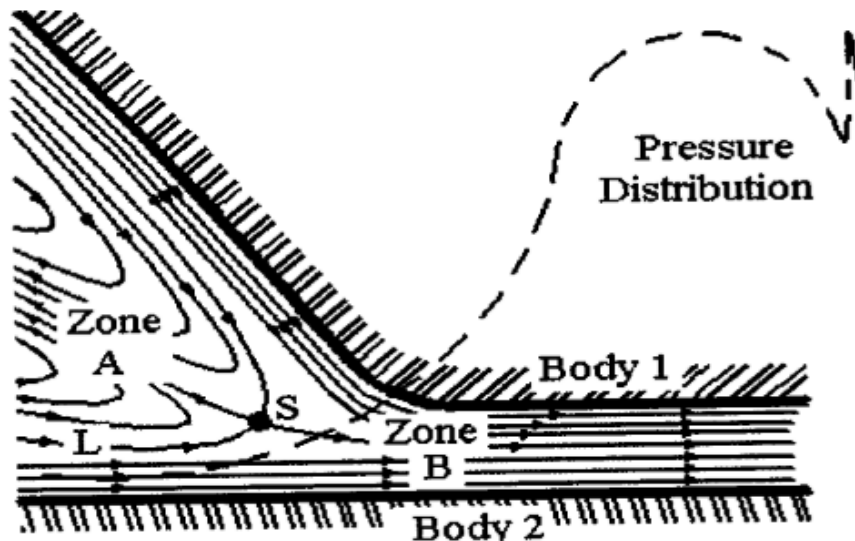


Figure 3.1 Typical flow velocity pattern and pressure distribution of a rolling EHD contact <sup>4</sup>.

The process of entrainment is also dependent on how the surfaces move with respect to each other, i.e. whether the contact is rolling or sliding <sup>166</sup>. In the case of mixed rolling-sliding contacts, the fluid flow pattern becomes asymmetrical as the stagnation point shifts towards the slower moving surface with increasing slide-roll ratios (SRR). Increasing the SRR decreases the critical speed at which particles are entrained in the contact, indicating that higher degree of sliding in the contact makes it harder for particles to become entrained. In the pure rolling case, frictional forces will drag colloidal particles into the contact if they move slowly or at the same speed as the mating surfaces. While a slow particle might experience appropriate frictional forces and subsequent entrainment in a mixed rolling-sliding contact too, a particle moving at an intermediate speed is likely to experience slip at the contact inlet and subsequent rejection by backflow. Thus, both fluid and frictional forces must coincide to favor particle entrainment as the SRR increases.

While mechanical entrainment is the result of purely mechanical action, adsorption involves physical and chemical interaction between the nanostructures and the tribosurfaces. These attractive interactions cause molecules and particles to spontaneously adhere to the tribosurfaces. This is believed to aid transportation of the nanostructures into the contact by reducing the likelihood of being rejected or swept away by lubricant flow. In other words, the strict conditions for mechanical entrainment might not need to be fulfilled to ensure presence of nanoparticles in the interfacial contact area.

It has been argued that some degree of adsorption is probably necessary to accumulate the requisite coverage of carbon nanostructures in the contact to keep the surfaces apart and provide for the drastic improvement in tribological performance reported in literature <sup>11,171</sup>. Specifically, Hugh Spikes <sup>11</sup> considered a circular contact of radius  $R$  lubricated by a dispersion of concentration  $C\%$  of nanoparticles with radius  $r$ , and supposed the film thickness was  $2r$  (just enough to be bridged by the undeformed nanoparticles). Assuming that all particles enter the contact unhindered by flow, a simple calculation yields the number of particles present in the contact at any one moment to be  $1.5CR^2/r^2$  and the fraction of the contact area covered by particles to be simply  $1.5C$ . For a quite high nanoparticle concentration of 1 vol%, this implies that only 1.5 % of the contact area will be covered by particles at any given time, which is probably insufficient to hold the surface apart. Consequently, this suggests that to separate the surfaces effectively, either the particles must become more concentrated in the contact inlet, or some adhesion of particles to the surfaces is required <sup>11</sup>.

However, even in the presence of adsorption effects, the ability to enter the contact area is still dependent on particle size. Specifically, larger particles may have difficulties entering the narrow contact area between the rubbing surfaces during boundary lubrication <sup>54,121</sup>. Due to their nanoscale dimensions, all the different types of carbon nanostructures discussed in this review have been shown to be able to enter the contact area between the rubbing surfaces under suitable conditions when properly dispersed <sup>54,77,93,98,121,144,149,163,172,173</sup>. However, the high surface area-to-volume ratio makes nanoparticles prone to agglomeration in most liquids <sup>13</sup>. The task of dispersing carbon nanostructures in lubricants is further complicated by their high chemical inertness, which means they have little to no affinity towards most base fluids <sup>174</sup>. Such undesired aggregation may not only render the nanoparticles too large to enter the contact area but can also inhibit lubricant flow through the contact area by accumulating at the inlet <sup>26</sup>. In some cases, nanoparticle aggregates may even intensify wear of the tribosurfaces by acting as third-body wear particles <sup>77</sup>. For these reasons, it is generally recognized that functionalization of carbon nanostructures is critical for their application in lubrication.

However, even functionalized nanostructures tend to agglomerate above a critical concentration. For this reason, both friction- and wear curves as a function of nanoparticle concentration tend to have a valley-like shape <sup>46,77,118,144,175</sup>, as exemplified by Figure 3.2. The higher friction and wear at low concentrations are generally attributed to insufficient nanoparticle coverage at the interfacial contact area. Meanwhile, the concentration at which the friction and wear are at a minimum are characterized by the optimal nanoparticle presence. Increasing the nanoparticle concentration beyond this point is generally associated with increasing degrees of agglomeration, which leads to increased friction and wear for the abovementioned reasons <sup>26</sup>.

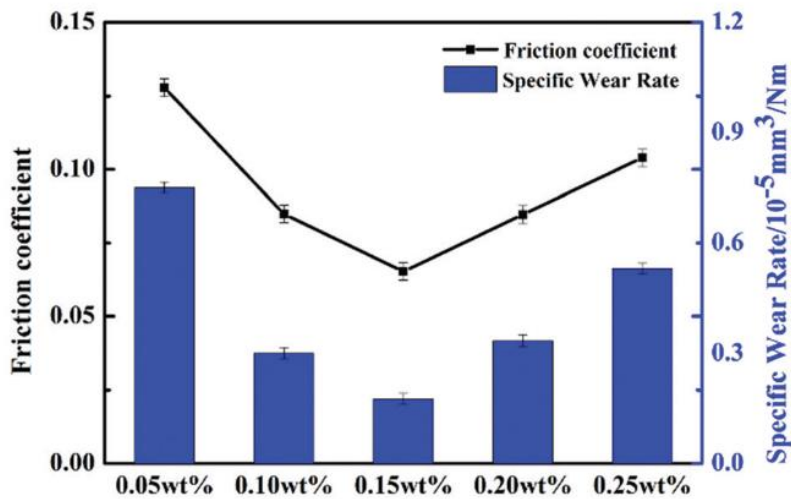


Figure 3.2: Comparison of average friction and specific wear rate of steel disks lubricated by urea-functionalized fluorinated MWCNTs at different concentrations <sup>118</sup>.

### 3.2 THE INTERLAMINAR SHEARING MECHANISM

One of the reasons for the great interest in carbon nanostructures (particularly graphene) within the field of tribology is the close relation with another carbon allotrope, namely graphite, which has been widely studied and used as a solid lubricant in industry for more than 40 years <sup>27</sup>. Graphite has a planar and layered structure in which the carbon atoms within each layer are arranged in a hexagonal lattice with strong in-plane bonding, while weak van der Waals forces act between the layers <sup>176</sup>. It is this contrast between intra-layer and inter-layer bonding strength that allows individual graphitic layers to slide over one another with relative ease and gives rise to the lubricous properties of graphite. Figure 3.3 illustrates how the relative motion of contacting surfaces supplies shear stresses to the multilayered material in the contact area, and how the low resistance towards interlaminar shear results in the formation of low-friction sliding system within the contact <sup>152</sup>.

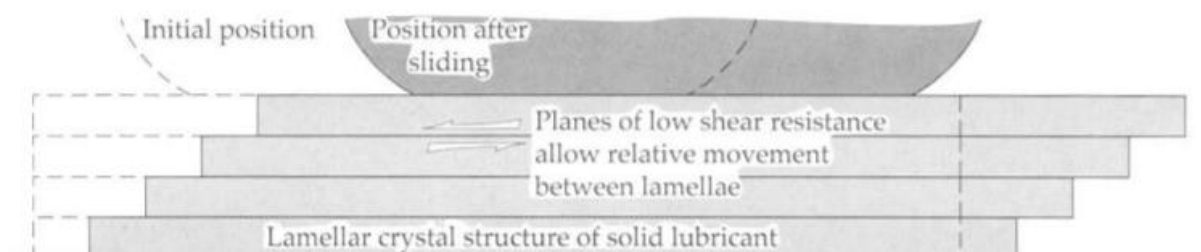


Figure 3.3: Interlayer shear mechanism of lamellar solids <sup>177</sup>.

Graphite and other solid materials with lamellar crystal structures that can reduce friction through this interlaminar shear mechanism are sometimes referred to as self-lubricating solids<sup>178</sup>. Herein, interlayer bonding strength and the ability of the solids stay adhered to the rubbing surfaces are important parameters for tribological performance<sup>177</sup>. The lubricity of lamellar solids is also influenced by environmental factors<sup>178</sup>. For instance, the friction-reducing ability of graphite is highly dependent on intercalation of water molecules or some other adsorbate between the graphitic layers in order to reduce interlayer bonding strength and resistance to interlaminar shear. For this reason, solid graphite performs best in humid environments where it typically provides a coefficient of friction in the range of 0.1-0.2, whereas it fails to provide low friction and wear in dry, inert or vacuum conditions<sup>27</sup>.

### **3.2.1 0D Carbon Nanostructures**

From the introduction above, it follows that a planar lamellar structure is a prerequisite for this friction-reducing mechanism. Among 0D carbon nanostructures, only graphene quantum dots (GQDs) are likely to satisfy this criterion. However, GQDs are only classified as a 0D carbon nanostructure due to its small lateral dimensions (<100 nm). While the associated quantum confinement and edge effects provide GQDs with interesting optical, electronic and photoelectric properties, their structure and associated lubrication mechanisms resemble that of its parent material graphene rather than the other 0D carbon nanostructures. For this reason, the reader is referred to Section 3.2.3 on 2D carbon nanostructures for a better understanding of the interlayer shearing performance of GQDs.

Even though the other 0D carbon nanostructures lack the flat-layered lamellar structure required for interlaminar shearing, it has been hypothesized that the concentrically-layered structure of carbon nano-onions (CNOs) might undergo structural exfoliation under the combined action of compressive and shear forces<sup>144,179</sup>. If so, the resulting graphitic wear debris could potentially stack and accumulate on the tribosurface in a way that resembles a lamellar surface film.

### **3.2.2 1D carbon nanostructures**

As in the case of most 0D carbon nanostructures, intact 1D carbon nanostructures lack the appropriate structure for interlaminar shear. However, since some studies have reported that multi-walled carbon nanotubes (MWCNTs) might be able to retain some of their layered graphene-like structure after structural collapse or due to exfoliation<sup>180-182</sup>, it has been hypothesized that the resulting third-body material might be able to reduce friction through interlaminar shear. This will be discussed in greater detail in Section 3.4.2. Either way, it is concluded that, with the exception of GQDs, neither 0D nor 1D carbon nanostructures have the appropriate structure to reduce friction through interlaminar shear in their intact state.

### 3.2.3 2D carbon nanostructures

The interlayer shearing mechanism is believed to be the main friction-reducing mechanism of graphene based lubricant additives<sup>151,152</sup>. As the building block of graphite, graphene and its derivatives possess the appropriate planar and lamellar structure characterized by the strong in-plane bonding and weak interplanar bonding required to undergo interlaminar shear. Nevertheless, the friction-reducing performance of the interlaminar shearing mechanism in graphene-based additives has been shown to be highly dependent on various structural features, including stacking, defects, and surface chemistry. This section aims to elucidate how structural, morphological, and chemical properties of 2D carbon nanostructures influence the resistance to interlaminar shear and the overall friction-reducing performance.

Firstly, it has been observed that few-layer graphene with a larger interlayer spacing exhibit significantly less friction and wear compared to few-layer graphene with smaller interlayer spacing, despite having otherwise similar dispersion state, size scale and elemental composition<sup>183</sup>. This difference in friction performance could be attributed to the reduced barrier for interlayer shear due to the weaker van der Waals forces acting between layers that are further apart. Secondly, the degree of exfoliation (i.e., the number of layers) has been shown to significantly influence the friction performance of graphene-based lubricant additives. On the one hand, several computational studies have predicted that the interlayer friction of graphene decreases with decreasing number of layers<sup>184,185</sup>. However, the opposite trend is generally observed in experimental studies due to the dominating friction contribution the interfacial contact between graphene and the tribosurface<sup>27,151</sup>. Specifically, several computational and nanoscale experimental studies have attributed the higher friction of highly exfoliated graphene (few layers) to the effect of out-of-plane deformations or puckering<sup>27,151,186</sup>, which is illustrated in Figure 3.4. The puckering effect could explain the observed increase in friction in terms of the larger interfacial contact area or the additional work required to move the puckered region forward. For thicker sheets (more layers), the puckering effect is expected to be less prominent owing to the larger bending stiffness of the sheet, and indeed, this has been supported by finite element modelling (FEM), as shown in Figure 3.4<sup>186</sup>. Then again, even though high out-of-plane flexibility may have an adverse impact on the friction performance, it has also been suggested to enhance the graphene-based additives ability to conform to the surface and yield a better protective film. Moreover, it is worth noting that the strong dependence of friction on the number of graphene layers is not observed when the graphene layer is strongly bonded to the surface<sup>27</sup>. Thus, strong adhesion to the tribosurfaces should be promoted.

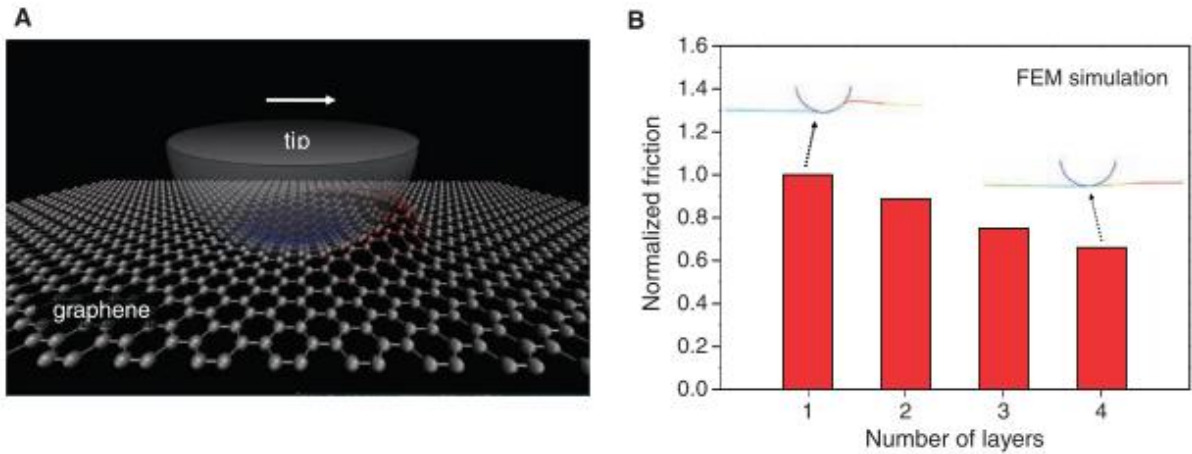


Figure 3.4: (A) An illustration showing the proposed puckering effect, where adhesion to the sliding top creates out-of-plane deformation of the graphene sheet, leading to increased contact area and friction. (B) The variation in friction as a function of sheet thickness based on finite element modelling (FEM) simulation.

The graphene stacking mode, given by the degree of relative rotation of adjacent crystalline graphene layers, also greatly affects the lubrication performance of 2D carbon nanomaterials as it forms the basis of so-called structural lubricity or *superlubricity*<sup>152,187</sup>. This phenomenon is characterized by extremely low friction and is attributed to the incommensurability of adjacent layers during intercrystallite slip. The concept of incommensurability and commensurability is perhaps most easily understood using the egg box model. Two graphene sheets are said to be in a commensurate state when their orientation and lattice constants are such that they perfectly match<sup>151</sup>. In the egg box model, this corresponds to the situation when two egg boxes are aligned and stacked so that they are embedded and stuck, as illustrated in Figure 3.5(a). In this state, the friction is relatively high. For the hexagonal lattice of graphene, this is true for every 60-degree rotation of one sheet relative to the other. However, when the sheets are rotated so that their lattices are misaligned in the incommensurate state, as shown in Figure 3.5(b), friction can become virtually non-existent during sliding. Since the friction forces between two solids in sliding motion remains finite at finite velocities, Müser have suggested an *ad hoc* definition of superlubricity as a kinetic friction coefficient of less than 0.001<sup>188</sup>.

According to Liu et al.<sup>151</sup>, the key to achieving superlubricity is to realize sustained incommensurability during sliding<sup>151</sup>. However, this is hard to achieve as the low-friction sliding regime can be disrupted by torque-induced rotations, temperature fluctuations and increased loads<sup>189</sup>. Consequently, until recently, superlubricity of 2D materials had primarily been studied and realized in a limited number of controlled and idealized nanoscale experiments supported by theoretical studies<sup>188,190–193</sup>. It has also been argued that, since superlubricity is a result of very specific nanostructural conditions, the effect is likely to be lost on macroscale due to finite sheet sizes, structural imperfections, and disorder caused by defects and deformation<sup>194</sup>. Nevertheless, in 2015, Berman et al.<sup>194</sup> showed that superlubricity could be realized at an engineering scale. Herein, the macroscopical superlubricity was attributed to graphene

patches on the interface wrapping around nanodiamonds to form nanoscrolls with reduced contact area that could achieve an incommensurate contact and substantially reduced coefficient of friction ( $\sim 0.004$ ) when sliding against a diamond-like carbon (DLC) surface under dry conditions. Since then, macroscale superlubricity have been reported in several graphene-based tribosystems<sup>195–199</sup>.

Li et al.<sup>196</sup> achieved instantaneous macroscale superlubricity of graphite against steel with a minimum friction coefficient of 0.001 for a maximal sliding distance of 131  $\mu\text{m}$ . The authors attributed this to the formation of many tribo-transferred multilayer graphene nanoflakes with different shapes, number of layers (2–100), and sizes (100 nm to 20  $\mu\text{m}$ ), on the steel contact zone after the initial sliding. However, because the presence of atomic steps and edges greatly reduces the probability of superlubricity from a statistical viewpoint, the macroscale superlubricity only appeared randomly with short durations. Recently, Ge and colleagues showed that robust macroscale superlubricity could also be realized in liquid-lubricated systems<sup>197,198</sup>. Specifically, the addition of GO nanosheets to a  $\text{LiPF}_6$ -based ionic liquid contributed to achieving a friction coefficient of 0.005 in a  $\text{Si}_3\text{N}_4$ /sapphire contact under a pressure of 600 MPa<sup>197</sup>. Similarly, a robust friction coefficient of 0.037 was achieved for a  $\text{Si}_3\text{N}_4$ / $\text{SiO}_2$  contact by adding graphene oxide nanoflakes to ethanediol<sup>198</sup>. In both cases, GO nanosheets were directly observed to adsorb onto the tribosurfaces, thereby contributing to the superlubricous behavior by transforming the shear interface from a  $\text{Si}_3\text{N}_4$ /sapphire contact or  $\text{Si}_3\text{N}_4$ / $\text{SiO}_2$  contact to a GO/GO contact with extremely low resistance to shear.

Even though macroscale friction values as low as these are still quite rare, the findings in the abovementioned studies suggest that occasional superlubricous contact between randomly oriented graphene-based nanoadditives within an adsorbed layer, transfer layer or tribofilm might be possible. Thus, it is hypothesized that, even though the observed macroscale friction does not fall within the range of superlubricity in most experimental studies, occasional and short-lived sliding in the superlubricous incommensurate state can occur with some statistical probability, which may contribute to reducing the overall average macroscale friction<sup>155,200,201</sup>.

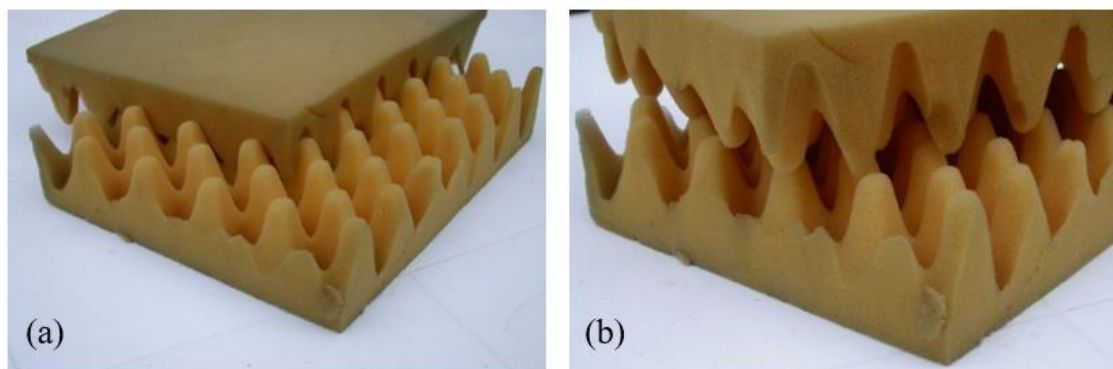


*Figure 3.5: The egg box model used to illustrate (a) the low-mobility commensurate state and (b) the high-mobility incommensurate state of graphene.*

Other factors that greatly influence the interlayer shearing potential of graphene-based nanoadditives are edge morphology, structural defects, and surface chemistry. For instance, the atoms located on edges and step edges of lamellar materials behave differently from the atoms of the basal plane both physically and chemically due to the presence of dangling bonds and functional group terminations <sup>202</sup>. The high reactivity of these edges increases the resistance to interlayer shearing, which is why larger graphene sheets are likely to experience less interlaminar friction than smaller sheets. Mao et al. <sup>144</sup> compared the lubricating performance of three types of reduced graphene oxide sheets with varying edge micromorphology and concluded that the larger perimeter of graphene types with irregular edges led to higher friction and more friction-induced wear than graphene types with more regular edges. Moreover, Zhao et al. <sup>183</sup> suggested that the larger edge regions of less exfoliated graphene stacks (more layers) could cause the highly oriented layers to adsorb perpendicularly relative to the friction surface and sliding direction due to edge instability and dangling bond action. In this case, the sliding motion would be directly impeded and the graphene more prone friction-induced damage.

On the one hand, molecular dynamics have shown the presence in-sheet wrinkles may contribute to the lowering of the interlayer shear stress by a factor of  $\sim 2$ , if other phenomena do not come into play <sup>199</sup>. However, once again, the overall friction behavior of actual tribosystems generally exhibits the opposite trend (i.e., increased friction in presence of wrinkles and similar defects). One reason for this could be the dominating contributions from tribosurface-graphene friction compared to interlayer friction. Analogous to the aforementioned effect of high in-sheet flexibility (see Figure 3.4), the presence of pre-existing wrinkles is likely to provide increased resistance to a tip or asperity as it slides across the graphene surface <sup>203</sup>. However, the main reason for the increased friction observed under lubrication with more wrinkled or defective 2D carbon nanostructures is likely attributable to the reduced mechanical properties and the associated susceptibility to wear, leading to loss of the lubricious 2D structure <sup>183,202,204</sup>. The effect of friction-induced structural evolution as a result of structural defects and morphology will be addressed in greater detail in Section 3.4.3.

Since surface chemistry can greatly influence the physical and chemical interactions between adjacent layers, chemical modification or functionalization of graphene can affect the interlaminar shear mechanism and lubrication performance. For instance, based on *ab initio* density functional theory (DFT) calculations, Wang et al. <sup>205</sup> predicted that the interlayer friction between two single-side hydrogenated graphene sheets would decrease compared to pristine graphene due to the accumulation of electrons between the carbon and the attached hydrogen atoms leading to a significant decrease in the potential interfacial energy. In contrast, *ab initio* DFT calculations predicted moderately increased interlayer friction in graphene oxide compared to pristine graphene <sup>206</sup>. On the one hand, the presence of oxygen functional groups such as epoxides and hydroxyls were found to increase the interlayer spacing, which is typically associated with reduced van der Waals forces, and reduced resistance to

interlaminar shear. However, in graphene oxide, the interlayer interactions are dominated by the electrostatic and hydrogen bond interactions that arise in addition to the  $\pi$ -orbital and van der Waals interactions<sup>206</sup>. As a result, the graphene oxide layers have to overcome a much larger energy barrier, resulting in higher energy dissipation and increased interlayer friction with increasing degree of oxidation. In contrast, Min et al.<sup>207</sup> attributed the more stable friction behavior obtained using fluorinated graphene oxide as a nanoadditive in water to the semi-ionic C-F bonds reducing the interlayer bond energy and making interlayer slippage more likely to occur, compared to graphene oxide.

In addition to altering the interlayer interactions, oxidation or other chemical modification of graphene is accompanied by wrinkling and local  $sp^2$ -to- $sp^3$  rehybridization of the carbon layers<sup>206</sup>. The latter not only reduces the mechanical strength and structural durability as discussed above<sup>201</sup>, but is also associated with increased out-of-plane flexibility<sup>208</sup>. Ko et al.<sup>208</sup> used friction force microscopy to show that hydrogenated, fluorinated, and oxidized graphene exhibit nanoscale friction that is 2, 6, and 7 times higher than that of pristine graphene, respectively. This increase in friction was primarily attributed to increased out-of-plane elastic characteristics after chemical modification, illustrating how dramatically  $sp^3$  hybridization can influence flexibility, mechanical properties, and friction performance. However, even though chemical modification of 2D carbon nanoadditives may have adverse effects on the interlaminar shear mechanism and mechanical properties in some cases, it is worth to keep in mind that it may still improve the overall lubrication performance by providing other beneficial effects such as enhanced dispersibility and adsorptivity. Thus, one must take into account several considerations when evaluating the potential effect of surface chemistry on the lubrication performance of functionalized graphene-based nanoadditives.

### 3.3 THE BALL- AND ROLLER BEARING MECHANISMS

In simple terms, the *ball bearing* mechanism is based on the idea of spherical or semi-spherical nanoparticles being able to act as nanoscale bearing balls that reduce friction and the associated wear by translating sliding friction into a combination of sliding and rolling friction. The proposed *roller bearing* mechanism is the corresponding action of a cylindrical or tubular structure and can be envisioned by considering transport of heavy objects using rolling tree trunks. On the macroscale, it is well established that the coefficient of friction realized under rolling friction is generally 100 to 1000 times lower than that of sliding friction for corresponding materials<sup>209</sup>. However, as will be discussed below, this macroscale behavior might not translate to the nanoscale.

### 3.3.1 0D Carbon Nanostructures

Owing to their spherical shape, the ball bearing effect has been credited for the observed friction-reduction in numerous experimental studies where CQDs<sup>77–79,156,165,210–212</sup>, NDs<sup>97,98,100,159,213,214</sup>, fullerenes<sup>18,36,37,215,216</sup>, and CNOs<sup>46,52–54,56</sup> have been used as lubricant additives. A prerequisite for this lubrication mechanism is thought to be stable and sufficiently low loading conditions so as to not impede the rolling motion or interfere with the structural integrity of the nanoparticle. Consequently, the mechanical properties and structural morphology of the nanostructure are likely to be important variables that influence to which extent a certain carbon nanostructure can reduce friction through the ball bearing mechanism. However, despite seemingly supportive experimental results, the ball bearing mechanism remains a topic of great debate with two fundamental questions at its core. Firstly, is rolling motion of nanoparticles even possible? And, secondly, if rolling motion of 0D carbon nanomaterials in the contact is plausible, to which extent does it reduce friction? That is, how does nanoparticle motion influence the observed friction and wear characteristics of a given tribosystem at the macroscale?

Answering these questions is made challenging by the lack of means and experimental techniques by which the nanotribological behavior between contacting surfaces can be probed *in situ* during conventional tribological testing using a tribometer. Since tribological experiments are usually limited to surface characterization before and after testing, the evolution of mechanical and chemical processes on surfaces during the experiment remains elusive. Thus, it can be argued that the theory of spherical nanoparticles being able to roll between surfaces under boundary lubrication is mostly speculative with little theoretical support or direct evidence. In recent years, researchers have taken advantage of advances in experimental and computational technologies in an effort to bridge this gap in our understanding. To date, this has mainly been done through two main approaches: molecular dynamics (MD) simulations<sup>217–219</sup> or the use of *in situ* imaging techniques, such as SEM or TEM, in combination with a nanomanipulator like AFM or SPM<sup>217,220–223</sup>. While it could be argued that these methods portray an idealized and simplified system, they are useful tools for ascertaining theoretical plausibility of nanotribological behavior.

For a long time it was believed that carbon nano-onions (CNOs) behave similarly to other nested fullerene-like structures, known as inorganic fullerenes (IFs)<sup>53</sup>. These IF supramolecules are typically comprised of concentric layered metal dichalcogenides,  $\text{MX}_2$  ( $\text{M} = \text{W}, \text{Mo}, \text{Ti}, \text{Nb}, \text{Hf}$ ;  $\text{X} = \text{S}, \text{Se}$ ), or other layered inorganic compounds. Their tribological behavior has been studied extensively<sup>220,221,224–227</sup>. Even though rolling motion of these structures has been realized and experimentally observed under low-loading conditions using electron microscopy and nanomechanical manipulators<sup>220,222</sup>, they generally tend to deform or collapse under larger mechanical loads and shear forces<sup>217,228</sup>. This causes individual nanosheets to exfoliate and dislodge from the nanoparticle surface. These exfoliated sheets are gradually transferred onto the mated surfaces to form a low-shear strength transfer film acting as a third-body that reduces friction and wear through a mechanism similar to that of

graphene sheets (see Section 3.4.3)<sup>220</sup>. The tendency of IFs to exfoliate readily under uniaxial pressure, even in the absence of shear stresses<sup>220,229</sup>, can be attributed to the high concentration of defects, dislocations and grain boundaries required to relieve inherent structural strains due to surface curvature<sup>230</sup>. IFs can be described as multiple flat nanosheets conjoined the edges by defects, resulting in a faceted or polygonal structure that easily exfoliates or collapses under low to moderate uniaxial loads, despite being able to withstand high hydrostatic pressures<sup>53</sup>. Hence, while rolling and sliding may contribute to the overall lubrication performance, the general consensus is that exfoliation and the associated third-body material transfer film is the primary lubrication mechanism of inorganic fullerenes<sup>11,217,220,229</sup>.

The obvious structural similarities between IFs and CNOs have led many researchers to assume analogous tribological behavior (i.e. that exfoliation and material transfer is the predominant lubrication mechanism for CNOs as well)<sup>53,144</sup>. However, the absence of graphitic exfoliation layers and occurrence of intact CNO *post* tribological testing under boundary lubrication conditions might suggest otherwise<sup>53,54</sup>. Joly-Pottuz et al.<sup>53</sup> used MD simulations and a combination of experiments across length scales (nano-, meso- and macroscale) to study the tribological properties of CNOs. Based on the collective results, they proposed that CNOs can indeed be considered genuine nanoscale ball bearings that achieve low friction by rolling and sliding individually on the tribological interface without exfoliation and structural collapse. They attributed this difference between IFs and CNOs to the latter being more resistant to compression due to the presence of pentagons in the curved structure, which permits smaller radius of curvature without residual stress. As a result, CNOs are not as faceted as IFs and do not suffer from structural weakness caused by defects concentrated at edges to the same extent.

This proposal was later supported by Bucholz et al.<sup>179</sup> who used MD simulations to investigate the proposed rolling/sliding mechanism of CNOs subjected to friction between sliding amorphous hydrogen-terminated diamond-like carbon (DLC) surfaces in an ultra-high vacuum environment. They found that, unlike IFs that have been experimentally demonstrated to exfoliate at contact pressures in the range 1-2.5 GPa even in the absence of frictional forces<sup>220</sup>, the MD simulations showed no indication of graphitic exfoliation during uniaxial compression of CNOs up to contact pressures of ~40 GPa<sup>179</sup>. Instead, the MD simulation demonstrated that CNOs can indeed reduce friction through a rolling/sliding mechanism in which the relative proportion of rolling and sliding behavior is governed by the formation of strong interfacial bonds between individual CNOs and the DLC surfaces. The number of interfacial bonds formed was found to increase with increasing contact pressure and the bond formation process of an individual CNO at high contact pressure (5 GPa) was elucidated as follows: (1) Initially, the surface adhesion was expected to be negligible relative to the applied lateral and normal forces due to the small apparent contact area of the CNO. Thus, before the onset of bond formation, weak van der Waals forces provided the CNO with sufficient angular momentum to roll whilst still being weak enough to not impede the rolling motion. (2) As the CNO became bonded to one or both of the DLC surfaces due to high contact pressure, the CNO was no longer able to roll and transitioned into

sliding behavior with a noticeably larger friction force. (3) As more interfacial bonds formed, the CNO was no longer able to slide across the surface, and further sliding of the DLC surfaces relative to one another was accompanied by a certain periodicity of the already quite large friction force due to continuous formation, stretching and breaking of interfacial bonds <sup>179</sup>.

In addition to contact pressure, the bond formation process was found to be influenced by the chemical nature of the CNO. As mentioned in Section 2.1.2, CNOs can be synthesized by annealing of nanodiamond precursors. Depending on the annealing procedure, CNOs with or without a residual nanodiamond core inside the concentric graphitic shells can be obtained <sup>52</sup>. In the MD simulations by Bucholz et al. <sup>179</sup>, CNOs without a diamond core exhibited a transition from rolling to sliding behavior due to interfacial bond formation at contact pressures beyond ~2.5 GPa. In contrast, the CNOs with residual diamond cores were found to predominantly slide under all the contact pressures investigated, due to prolific bond formation across the contact pressure range. This difference was attributed to dangling bonds at the periphery of the diamond core inducing localized strain to the fullerene shell in the surrounding region during compression, making neighboring atoms more prone to form interfacial bonds as a means of strain reduction.

According to Bucholz et al. <sup>179</sup>, rolling versus sliding behavior at the interface corresponded to the friction coefficients differing by an order of magnitude in their modelled systems <sup>179</sup>. This is unlike Joly-Pottuz et al. <sup>52</sup> who found experimentally that CNOs with and without residual diamond cores have comparable friction-reducing capabilities. However, this discrepancy could be attributed to a few key considerations. Firstly, in the MD simulations by Bucholz et al., there was only one C<sub>540</sub> shell covering the 275-atoms residual diamond core, thus, the dangling bonds on the nanodiamond surface were quite poorly shielded from the surrounding environment and readily available to induce CNO interaction with the tribosurfaces. In contrast, the CNOs used in the experiment by Joly-Pottuz et al. were comprised of significantly more concentric layers that shield the chemically reactive nanodiamond surface. A second key difference is that the experimental study was performed using CNOs as additives (0.1 wt%) in a liquid medium (PAO) <sup>52</sup>, whereas the simulation was done in a perfect ultra-high vacuum <sup>179</sup>. Lastly, it is worth noting that the experimental study and the simulation used different materials for the mated surfaces. Joly-Pottuz et al. <sup>52</sup> used AISI 52100 steel, while Bucholz et al. <sup>179</sup> modelled amorphous hydrogen-terminated DLC.

Unsurprisingly, the tribological behavior of CNOs seems to be closely related to that of its parent material fullerene. That is, fullerenes are believed to reduce friction through a rolling mechanism that may transition into sliding behavior depending on the tribological conditions <sup>18,36,37,215</sup>. Li et al. <sup>216</sup> used reactive molecular dynamics (RMD) simulations to investigate the friction behavior of a mated amorphous carbon (a-C) contact lubricated by a linear alpha olefin with C<sub>60</sub> fullerene as an additive under a contact pressure of 5 GPa. The addition of C<sub>60</sub> to the base oil was found to reduce the friction coefficient from 0.21 to 0.05. Initially, the fullerene additive was found to act as a miniature ball bearing

that lubricated the tribosurfaces through rolling or caterpillar motion, but, eventually, the C<sub>60</sub> molecules underwent partial structural collapse due to chemical bonding with both the a-C surfaces. The fullerene essentially served as a bridge to cross-link the mated surfaces, which was accompanied by an increase in friction.

Several factors, other than different simulation environments, could explain why C<sub>60</sub> underwent structural collapse whilst CNOs remained mostly intact. Firstly, the C<sub>60</sub> is much smaller and therefore has a much smaller radius of curvature than the outer C<sub>540</sub> layer of the CNO modelled by others<sup>53,179</sup>. Since the chemical reactivity of fullerene structures arise mainly from the strain imposed on C=C bonds by surface curvature<sup>28</sup>, C<sub>60</sub> is likely to be more chemically reactive and thus more prone to form interfacial bonds with the surface as a means of strain relief than the larger C<sub>540</sub> shell. Moreover, the tribosurfaces in the simulation by Li et al. were highly reactive non-passivated a-C surfaces which promote the formation of interfacial bonds<sup>216</sup>, whereas Bucholz et al.<sup>179</sup> and Joly-Pottuz et al.<sup>52</sup> used passivated DLC and steel, respectively. Hence, reduced intermolecular and chemical interaction associated with a passivated tribosurface is likely to result in improved lubrication performance in the case of 0D carbon nanostructures.

The ball-bearing abilities of nanodiamonds (NDs) was first proposed by Tao et al.<sup>97</sup> in 1996, and have since been suggested as a contributing friction-reducing mechanism by numerous experimental studies where NDs were employed as lubricant additives<sup>98,100,159,213,214</sup>. Hu et al.<sup>218</sup> used MD simulations to study the tribological behavior of NDs confined between two iron blocks. At low sliding velocity (10 m/s) and low normal load (500 MPa), the NDs were found to effectively separate the rubbing surfaces. More importantly, through analysis of nanoparticle displacement and angular velocity, the authors claimed to have found direct evidence for the ability of spherical nanoparticles to roll between rubbing surfaces<sup>218</sup>. Owing to their high hardness, the shape and rolling action of the NDs remained unaffected by increased loading (1 GPa), unlike hard SiO<sub>2</sub> nanoparticles which were crushed under the high pressure. The deformation-induced loss of rolling effect in the case of SiO<sub>2</sub> nanoparticles highlights the importance of hardness and structural integrity on the ball bearing potential of nanoparticles. Similarly, Kang and Hwang<sup>219</sup> concluded that C<sub>60</sub> fullerene with an internal potassium atom have better ball bearing capabilities than those without due to increased compressive strength and structural integrity. The nanoparticles have to be hard enough to withstand plastic deformation under the high uniaxial pressures and shear experienced under boundary lubrication conditions. However, extreme hardness of NDs may also have adverse effects. More specifically, hard nanoparticles have been shown to enhance wear or become embedded in the comparatively soft tribosurfaces<sup>54,97,98,159,213,214,218</sup>. This suggests that the relative hardness of the nanoparticle and the surface may have a significant influence on the wear behavior<sup>171</sup>.

Using non-equilibrium MD simulations, Ewen et al.<sup>171</sup> probed the friction and wear behavior of both NDs and CNOs between  $\alpha$ -iron slabs over a range of coverages, pressures and sliding velocities. At high nanoparticle coverage and low pressure, the nanoparticles did not indent into the tribosurfaces, resulting in almost zero wear and a low friction coefficient arising purely from van der Waals interactions between the nanoparticles and the iron slabs. On the other hand, at low nanoparticle coverage and high pressure, the nanoparticles indented and ploughed through the tribosurfaces during sliding, leading to atomic-scale wear and a much higher friction coefficient. After the onset of nanoparticle indentation, both the indentation depth and the friction coefficient were found to increase linearly with increasing pressure. However, even at the highest pressures and lowest coverages simulated, both types of nanoparticles were still able to maintain separation of the mated iron surfaces and reduce friction by approximately 75% compared to when no nanoparticles were present<sup>171</sup>. Yet, CNOs were shown to indent the iron surfaces to a lesser extent than NDs at the same coverage and pressure because of their comparatively softer layered structure. The 25% smaller indentation depth of CNOs was accompanied by a corresponding reduction of both wear depth and coefficient of friction in these simulations<sup>171</sup>. In other words, the harder diamond nanoparticles caused more wear and higher friction under the same conditions due to deeper indentation into the tribosurfaces. This agrees well with experimental results by Joly-Pottuz et al.<sup>52</sup> who found that the increased hardness of CNOs with a residual diamond core enhanced detrimental abrasive wear compared to CNOs without a diamond core.

Even though rolling of nanoparticles could be observed in the simulations by Ewen et al.<sup>171</sup>, it did not seem critical in reducing the friction coefficient. Contrary to macroscale behavior, simulations where rolling motion was more predominant did not yield lower friction and no detectable difference in friction in periods of sliding and rolling was found. Moreover, these findings contradict the previously discussed simulation results in which the friction obtained during rolling and sliding differed by one order of magnitude, and it was stated that the tribological performance of spherical CNOs is determined primarily by the relative occurrence of rolling compared to sliding<sup>53,179</sup>. Instead, Ewen et al. suggested that these observed differences in friction during rolling (low loads) and sliding (high loads) originated from an increase in adhesive forces, due to interfacial bonding, rather than the changes in the motion of the nanoparticles<sup>171</sup>.

Others have also questioned the contribution and relevance of nanoparticle rolling motion in obtaining low friction. Liang et al.<sup>223</sup> used atomic force microscopy (AFM) to study C<sub>60</sub> with different degrees of rotational motion. In defiance of the macroscale analogy, the friction was found to be higher for the more freely rotating layers and the change in frictional force was quantitatively consistent with an observed change in adhesion. This led to the conclusion that the rotational degree of freedom on C<sub>60</sub> molecules does not significantly participate in the energy dissipation of the friction process. Later, Coffey and Krim<sup>231</sup> used a quartz crystal microbalance, which probes shorter time scales than AFM, to

measure friction levels for molecularly thin methanol films sliding along C<sub>60</sub> substrates in rapid and repressed rotational states. They also reported increased friction in the case of rapid rotation compared to repressed rotation.

To further investigate the influence of nanoparticle motion on friction, Zhao and Duan<sup>232</sup> ran a simulation in which the effect of interfacial bond formation and nanoparticle indentation was minimized. Their simulated system involved sliding a hard and inert DLC surface over nanodiamonds supported by an amorphous silica (a-SiO<sub>2</sub>) slab. Since they achieved a much lower maximum friction for diamond nanoparticles than the abovementioned experimental and simulated results<sup>53,171,179,218</sup>, it was concluded that, for the lubrication of nanoparticles, the increase of indentation depth and formation of interfacial bonds can significantly increase the friction force. Under low loads (<50 nN), the NDs were found to roll stably along the DLC sliding direction, whereas, under high loads (≥ 50 nN), the NDs became trapped in the soft a-SiO<sub>2</sub> substrate where it continuously rolled back and forth in an oscillating motion. When comparing the rotational and translational motion of the NDs, the peaks and valleys of the friction force curve coincide with those of the motion curves. However, under low loads, this correlation between nanoparticle motion and friction force was not evident. The authors argued that even though there is no consistent correlation in one single direction, this does not mean the nanoparticle motion has no effect on the friction force. Instead, based on results showing that NDs rotate about all three axes during rolling under low loads, they suggested that nanoparticle motion in multiple directions may explain the observed friction behavior. In order to verify whether repressed nanoparticle motion can enhance friction-reducing effects as proposed by Coffey and Krim<sup>231</sup>, they artificially fixed the center for the nanoparticles to prevent them from moving. Under equal load, the average friction force for the fixed nanoparticles was indeed much lower than that for the free nanoparticles. Zhao and Duan<sup>232</sup> attributed this phenomenon to rolling motion providing an additional energy dissipation channel for frictional heating. Hence, contrary to the rolling motion of ball bearings on the macroscale, the repressed motion of nanoparticles reduces the system's friction dissipation, suggesting that the rolling force is larger than the sliding force at the nanoscale<sup>232</sup>.

In summary, it has been shown that rolling motion of spherical and semi-spherical 0D carbon nanoparticles under boundary lubrication is plausible under the appropriate conditions. Specifically, the load must be sufficiently low so as to not impede rolling motion or compromise the structural integrity of the nanoparticle. Furthermore, the nanoparticle itself should be chemically inert, have high compressive strength and a high resistance towards shear stresses. High hardness is beneficial in order to minimize the interfacial contact area with the tribosurfaces during compression. However, such high hardness is generally at the expense of elasticity which may allow the nanoparticles to accommodate increased local compressive forces without indenting or embedding into the tribosurfaces. The tribosurfaces themselves should in turn be smooth, inert, and hard in order to prevent pinning, interfacial bonding, and nanoparticle indentation, respectively. It has also been shown that high nanoparticle

coverage is favorable in order to distribute load and reduce contact pressures<sup>171,233</sup>. This suggests that effective dispersion methods are critical to the performance of these additives so that they may enter the contact at the requisite coverage.

However, even though rolling motion of 0D carbon nanoparticles can be realized between sliding surfaces, it remains unresolved whether rolling resistance reduces energy losses relative to sliding friction. Instead, some have suggested that the low friction observed in experimental studies where 0D carbon nanostructures have been used as lubricant additives is the collective result of other lubrication mechanisms and surface separation, rather than the ball bearing mechanism. All in all, more research is needed to investigate and confirm the role of the ball bearing mechanism in the tribological performance of 0D carbon nanostructures. MD simulations are useful for building fundamental understanding of tribological phenomena at the atomic scale and is therefore likely to play an increasingly important role in this effort. Yet, to date, most MD simulations have been used to study nanoparticles confined between solid surfaces in absence of a liquid lubricant – despite being intended as additives<sup>234</sup>. This is because the simulation of dispersed nanoparticles in a liquid lubricant confined between solid surfaces remains a complex problem for MD simulations. Another limitation of classical MD simulation is the inability to accurately model chemical reactivity. Even though solid nanoadditives are believed to enhance lubrication performance primarily through mechanical action, it would be interesting to study the influence of chemical interaction and reactivity. Hopefully, future advances in the field on MD simulations will enable more accurate representation of dispersed nanoadditives under boundary lubrication conditions between realistic rough surfaces.

Lastly, the attentive reader may notice that the 0D carbon nanostructures graphene quantum dots (GQDs) and carbon quantum dots (CQDs) have not been mentioned in this section. While GQDs are classified as a 0D nanostructure due to its nanoscale lateral dimensions, they are still sheet-like in shape, rather than round. Thus, any significant rolling motion is deemed unlikely. As for CQDs, even though several recent experimental studies have claimed friction-reduction by CQDs through ball bearing action<sup>77–79,156,165,210–212</sup>, no direct evidence has yet been presented. That is not to say that CQDs are not capable ball bearing behavior, but rather that these suggestions are still based on indices and assumptions of analogous behavior among 0D nanoparticles. To the best of the author's knowledge, there is still no theoretical support (e.g., MD simulations) or nanoscale experimental studies (i.e., tracking of individual nanoparticles under nanomanipulation) available on the nanoparticle motion of CQDs during tribological operation.

### **3.3.2 1D Carbon Nanostructures**

Owing to the tubular structure of 1D carbon nanostructures, numerous experimental studies where carbon nanotubes (CNTs) were used as lubricant additives have attributed the observed friction reduction to the roller bearing mechanism<sup>117,118,121,182,235,236</sup>. However, once again, verifying this

hypothesis is made challenging by the lack of experimental methods by which to probe the behavior of individual nanoparticles *in situ* during lubrication. Thus, researchers have utilized theoretical approaches and nanoscale experiments in the search of theoretical evidence in support of this mechanism<sup>237–243</sup>.

Several experimental studies used AFM tips to laterally manipulate CNTs on different surfaces and concluded that CNTs display preferential sliding<sup>242,243</sup>. In fact, rolling motion could only be observed when the crystal lattice of the CNT was in commensurate contact that of the underlying surface and the AFM tip pushed on the CNTs in a very particular way. This was achieved on atomically smooth highly oriented pyrolytic graphite (HOPG) substrates, where structural symmetry and long-range order of both the CNT and the graphite surface allowed the two hexagonal crystal lattices to maintain commensurate contact throughout the rolling period. Once commensurability was lost, nanotube motion transitioned back to sliding. These findings agree with several computational studies which also concluded that commensurate contact is a prerequisite for rolling motion of CNTs<sup>238,239</sup>. In other words, extremely specific and highly controlled conditions are required for CNT rolling, and these conditions are unlikely to be met during liquid lubrication of rough engineering materials in macroscale systems.

Furthermore, it remains uncertain whether rolling motion would exhibit lower friction compared to sliding motion on the nanoscale at all. Simulations by Schall and Brenner<sup>238</sup> suggested that the relative friction coefficient for the incommensurate sliding behavior is approximately 80% of that of the commensurate orientations in which periodic sliding and rolling was observed<sup>238</sup>. This is qualitatively consistent with experimentally observed phenomena<sup>242,243</sup>. Thus, based on available literature, it is deemed highly unlikely that rolling of individual CNT additives could have contributed to the observed friction-reduction of CNT-enriched lubricants to any significant extent, even if rolling motion was realized. That is not to say that some rotational motion of individual CNTs within bundles or between sliding surfaces cannot occur during lubrication<sup>237</sup>, but rather that this does not account for the reduced friction reported in literature when CNTs are used as lubricant additives.

In Section 3.3.1, it was concluded that 0D carbon nanostructures can reduce friction regardless of nanoparticle motion due to their high mechanical strength which allows them to act as physical separators between the tribosurfaces and reduce the real interfacial contact area<sup>233</sup>. In the case of 1D carbon nanostructures, however, it is questionable whether CNTs would be able to bear enough load to effectively separate the sliding surfaces in their intact state during boundary lubrication and under higher compressive loads. Due to their very low Young's modulus perpendicular to the tubular axis<sup>240,244</sup>, carbon nanotubes are unlikely to retain their spherical cross-section under compression and are therefore prone to structural collapse during lubrication<sup>117,120,121,216,245</sup>. Ni and Sinnott<sup>240</sup> simulated the behavior of horizontally aligned bundles of nanotubes between two hydrogen-terminated diamond surfaces when subjected to compressive and shear forces. Under low compression, the nanotubes first slid in the direction opposite to the sliding motion, but as the load increased the nanotubes were flattened

until eventually cross-linking with each other or even merging. Li et al.<sup>216</sup> used reactive MD simulations to study the frictional behavior of CNTs in a linear alpha olefin oil (C<sub>8</sub>H<sub>16</sub>) and found that the CNTs could not exist stably on the unpassivated amorphous carbon surface. Instead, strong chemical interaction and bonding with both of the surfaces resulted in structural collapse of the nanotube structure and significantly increased friction. The severe plastic deformation described in these works would explain the formation of the flake-like wear debris of amorphous carbon that is often found on the rubbing surfaces after tribological testing with CNT additives<sup>120</sup>.

MD simulations suggest that nanotubes comprised of more concentric layers (i.e., multi-walled carbon nanotubes) should be able to sustain higher compressive loads owing to their increased hardness and rigidity perpendicular to the nanotube axis<sup>237,241</sup>. This is corroborated by experimental observations<sup>120</sup>. Shorter nanotubes are also predicted to perform better under the combined action of compressive and shear forces as they are more mobile and have more degrees of freedom to rotate and slip over each other<sup>237</sup>. Optimizing these parameters should theoretically make CNTs more resistant towards structural collapse during lubrication and increase their load carrying ability. However, the extent to which this improves the lubrication performance of real tribosystems remains uncertain.

In light of the above discussion, it is concluded that CNT lubricant additives are unlikely to act as nanoscale roller bearings for several reasons. Firstly, ensuring the presence of individual cylindrical CNTs in the contact area is made challenging by their long length and tendency to form large agglomerates, as established in Section 2.2.1. Secondly, MD simulations and highly controlled nanoscale experiments have shown that sustained rolling of CNTs is only achieved under very specific and idealized conditions that are not likely to be met under liquid lubrication of real tribosurfaces with more complex surface chemistries and roughness. And, thirdly, it even remains questionable whether CNTs additives would be able to collectively withstand the compressive and shear forces required to effectively bear the load and keep tribosurfaces apart under boundary lubrication without deforming or collapsing. All this to say, without the ability to roll and without the mechanical strength to bear the load, not much is left of the roller bearing mechanism. Hence, there must be other lubrication mechanisms at play. The potential influence of the CNT wear debris on tribological performance will be discussed in Section 3.4.2.

### **3.3.3 2D Carbon Nanostructures**

Just like a prerequisite for interlaminar shear was a planar lamellar structure, a prerequisite for the ball bearing or roller-bearing mechanism is a quasi-spherical or cylindrical shape. The flat 2D carbon nanostructures do not satisfy this criterion and are therefore unlikely to reduce friction and wear through the ball- or roller bearing mechanism.

### 3.4 PROTECTIVE FILM FORMATION

The main way by which carbon nanostructures prevent wear of the surfaces in sliding contact is through formation of protective surface films. These films prevent wear by acting as physical barriers that limit direct contact between the sliding surfaces. In other words, metal-on-metal contacts are replaced by metal-on-additive or additive-on-additive contacts, which is associated with several benefits:

- The surface asperities are protected from microwelding and subsequent adhesive wear.
- The interposed nanostructures bear the loads rather than the surface asperities.
- The surfaces are protected from abrasive interactions with the asperities of its countersurface.
- The load- and shear-induced elastic and plastic deformation of the interfacial contact area now occurs in the protective film layers, rather than the tribosurfaces themselves, which also reduces contact fatigue.

The extent to which protective surface films can improve tribological performance is highly dependent on the quality of the film. In this respect, factors such as surface coverage, structural morphology, mechanical properties, and strength of bonding with the underlying substrate are of utmost importance. The protective surface films formed by solid nanoadditives are generally classified as adsorption films, third-body material transfer films or tribofilms. A brief introduction to each of these categories, with emphasis on their formation mechanisms, is presented below before going into greater detail about the film forming capabilities of 0D, 1D and 2D carbon nanostructures in Section 3.4.1, 3.4.2, and 3.4.3, respectively.

#### Adsorption Film

Adsorption is a surface phenomenon in which particles or molecules spontaneously adhere to solid surfaces as a consequence of surface energy. The exact nature of the bonding is highly dependent on the chemical species involved, but adsorption is generally classified as either physical adsorption (*physisorption*), chemical adsorption (*chemisorption*), or the result of electrostatic attraction.

In lubrication, physisorption occurs when particles or molecules from the lubricant are held to the tribosurfaces by attractive Van der Waals forces originating from intermolecular interactions between induced or permanent electric dipoles<sup>246</sup>. For example, the organic friction modifiers (OFMs) described in Chapter 1 can physisorb to the tribosurfaces as a result of their polar functional head groups. Although relatively long-range, these dipole-dipole interactions are quite weak. Thus, physisorption is characterized by minimal perturbation of the electronic structure and reversibility of the bonding<sup>247</sup>. In contrast, chemisorption involves sharing or exchange of electrons (i.e. chemical bonding of covalent or ionic nature) between the surface and the adsorbate, and is accompanied by changes in the electronic structure of the bonding atoms or molecules<sup>247</sup>. Consequently, the bonding strength of chemisorption is higher, and the chemical nature of the species involved may be altered by the process in a way that is not necessarily reversible upon desorption. A well-known example of chemisorption in the boundary

lubrication regime, is the reaction of stearic acid with the surface iron oxide on the tribosurface of carbon steel in the presence of water, which results in a surface film of iron stearate <sup>246</sup>. However, the existence of intermediate cases, such as strong hydrogen bonding and weak charge transfer, means that there is no sharp distinction between physisorption and chemisorption <sup>247</sup>. Yet, it is conventionally accepted that the energetic threshold separating the binding energy of physisorption from that of chemisorption is about 0.5 eV (48 kJ/mol) per adsorbed specie <sup>248</sup>.

The ability of various carbon nanostructures to adsorb onto the moving surfaces during lubrication is highly system specific as the adsorption potential is dependent on numerous factors, including the surface energy and surface chemistry (i.e. the reactivity of surface functional groups) of both the tribosurfaces and the nanoparticles themselves, as well as the chemical nature of the lubricant and its numerous components. It is essentially a question of whether it is more energetically favorable for the tribosystem to have the nanoparticle adhere to the tribosurfaces or remain in the lubricant phase. Structural features that promote adsorption onto certain metal surfaces include surface functional groups with electronegative heteroatoms (such as oxygen, sulfur, nitrogen or phosphorous), aromatic rings and  $\pi$ -bonds that can adsorb onto the metal surface via the formation of coordinate covalent bonds or through electrostatic interaction with the metal surface <sup>249</sup>.

It has also been hypothesized that adsorption of carbon-based nanoadditives could be facilitated by so-called exo-electron emission (EEE) <sup>153,211,250,251</sup>. This is a process in which low-energy electrons are allegedly emitted from convex points on the metal surface as a result of rubbing action, resulting in positively charged surface asperities that can attract nanoadditives through electrostatic interactions <sup>252,253</sup>. The theory has a long history reaching back to the 1950's <sup>254</sup>, however, research interest has dissipated in later decades due to the shortcomings of experimental techniques by which to study and verify the theory. Hopefully, future advancements in experimental techniques will help shed light on the validity and mechanisms of EEE as well as its potential influence on tribological processes.

In the adsorption process, an equilibrium is established between the species present on the surface and those remaining in the bulk of the lubricant <sup>246</sup>. This equilibrium governs the surface coverage, uniformity, and thickness of the adsorbed layer under static conditions, and is highly dependent on parameters such as additive concentration, pressure, and temperature. For example, increased temperature can cause adsorbed molecules or particles to disorientate, desorb or melt. Because physisorption is weaker than chemisorption, a surface film of physisorbed molecules will desorb at a much lower temperature than a chemisorbed film. Moreover, due to the dynamic nature of lubricated contacts, factors such fluid shear and interfacial contact may cause mechanical removal of the adsorbed species. For this reason, the lubrication performance of friction reducing additives is not only dependent on the adsorption strength, surface coverage and thickness of the adsorbed layer, but also on its mechanical properties (e.g., its durability, rigidity, and viscoelastic behavior) and adsorption kinetics. Characterizing the adsorption kinetics of friction modifying lubricant additives is particularly important

as it governs how fast the adsorbed layer can be replenished in case of removal, which in turn dictates the frictional response of the tribosystem.

### **Tribofilm**

Tribofilms are strongly bound solid thin films that are formed *in situ* on contacting surfaces in relative motion<sup>255</sup>. Although tribofilms are adhered to their parent worn surfaces, their chemical composition, structure and tribological properties differ from that of the underlying material, which can significantly alter the friction and wear behavior of the tribosystem. Since tribofilm formation essentially involves the generation of a brand-new solid material at the interface between the sliding surfaces, the term *tribofilm* does not pertain to sliding-induced plastic deformation layers without changes in the crystalline structure and/or chemical composition; weakly bonded surface layers (gaseous, liquid, or solid) that arise due to adsorption or ionic interaction; or discontinuous films of solid particles at the interface<sup>255</sup>.

Despite being a research subject of much interest, tribofilm formation is still not well understood as it is the result of complex interplay between physical and chemical interactions and mechanical agitation. Generally, tribofilms can be classified as either mechanically mixed or tribochemically generated. Mechanically mixed tribofilms are composite material films formed by mechanical mixing of wear particles from the sliding surfaces. Biswas<sup>256</sup> outlined a process in which cracks are nucleated in the deformed subsurface during sliding, giving rise to detached wear particles that are subsequently comminuted at the interface. The resulting particles have high surface energies due to their high surface area-to-volume ratio and lack of oxide layers on their freshly fractured surfaces. For this reason, even dissimilar materials, that would not otherwise be particularly compatible, are likely to adhere quite strongly to each other, thereby forming a new composite material. When such composite particles adhere to one of the sliding surfaces, a mechanically mixed tribofilm can be formed. Unlike tribochemically generated films, the mechanically mixed particles making up a composite tribofilm are recognized to have the same physical structure and chemical composition as its parent materials<sup>256</sup>.

In contrast, tribochemically generated tribofilms contain chemical reaction products formed over the course of tribological operation in the boundary lubrication regime<sup>256</sup>. The term *tribochemical reaction* generally includes both chemical reactions that occur only under rubbing conditions (so-called *mechanochemical reactions*), and reactions that would otherwise occur independently under the specific environmental conditions, such as temperature and pressure, in the contact<sup>9</sup>. The latter category includes phenomena such as oxidation, thermal degradation, catalysis, and polymerization. However, it is worth noting that the two sets of tribochemical reactions are intimately intertwined, and that the lack of suitable *in situ* characterization techniques makes it difficult to distinguish whether a tribochemical reaction film is the direct result of mechanical action or just the environmental

implication of the said action <sup>9</sup>. Thus, the term *tribochemical* will hereafter be used to denote both mechanochemical and environmentally activated chemical reactions.

According to Luo <sup>255</sup>, tribofilms may also be classified into the following four types, based on the origin of the chemical elements and compounds constituting the tribofilm:

1. Tribofilms generated through the wear of major constituents of the sliding surfaces.

For example, Luo <sup>257</sup> reported on the formation of a strong nanocrystalline or amorphous multicomponent oxide tribofilm formed on a magnetron sputtered multilayer TiAlN/VN coating under unlubricated sliding by wear particles from the parent sliding surfaces becoming comminuted, self-agglomerated, adhered to the parent worn surface, and oxidized. In this case, the tribofilm resulted in increased friction.

2. Tribofilms generated by preferential wear of the soft or lubricious constituents in a multi-phase or composite material.

Preferential wear or smearing of soft component in alloys can result in a tribofilm that breaks adhesive joints between surface asperities, resulting in reduced friction. For instance, preferential wear of the relatively soft graphite flakes in multi-phase grey cast iron can result in a carbon-based tribofilm on the worn surface that breaks adhesive joints between the ferrous asperities, thereby reducing friction <sup>255</sup>. Alternatively, the soft inclusions of sulfur, phosphorous or lead in special grade cutting steel can be worn during cutting and be transferred onto the tool surface where it acts as a lubricious tribofilm that can facilitate high machining speeds <sup>255</sup>.

3. Tribofilms that are different from the parent material in chemical composition and/or crystalline structure due to the sliding contact causing either chemical reactions or phase transformations.

For example, diamond-like carbon (DLC) surfaces have been found to undergo sliding-induced graphitization, which can result in a low shear strength carbon tribofilm with  $sp^2$ -type chemical bonding <sup>255</sup>. Another example is the hardened  $\epsilon$ -martensite layer that can be found on worn surfaces of high-carbon and high-manganese austenitic steel after severe wear <sup>255</sup>.

4. Tribofilms generated as the result of tribochemical reactions between wear products (wear debris or worn surface) and the environment.

This is a very common type of tribofilm as most tribosystems are exposed to environments containing chemically reactive species. This category would for instance include oxide films formed during rubbing in the presence of oxygen or water, particularly in high speed or high temperature environments. Oxide tribofilms may not only provide wear protection but could also inhibit further corrosion of the sliding

surface if it has sufficient barrier properties to limit diffusion of oxygen or other corrosive species to the metal surface beneath.

In the context of liquid lubricated tribosystems, tribofilms resulting from tribochemical reactions involving the lubricant components and the worn surface are arguably the most common. This is due to several reasons including high concentration of chemically active species in close vicinity to the surface, the shear flow continuously washing away wear particles, and the cooling effect of many liquids which reduce temperature in the contact. Understanding the tribofilm formation mechanisms of various lubricant additives has been of great interest in later years, but the lack of appropriate *in situ* experimental methods means that the precise nature of tribofilm formation and tribochemical reactions remains elusive and a subject of much speculation. In most cases, surface and near-surface analysis of reaction products *ex situ* is simply not enough to fully understand the complex nature of tribochemical processes. However, in recent years, our understanding of tribofilms has been increasingly enriched due to advances in material characterization techniques and computational technology, but much still needs to be resolved.

To date, most research on the tribological action of lubricant additives have focused on conventional molecular friction modifiers and anti-wear additives, such as ZDDP, rather than solid nanoadditives, such as carbon nanostructures. For this reason, not much is known about the role of carbon nanostructures in tribofilm formation. Nonetheless, formation of tribofilms have been reported in literature where carbon nanostructures have been used as lubricant additives. However, because research into the tribological properties of carbon nanostructures and other solid lubricant additives is still relatively new, literature on the tribochemical action of carbon nanostructures is still scarce. Specifically, most publications on the matter have, to date, focused primarily on reporting the overall friction and wear characteristics of the tribosystem, and less attention has been paid to potential tribofilm formation. Often, it is simply stated that a tribofilm was likely formed during tribological testing based on simple surface analysis, without going into a more detailed characterization of the tribofilm or attempting to elucidate its formation mechanisms or the role of the carbon nanostructure in said formation. Moreover, herein lies the challenge of distinguishing the contribution of the carbon nanostructure from that of its surface functional groups and dispersing agents.

### **Third-body Material Transfer Film**

When using conventional molecular friction-modifying additives, the transition from adsorbed layer to tribofilm is clearly indicated by the onset of significant structural and chemical changes. However, in the case of solid nanoparticulate additives, this transition is not always as easily identifiable. Specifically, many carbon nanostructures tend to degrade into an intermediate state that is no longer an adsorbed layer of intact nanoparticles and not yet something that would qualify as a tribofilm. For example, several 0D carbon nanostructures have been known undergo bond-rearrangement or structural

collapse in response to high contact pressures (as seen in Section 3.3.1), and some multi-walled carbon nanotubes (MWCNTs) have been shown to exfoliate into graphene-like fragments<sup>181,182</sup>. The resulting carbon-based wear debris may adhere onto the tribosurface and form a surface film that is fundamentally different from the adsorbed layer of intact carbon nanostructures in terms of properties and performance. Yet, despite having undergone significant structural changes, the adhered wear debris may still not qualify as a tribofilm due to reasons such as insufficient bonding strength with the underlying substrate or discontinuous coverage. In other words, it is simply not stable, substantial, or cohesive enough to be considered a new material on the tribosurface, in accordance with the abovementioned tribofilm definition.

Instead, this intermediate case of adsorbed wear debris may be called a third-body material transfer film. That is, material from the third body in the contact area (in this case the carbon nanostructures) has been transferred to the contacting bodies in relative motion. The friction-reducing and antiwear performance of such transfer films is highly dependent on the quality of the deposited material in terms of interfacial bonding, morphology, surface chemistry, and mechanical properties.

### **3.4.1 0D Carbon Nanostructures**

For conventional molecular friction modifiers, it has been shown that the tribological characteristics of additive modified lubricant compositions are improved by increased adsorption capacity of the additives<sup>13</sup>. This is because the increased interaction and bonding energy between the adsorbents and the metal surface yields a more strongly bonded protective film. Moreover, computational studies have predicted that higher nanoparticle coverage and narrower particle size distribution is beneficial for friction and wear reduction due to improved load distribution<sup>233</sup>. In other words, nanoparticle adsorptivity is likely to be a highly influential parameter governing the tribological behavior of carbon nanostructures. However, despite the importance of the adsorbed layer in the friction modifying and antiwear performance of surface-active lubricant additives, there is a serious lack of studies relating the tribological performance of carbon nanostructures to their adsorption behavior (e.g., the adsorption potential, strength, and kinetics) as well as the mechanical and viscoelastic properties of the resulting adsorbed layer. This is a gap in our understanding of solid nanoparticle lubrication that needs to be filled.

Due to the system-specific nature of nanoparticle adsorption processes, attempting to predict or rank the lubrication performance of the various 0D carbon nanostructures on the basis of adsorption potential alone would be misleading. It is, however, possible to highlight some properties that may facilitate or promote their adsorption to the tribosurfaces. For example, since adsorption is a means of surface energy reduction, high specific surface area is likely to improve adsorption capacity. As stated by Manyangadze et al.<sup>258</sup>, high specific surface area might not automatically translate to a higher adsorption capacity, but it is worth noting that the adsorption capacity is to a large extent a function of the specific surface

area of the particle. Surface functional groups exhibiting dipole moment or partial electrical charges are likely to promote physisorption and electrostatic interaction. Moreover, chemisorption and electron transfer is facilitated when the adsorbent or its functional groups have an availability of  $\pi$  electrons due to the presence of aromatic rings or multiple bonds, or unshared lone electron pairs that can interact with the d-orbitals of the metal surface <sup>259</sup>.

Owing to their high surface-to-volume ratio, all the 0D carbon nanostructures introduced in Section 2.1 are expected to exhibit some degree of adsorptivity in most tribosystems. For instance, Ewen et al. <sup>171</sup> argued the high specific surface area of NDs and CNOs (up to 400 m<sup>2</sup>/g) should provide reasonably strong surface-active and adsorption processes. However, they also argued that their nonpolar nature and relatively weak short-ranged Van der Waals interactions with the surface, they probably show less surface activity than, for example, conventional amphiphilic organic friction modifier additives. Hu et al. <sup>156</sup> reported that the presence of oxygen and nitrogen surface functional groups promoted the formation of a monomolecular adsorption film on 316 stainless by forming coordinate covalent bonds with the electron-deficient d-orbitals of the metal surface elements. Cui et al. <sup>249,260</sup> found that the adsorption process of three different nitrogen-doped CQDs obeyed a Langmuir isotherm on Q235 carbon steel in 1 M HCl solution, and the estimated adsorption free energy ( $\Delta G_{ads}^0$ ) indicated that interactions between the CQDs and the steel surface involved a mixture of both physisorption and chemisorption. The ability and tendency of 0D carbon nanostructures to adsorb onto tribosurfaces is also supported by the fact that some affinity and adhesion is arguably necessary to ensure sufficient coverage to effectively separate the surfaces and provide the drastic increase in load carrying capacity reported in literature <sup>11</sup>, as discussed in Section 3.1.

The ability of 0D carbon nanostructures to form third-body material transfer films is closely related to their tendency to undergo structural deformation, exfoliation, or collapse. As seen in Section 3.3.1, several 0D carbon nanostructures are prone to pressure-induced re-bonding as a means of strain reduction under high compressive loads. Moreover, the combined action of compressive and shear forces can cause severe plastic deformation in the form of crushing, rupture, or scission of intramolecular bonds. The tendency to deform or collapse is also influenced by the nature of physical and chemical interactions between the nanoparticles and the tribosurface. Stronger adsorption or interfacial bonding is generally accompanied by loss of mobility which in turn makes the nanoparticle more susceptible to sliding-induced damage. Larger nanoparticle aggregates are also more prone to mechanical deformation during tribological operation. In other words, the ability of 0D carbon nanostructures to form third-body material transfer films is highly dependent on the dispersion state and mechanical properties of the nanoparticle itself, as well as the operating conditions and chemical nature of the tribosurface.

As previously mentioned, the tribological performance of the resulting third-body material transfer films is highly dependent on the quality and properties of the deposited material. For instance, Li et al.<sup>216</sup> reported on the deteriorating effect of dangling bonds after structural collapse of C<sub>60</sub> fullerene. The presence of dangling bonds not only caused interfacial cross-linking of the two tribosurfaces, but also severely limited the mobility of the lubricant base fluid. In contrast, Xiao et al.<sup>78</sup> reported that, as the tribological experiment proceeded, some of the CQD nanoparticles were crushed under the influence of normal and shear stresses, resulting in lamellar-like wear debris that could potentially undergo interlaminar shear. Based on this, it stands to reason that the tribological performance of transfer material in some cases can be related to the structural morphology of the original structure and its ability to retain beneficial structural elements, such as lamellar segments.

The ability to retain structural elements, in turn, is dependent on the nature of the deformation process. For instance, Ye et al.<sup>211</sup> investigated the influence of load in the transfer film formation process of oleylamine-functionalized nitrogen-doped CQDs in PAO on AISI 52100 steel. SEM-EDS elemental mapping revealed that the deposited carbon content on the worn surface increased with increasing loads from 196 to 588 N. Under low loads (196 N), the deposited carbon material still exhibited fluorescence, but this was not detected after tribological testing at higher loads. Moreover, Micro-Raman mapping revealed increasing I<sub>D</sub>/I<sub>G</sub> ratios with increasing loads. These findings illustrate how friction-induced defects and degree of disorder increase with increasing loads. All in all, the authors concluded that the functionalized CQDs first adsorb uniformly onto the tribosurfaces via physical and electrostatic interactions, where they act as ball bearings under the initial stages. Then, traction and compression created by the contact pressure eventually damage both the hydrocarbon functional groups and the CQDs themselves, resulting in the deposition of increasingly defect carbon-based material. Over time, a thin protective film containing iron oxides, inorganic carbon and nitrogen element was built up on the worn surface, which protects the tribosurfaces from directly contacting and bears the load from the steel balls<sup>211</sup>.

This example also illustrates another important aspect of protective film formation, namely that the transition from third-body material transfer film to tribochemical film can sometimes be difficult to discern. This is because the same structural deformation that gave rise to the third-body wear material may also provide a path to tribofilm formation through mechanochemical activation. Specifically, accumulated deformation-induced strain or highly reactive dangling bonds can act as tribochemically active sites and react with either the tribosurfaces, neighboring nanostructures, wear debris, or other lubricant components. Over time, the accumulation of nanoparticles, transfer material, wear debris, and potential tribochemical reaction products may become substantial enough to qualify as a proper and firmly bonded tribofilm in accordance with the previously established definition. In other words, mechanochemical activation of the carbon nanostructure through structural degradation is believed to

be a possible tribofilm formation mechanism. This theory is supported by the presence of degraded or deformed carbon nanostructures in several reported tribofilms.

For instance, Joly-Pottuz et al.<sup>53,54</sup> found evidence of tribologically transformed carbon nanostructures in composite tribofilms formed on AISI 52100 steel surfaces during lubrication with PAO containing carbon nano-onions (CNOs). The tribofilm was subjected to Raman spectroscopy and extensive TEM analysis, and was described as a mosaic of graphitic sheets and intact CNOs bound by iron oxide nanoparticles<sup>54</sup>. Herein, the graphitic structures were thought to originate from the nested and layered CNOs, likely through tribologically-induced deformation as seen in previous studies by the same group<sup>55</sup>.

Wu et al.<sup>100</sup> reported on the tribofilm formed on the  $\text{Si}_3\text{N}_4$  surface of a  $\text{Si}_3\text{N}_4$ -Si contact lubricated by water containing 0.6 wt% NDs. High resolution TEM analysis and elemental mapping revealed that the tribofilm was comprised of intact NDs distributed within an amorphous matrix of primarily carbon and oxygen, as shown in Figure 3.6. Some areas of Si enrichment could also be seen, likely due to wear debris from the Si substrate. Since the nanodiamonds were the only source of carbon in the given tribosystem, the amorphous carbon making up the matrix of the composite tribofilm must surely be a product of the nanodiamond additives. While some defects could have been introduced in the NDs during detonation method synthesis, the authors also suggested that defects could have been introduced by the mechanical interaction owing to the sliding process, which could have led to the amorphization of NDs over time.

Surface functional groups are also believed to be a likely source of tribochemical activity. Since carbon nanostructures are generally known for their high chemical inertness, functionalizing carbon nanostructures with more chemically reactive groups could potentially promote tribofilm formation. How functionalization can be used to exploit tribochemical interactions will be discussed in greater detail in Chapter 4. Another interesting way in which surface functional groups may influence tribofilm formation is through enhanced adsorption, which promotes the presence of carbon-based nanoadditives on the surface.

For instance, Hu et al.<sup>156</sup> synthesized water-dispersible CQDs with hydrophilic oxygen-containing groups and nitrogen element by tuning the carbonization degree of ammonium citrate and investigated their lubrication performance as additives in water in an  $\text{Al}_2\text{O}_3$ -316 steel contact. The addition of 0.1 mg/mL significantly improved both friction and wear performance of the lubricant, and the resulting wear scar was both narrower, shallower, and smoother than that on the steel surface lubricated by pure water. SEM analysis with elemental distribution mapping showed increased carbon content in furrows of the wear scar of the steel surface lubricated with CQDs, and the Raman spectra exhibited the characteristic D and G peaks indicative of the graphene structure found in CQDs. TEM imaging of the wear scar cross-section revealed the presence of a firmly bonded tribofilm of uneven thickness and with

several intact CQDs embedded near the substrate surface, as seen in Figure 3.7. While the specific mechanisms of the tribofilm formation process remained unidentified, the enhanced adsorptivity of CQDs due to the presence of functional groups with oxygen and nitrogen elements was believed to play an important role in the effective buildup of the tribofilm.

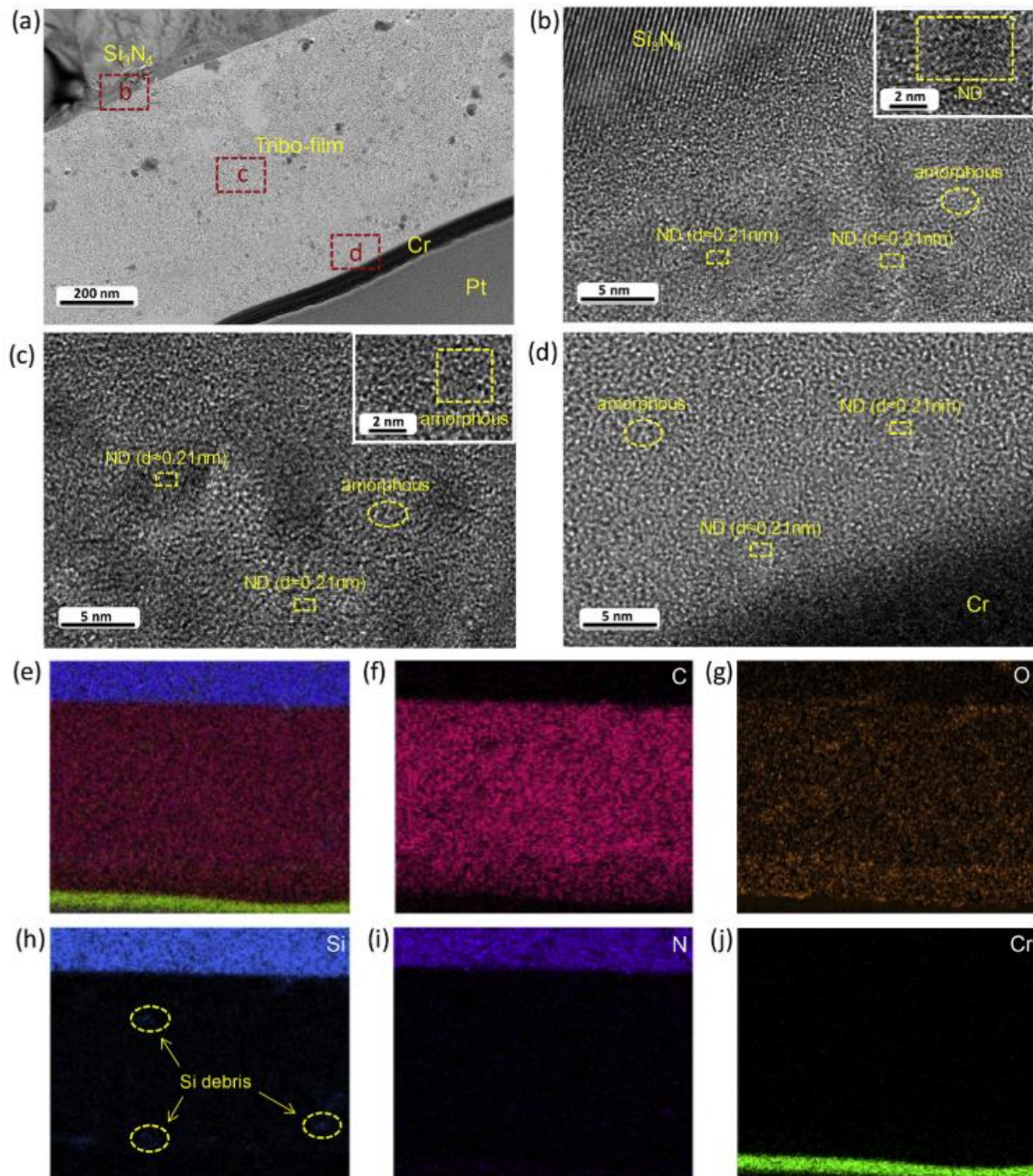


Figure 3.6: (a) TEM picture of the tribofilm in the contact area on the  $\text{Si}_3\text{N}_4$  ball, and high-resolution TEM pictures of typical regions (b) near the  $\text{Si}_3\text{N}_4$  substrate, (c) inside the tribofilm and (d) around the Cr/tribofilm interface. (e-j) Elemental mapping of the tribofilm on the  $\text{Si}_3\text{N}_4$  ball lubricated by water with NDs<sup>100</sup>.

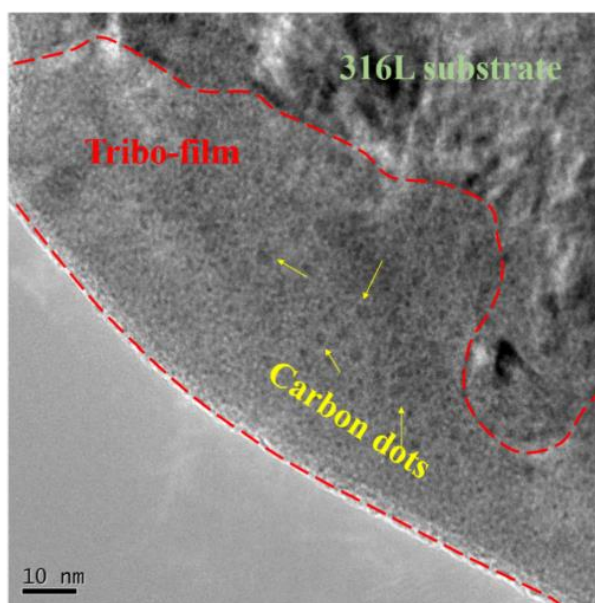


Figure 3.7: Cross-sectional TEM image of the wear scar on 316 steel lubricated by CQDs dispersed in water <sup>156</sup>.

This theory corresponds well with the findings of some recent studies in which the tribofilm formation of conventional molecular antiwear additives have been correlated to their adsorption strength and kinetics <sup>261,262</sup>. Khan et al. <sup>261</sup> found that strong adsorption of surface-active additives was necessary for efficient tribofilm formation as weaker adsorption resulted in desorption from the surface due to flash heating before they had the chance to participate in the mechanochemical reactions required for tribofilm formation. Moreover, Khanmohammadi et al. <sup>262</sup> used Quartz Crystal Microbalance with Impedance (QCM-I) to demonstrate that adsorption kinetics play a critical role in determining whether ionic liquid will yield tribofilms when used as additives in water-based lubricants for stainless steel surfaces. Since adsorbed species are continuously removed from the contact during tribological testing, faster adsorption kinetics allow for more effective re-adsorption of additives. This continuous replenishment of adsorbed species likely helps ensure sufficient presence of additives in the contact for a tribofilm to form on the surface. The evident significance of adsorption in the tribofilm formation process of other tribofilm-forming additives should serve as a persuasive argument for the inclusion of adsorption studies in future research on the lubrication potential of carbon nanostructures.

It has also been suggested that carbon nanostructures may partake in tribochemical film formation through their inherent chemical reactivity, rather than through their surface functional groups or by mechanochemical activation such as the formation of dangling bonds. Even though carbon nanoallotropes are generally regarded as stable and relatively inert materials owing to their low reactivity towards substances such as gases of acids, they still exhibit a degree of chemical reactivity in that they can undergo various organic reactions and modifications at their surfaces, sometimes within their internal spaces <sup>28</sup>. For instance, although C<sub>60</sub> fullerene is a quite stable structure, its small round

shape imposes a certain degree of strain on the molecule, which is responsible for much of its chemical reactivity. For this reason, C<sub>60</sub> can participate in most organic reactions that involve sp<sup>2</sup> carbons, such as addition of nucleophiles or radicals to C=C bonds, cycloaddition with dienes, or polymerization processes<sup>28</sup>. In an effort to explain the formation of a polymeric tribofilm (≤ 100 nm) comprised of fullerenes and covalently bound hydrocarbon fragments, Ginzburg et al.<sup>35</sup> proposed a tribofilm reaction mechanism in which C<sub>60</sub> additives act as radical scavengers for various mechanochemically generated base oil radicals, and undergo polymerization. While this mechanism seems promising at first glance, there is still a considerable lack of literature supporting this theory, thus, more research is needed to corroborate and substantiate these claims.

In recent literature, there are also some cases in which the reported tribofilm seem to be the reaction product of other components in the lubricant formula, rather than the carbon nanostructure additives themselves or their surface functional groups. In these cases, the role of the carbon nanostructure might be more difficult, yet perhaps more interesting, to discern. For instance, would the tribofilm form in the otherwise identical tribosystem in the absence of the carbon nanostructure? If yes, did its presence cause any changes in the resulting tribofilm or its formation process? If no, what role did the carbon nanostructure play in the formation process? One possible explanation could of course be that the tribofilm formed solely due to the environmental implications of the nanostructure's presence, rather than the nanostructure itself. Such implications could, for instance, include higher and more localized contact pressures or frictional heat. Alternatively, is it possible that the nanostructures could somehow play an active part in the tribofilm formation process, even though the resulting film is the reaction product of other lubricant components or wear debris? Interestingly, there are some examples in recent literature which may indicate that this could be the case.

Firstly, it has been suggested that the presence of carbon nanostructures have the ability to stabilize the formation of certain tribochemical reaction products that may not have been formed otherwise<sup>53,54</sup>. Secondly, it seems as if carbon nanostructures may aid the transportation of other lubricant components through adsorption or related phenomena<sup>19,78,213</sup>. For example, Xiao et al.<sup>78</sup> suggested that the presence of CQDs promoted the formation of a partial tribosintered film by helping ceramic wear debris from the parent worn surfaces to accumulate. Similarly, Ivanov and Shenderova<sup>213</sup> proposed that NDs may enhance the delivery of other tribofilm-forming additives to the tribosurfaces by allowing them to adsorb onto their surface during preliminary mixing and effectively transporting them. As a result, the amount of the other tribofilm-forming antiwear additive needed for wear protection could be reduced by up to five times. In other words, even though the NDs did not react themselves to form the tribofilm in this case, they still played a role in the tribofilm formation process. Chapter 5 will go into greater detail about this type of potential synergistic action of carbon nanoadditives.

Furthermore, the formation of tribochemical tribofilms, as opposed to mechanically mixed tribofilms, is inevitably accompanied by changes in the chemical nature of alloying elements of the surface. In the

case of steel, for instance, this often involves the formation of compounds such as iron oxides<sup>81,165</sup>, sulfates<sup>142</sup>, sulfides<sup>37</sup> or iron fluoride<sup>263,264</sup>, depending on the reactive elements of the other reactant. These surface reaction products will of course also influence the friction and wear behavior of the tribofilm. Moreover, the presence of these tribochemical reaction products may also in turn affect the various other lubrication mechanisms of the carbon nanostructures. Thus, exploring their conditions and mechanisms of formation and their various properties is not only beneficial in of itself, but is also essential to our understanding of carbon nanostructures as lubricant additives as a whole.

Regardless of what kind of role the carbon-based nanoadditives play in tribofilm formation processes, intact carbon nanostructures are very often found embedded in the tribofilms as a result of their high mechanical strength. This means that that the resulting tribofilms are effectively composite materials. By an extension of the tribofilm term, purely mechanical embedment of nanostructures into comparatively softer tribosurfaces (in absence of any chemical reaction products) could perhaps also be considered a tribofilm if the embedment is widespread and consequential enough for the composite stratum on surface to be considered a different material from the underlying surface. In either case, the presence of embedded nanostructures will undoubtedly affect the mechanical properties and durability of the composite tribofilm layer. Particle reinforced materials usually exhibit enhanced stiffness as well as increased strength and toughness, which is generally associated with greater wear resistance. For this reason, it has been conjectured that the incorporation of carbon nanoadditives into the tribofilms and metal tribosurfaces is an advantageous step towards improved tribological performance<sup>213</sup>.

However, this may not always be the case as the effects of nanoparticle incorporation are highly dependent on the mechanical properties of both the constituent materials and the nature of the bonding between them. For example, embedment of hard nanoparticles into already high-strength materials have been known accelerate the transition into severe wear regimes by initiating nucleation of fatigue microcracks, whereas embedment into ductile materials can aid development of beneficial subsurface microstructures<sup>265</sup>. In other words, even though embedment or incorporation of solid nanostructures can benefit the wear resistance of the tribofilm or tribosurfaces in some cases, more research is needed to establish the effects of different nanostructures embedded in various matrix materials under a wide range of tribological conditions. Either way, if embedment of nanoparticles is found to be a desirable feature, the adsorption proficiency is likely to be an important parameter as it controls the presence of nanostructures at the interface.

In summary, tribofilm formation remains elusive and is a subject of speculation due to the lack of experimental methods by which to monitor the evolution of tribofilms *in situ* and the complex interplay of the processes involved. Still, tribofilms have been reported in several instances where carbon nanostructures have been employed as lubricant additives. Based on preliminary results, it seems as if carbon nanostructures are able to contribute to tribofilm formation in a number of different ways. Due to their relatively high chemical inertness, carbon nanostructures are generally thought to participate in

tribochemical film formation by undergoing structural degradation (i.e., through mechanochemical activation) or by the virtue of more tribochemically active surface functional groups. In addition, it has been proposed that carbon nanostructures may play other less direct roles in tribofilm formation, for instance by facilitating transport of other tribofilm-forming additives to the sliding surfaces or stabilizing the formation of certain tribofilm species. These mechanisms are particularly speculative, and more research is needed to investigate and discern their validity. Lastly, it is also possible that carbon nanostructures aid tribofilm formation by altering the environmental conditions (e.g., temperature, contact pressure etc.) in the contact, which could facilitate the occurrence of thermally activated or pressure-induced tribochemical reactions.

Now that the possibility of tribofilm formation in the presence of carbon nanoadditives has been established, more extensive characterization and reporting of tribofilm composition and properties is strongly encouraged as the field moves forward. This is an important first step towards being able to exploit the tribofilm-forming ability of carbon nanostructures in a more deliberate and competent manner. In present literature, there is an unfortunate occurrence of tribofilm formation being claimed based on insufficient or unsatisfactory experimental evidence. Such claims are often based on a single and superficial surface analysis of the wear scar, which on its own may not be enough to differentiate between adsorbed layers and an actual tribofilm. Since tribofilms differ from their parent worn surfaces in terms of morphology, microstructure, chemical composition, and the elastic and plastic properties, the characterization of tribofilms should aim to reveal these differences. Thus, it stands to reason that a combination of characterization techniques should be employed to obtain a more complete picture of generated tribofilms, which in turn could help improve our understanding of the tribofilm formation process.

### **3.4.2 1D Carbon Nanostructures**

As discussed in Section 3.1, adsorption of carbon nanostructures play an important role in the performance of surface-active additives such as friction-modifiers and antiwear additives, and it is believed that nanostructures with a certain affinity towards the surface are more resistant towards being squeezed out of the contact. While pristine CNTs are generally recognized for their high chemical inertness, the artefacts left over from synthesis can often be regarded as defects with higher chemical activity which may promote adsorption and the formation of protective layers. For instance, based on experimental results, Joly-Pottuz and Ohmae<sup>120</sup> concluded that the nature of the catalytic particles used in chemical vapor deposition (CVD) synthesis of CNTs may positively influence the tribological properties of the nanoadditive, and suggested that purification of CNTs might not be necessary for future tribological applications. These results are promising as the need for purification of CNTs are accompanied by a drastic increase in cost.

Similarly, Salah et al.<sup>235,236</sup> used oil fly ash a catalyst and co-precursor in CVD synthesis of CNTs and hypothesized that the existence of active radical sites on their side walls might promote adhesion to the metal tribosurfaces. It is also worth noting that the covalent or non-covalent functionalization required for effective dispersion of CNTs will inevitably affect the chemical activity of the additive as well. In other words, it is not unlikely that selective choice of surface functional groups can be used to promote the adsorption of additives on the tribosurfaces and thereby enhancing retention of nanostructures in the interfacial contact area during sliding. This will be addressed and discussed further in Chapter 4.

Because of the low Young's modulus perpendicular to the tubular axis<sup>240,244</sup>, adsorbed carbon nanotubes are prone to deformation followed by structural degradation during lubrication<sup>117,120,121,216,245</sup>, as established in Section 3.3.2. As the resulting CNT wear debris deposit and accumulate on the tribosurface, a third-body material transfer film is formed. However, these films have been shown to exhibit very varying tribological properties. That is, some studies praise the friction- and wear reducing characteristics<sup>19,117,120</sup>, while others emphasize their poor lubrication properties<sup>216,245</sup>. For instance, Nunn et al.<sup>19</sup> obtained a friction coefficient as low as 0.013 using 0.5 wt% MWCNTs in PAO. The friction-reduction was also accompanied by a greater than 15% reduction in wear area compared to pure PAO. Similarly, Joly-Pottuz and Ohmae<sup>120</sup> reported having achieved a low and stable friction coefficient of 0.07 using 1 wt% SWCNTs in PAO under a contact pressure of 0.83 GPa, and Cornelio et al.<sup>266</sup> obtained friction coefficients as low as 0.063 in an undisclosed base oil. Salah et al.<sup>236</sup> ascribed both the reduced mean friction coefficient and reduced friction curve fluctuations to the smoothing effect of CNT deposits.

In contrast, Li et al.<sup>216</sup> labelled the increased surface roughness caused by the re-bonding of dissociated CNT flakes as a contributing factor in the obvious friction increase. Similarly, Upadhyay and Kumar<sup>245</sup> attributed the deteriorated friction and wear performance of CNT-enriched lubricants to the poor lubrication properties of both intact MWCNTs and the resulting transfer material deposits, which were described as both unstable and abrasive. While some of these differences can likely be ascribed to tribosystem-specific considerations such as the tribosurface material, lubricant base fluid and operating conditions, there are probably other factors at play as well. Specifically, differences in the surface coverage, cohesive and adhesive strength, roughness, and structural morphology are expected to account for some of the variations in tribological performance. Herein, understanding what kind of carbon nanotube gives rise to what kind of transfer film and under which conditions would be of great interest.

The antiwear properties of CNT-based transfer layers are generally attributed to their ability to act as effective spacers and separate the sliding tribosurfaces, thereby limiting abrasive and adhesive contact<sup>117,266,267</sup>. The separating films have also been shown to exhibit excellent load-bearing capacity, also under loads where liquid lubricants would normally be squeezed out, which drastically improves the extreme pressure properties of the tribosystem<sup>117,268,269</sup>. For instance, Peng et al.<sup>117</sup> found that the

addition of 0.1 wt% MWCNTs not only reduced friction and wear of pure water, but also greatly increased the maximum non-seizure load and the weld load by a remarkable 560% and 151%, respectively. Moreover, the presence of iron oxide wear particles in a transfer layer led Joly-Pottuz and Ohmae<sup>120</sup> to propose yet another wear-reducing mechanism. They suggested that the transfer layer may be able to trap or ‘digest’ abrasive surface wear particles so that they are no longer active in the contact.

While there is a general consensus on the antiwear mechanisms of the transfer layers, their friction-reducing properties have been the subject of much speculation and remain largely unexplored. On one hand, it is certainly possible that the friction reduction can be attributed to general effects such as smaller interfacial contact area, reduced asperity ploughing, and limited adhesive asperity interactions. Alternatively, perhaps it is possible that the transfer films have some inherently lubricious properties. In several instances, there is strong experimental evidence for severe shear-induced amorphization of CNTs during lubrication<sup>120,266,270</sup>. For example, using *in situ* Raman analyses during steel sliding on a sapphire flat, it was observed that the radial breathing mode and characteristic peaks of the SWCNTs disappeared completely after only 1 minute<sup>270</sup>. This was accompanied by a rapid increase in the  $I_D/I_G$  ratio, indicating the formation of more disordered carbon species inside the contact area. In another study<sup>120</sup>, TEM-EELS analysis of wear debris collected on the surface after lubrication with SWCNTs showed that the characteristic peak for  $sp^2$ -hybridization, which is clearly visible in the spectra for graphite and pristine carbon nanotubes, was not present in the spectrum of the wear particles. Here too was the amorphization of carbon supported by the growth of the D band in the Raman spectra, and it was eventually concluded that the carbon of wear debris was entirely amorphous. How these amorphous carbon transfer films can reduce friction remains unresolved and severely understudied, but perhaps an analogy to DLC coatings could be envisioned<sup>120</sup>. However, this has not yet been investigated or studied.

While transfer films from SWCNTs are generally reported to be comprised almost entirely of amorphous carbon<sup>120,266,270</sup>, it has been observed that wear debris of MWCNTs may retain some of its graphitic structure after tribological testing<sup>117,180–182</sup>, which could potentially contribute to reducing friction in a manner similar to graphite or few-layer graphene. While more research is needed to verify the friction-reducing effects and longevity of these graphene-like sheets and lamellar segments, it could potentially explain why MWCNTs tend to perform slightly better than SWCNTs in the few comparative studies that are available<sup>19,236</sup>. However, this tendency could also potentially be attributed to another key difference between SWCNTs and MWCNTs, namely their intrinsically higher resistance towards structural collapse from the outset. MD simulations have shown that the larger number of concentric layers make MWCNTs more rigid and resistant towards deformation under the combined action of compressive and shear forces<sup>237</sup>. For this reason, there are instances where MWCNTs have remained mostly intact, albeit significantly shortened and slightly deformed, rather than completely amorphized<sup>117,236,267</sup>.

All in all, owing to their low strength perpendicular to the nanotube axis, adsorbed layers of CNTs are rapidly transformed to third-body material transfer films. These transfer films are most often described as flake-like wear debris of mechanically flattened and intermingled carbon nanotubes, or amorphous carbon, without any mention of additional constituents or tribochemical reaction products. Despite the great importance of these films in tribological behavior, they have not been studied extensively and there is still much to learn about their formation process and lubrication mechanisms. One reason for the lack of research into CNT-based additives and their transfer films could be their very varying performance. While some achieve promising friction- and wear-reduction, others report on the unstable and abrasive nature of CNT deposits<sup>216,245</sup>. This, along with their tendency to agglomerate, and the difficulty of dispersing them, it is understandable that research interest has dissipated in later years.

### 3.4.3 2D Carbon Nanostructures

Once the graphene has entered the contact area, its high specific surface area allows it to easily adsorb onto the tribosurfaces and form a conformal adsorption film<sup>151,152</sup>. The wear-reducing properties of these graphene-based protective films are primarily attributed to the separating effect, which prevents the tribosurfaces from directly contacting, while the friction-reducing performance is primarily attributed to the interlaminar shearing mechanism and the so-called passivating effect. Since the interlayer shearing mechanism has already been addressed in Section 3.2.3, this section will primarily focus on introducing the passivation effect before going into more detail about the factors affecting the structural-evolution, wear resistance, and durability of graphene-based protective films. Lastly, as the section is summarized, a brief discussion about classification and characterization of graphene-based protective layers will follow.

The passivation effect was first proposed by Restuccia and Righi<sup>160</sup> who used *ab initio* spin-polarized density functional theory (DFT) calculations to show that graphene adsorption greatly reduces the surface energy of native iron surfaces. As a result, metal surfaces covered by graphene become almost inert and present very low adhesion and shear strength when mated in a sliding contact. Specifically, their calculations showed that interfacial adhesion between native iron surfaces could be reduced by as much as 88% when both the surfaces in the contact were covered by graphene. Furthermore, this reduction in adhesion was accompanied by a 98% decrease in ideal shear strength, indicating that the lubricating properties of graphene partially reside in the ability to passivate the surface onto which it is adsorbed<sup>160</sup>. In other words, adsorbed graphene layers do not only provide a mechanical separation effect, but also a chemical screening effect that reduce metal-metal interactions. Other studies have also concluded that the presence of adsorbed graphene can reduce friction between tribosurfaces due to shielding of dangling bonds at the interface<sup>216,271</sup>. While more research is needed to verify the passivation effect, these findings collectively highlight the importance of considering chemical interactions, as well as mechanical contributions, arising from carbon nanostructures in the interfacial contact area.

Similar to the case of the interlaminar shearing mechanism, the friction-reducing contribution of the passivation effect is dependent on the surface coverage of the adsorbed layer <sup>161,183</sup>. As explained by Marchetto et al. <sup>161</sup>, if the graphene coverage is incomplete, the countersurface asperities would have to transverse both graphene-covered areas of low friction and uncovered areas of higher friction, resulting in increased and fluctuating friction behavior <sup>161</sup>. As previously established, the surface coverage of the protective layer is primarily governed by the adsorption behavior of the additives – both in terms of strength and kinetics. However, high adsorption strength and fast kinetics is not only important for friction-reducing purposes. It is also essential to the antiwear performance and durability of the protective layer. This is because more strongly bonded films are more resistant towards being removed from the contact area, as schematically illustrated in Figure 3.8. And, in case of removal, fast adsorption kinetics is beneficial for rapid replenishment of the film.

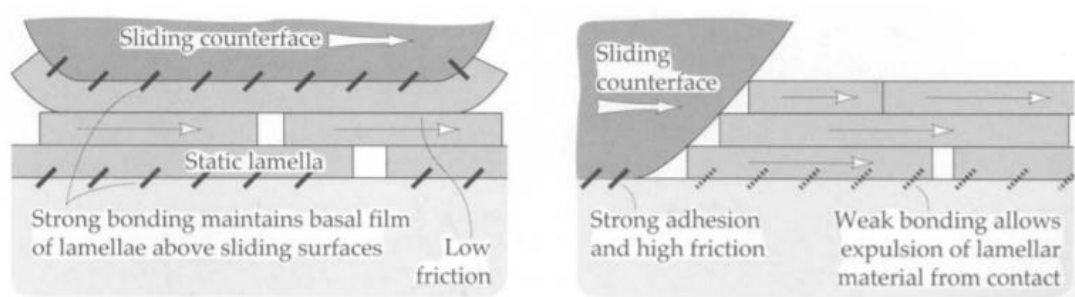


*Figure 3.8: Effect of adhesion strength of lamellar additives and the underlying substrate on friction. Although adhesion between lamellae is highly undesirable, adhesion of lamellae to the worn surface is essential. In general, material that is weakly adhered is quickly removed by the sweeping action of the sliding surfaces <sup>177</sup>.*

Factors that can promote adhesion and the formation of a more strongly bonded protective layer include, but are not limited to, dangling bonds <sup>160</sup> and surface functional groups that can interact with the surface through the formation of coordinate covalent bonds or electrostatic interactions <sup>249</sup>. The strength of adsorption is also dependent on the underlying material. For instance, based on density functional theory (DFT) calculations, Marchetto et al. <sup>161</sup> concluded that graphene only physisorbs on copper while it chemisorbs on iron where the  $\pi$ -orbitals of graphene can hybridize with electron-deficient d-states of iron. This difference in adsorptivity is likely why graphene (albeit damaged and defective) could be found inside the wear scar on the iron specimen, but not on copper, after rubbing against steel countersurfaces <sup>161</sup>.

Even trace impurities have been shown to influence the adhesion and durability of the adsorbed layer. Kim et al. <sup>272</sup> studied the microscale adhesion and frictional properties of graphene grown by CVD on two different catalysts, Cu and Ni, to investigate the feasibility of graphene as a thin solid lubricant between contacting surfaces in ambient environment at room temperature. They found that even though both Cu-grown and Ni-grown graphene could significantly reduce the adhesion and friction when

covering various surfaces, the graphene grown on Ni showed the lowest coefficient of friction (0.03). The difference in tribological performance of the graphene grown on different catalyst metals was attributed to the weaker adhesion between Cu-grown graphene and the substrate, resulting in a more easily worn graphene film. These findings illustrate that strong adhesion of graphene not only reduces the surface friction, as discussed in Section 3.2.3, but may also improve the retention of the protective layer on the surface during the tribological process.

However, various structural features and defects can also cause detachment or degradation of the protective film on the rubbing surface. Mao et al.<sup>144</sup> compared the lubricating performance of three types of reduced graphene oxide (rGO) sheets with varying edge micromorphology in the form of regular edges (r-rGO), irregular edges (ir-rGO) and both irregular edges and wrinkles (ir-W-rGO), as depicted in Figure 3.9. The antiwear behavior of the three different graphene types varied dramatically. While r-rGO reduced wear significantly, the two other structures exhibited little wear resistance or even enhanced wear. The authors attributed this to r-rGO forming a firm and thick adsorbed film, while ir-rGO and ir-w-rGO formed thin, partial, and unstable films. Specifically, the larger perimeter of the graphene types with irregular edges was associated with more dangling bonds and edge defects, which possibly led to an already partially broken layer that was more susceptible to wear during the friction process. Moreover, as discussed in Section 3.2.3, wrinkles are more susceptible to friction-induced wear.

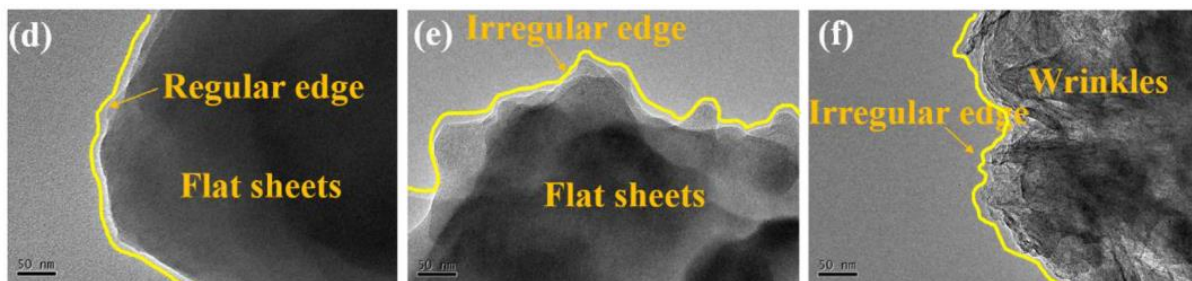


Figure 3.9: TEM micromorphological images of the three types of graphene sheets: (d) for r-rGO; (e) for ir-rGO; (f) for ir-W-rGO<sup>144</sup>.

Indeed, the presence of wrinkles have been linked to earlier onset of wear as the load bearing capacity of graphene drops nearly one order of magnitude in the presence of wrinkles<sup>204</sup>. Moreover, Vasic et al.<sup>204</sup> found that wear of graphene edges was generally initiated by wrinkle formation, and that wear was enhanced on irregular and already wrinkled graphene sheets. In other words, the introduction of structural defects in graphene tend to increase friction and susceptibility to wear<sup>27</sup>. Tripathi et al.<sup>202</sup> studied the effect of prevalent structural defects on friction and normal load bearing capacity of graphene and found that edges, step-edges, wrinkles, grain boundaries, and vacancies can all severely compromise the mechanical properties of graphene during tribomechanical operation, resulting in reduced tribological performance. Moreover, wrinkles and grain boundaries have been found to have a

higher binding energy towards foreign particles than the rest of the basal plane, which may also cause higher friction and accelerated wear <sup>273</sup>. As discussed in Section 3.2.3, surface functionalization of the graphene basal plane is generally accompanied by an increase in in-plane flexibility which can make the 2D structure more prone to friction-induced damage. This, along with the reduced mechanical properties, may explain the higher wear rate of graphene oxide compared to graphene <sup>27</sup>. However, as previously mentioned, adverse effects from increased in-plane flexibility can in some cases be mitigated by strong interfacial adhesion.

However, structural evolution of adsorbed graphene during tribological operation does not necessarily compromise or yield a less effective protective film. For instance, Hu et al. <sup>201</sup> observed that during sliding tests, the lamellar graphene-based protective film was prone to slipping and was broken into smaller pieces, resulting in a thicker film due to overlapping and curling. Similarly, Zhang et al. <sup>182</sup> reported that, after 4 hours, the graphene nanostructures had been divided into smaller pieces and became significantly thicker due to overlapping. TEM imaging showed that additional graphene layers with different orientations had stacked on top of underlying sheets and revealed that the thickened graphene structure still had a lamellar structure. Based on their findings, the authors concluded that graphene nanosheets can effectively restack over time under high applied loads. Additionally, it was observed that the intrinsic corrugation and puckering of the graphene had been significantly reduced due to the larger bending stiffness of the thickened structure, which is also believed to contribute to friction- and wear reduction <sup>182</sup>.

Another potentially beneficial consequence of structural evolution is mechanically induced tribochemical activity. Due to the high chemical inertness, the main source of tribochemical activity in graphene itself is thought to arise from friction-induced defects. Specifically, tearing or rupturing of graphene sheets during the frictional process result in the formation of highly reactive dangling bonds that may subsequently be passivated by the formation of new bonds. Such disruption of the graphene lattice structure is often characterized by a transition from  $sp^2$  to  $sp^3$  hybridization and accompanied by an increased D band in the Raman spectra <sup>274,275</sup>. Amorphization, oxidation and chemical interactions with the tribosurfaces, wear debris or other lubricant components are ways by which mechanically activated dangling bonds may be re-passivated. Rupture of graphene-based protective surface layers may also allow the underlying tribosurface material to come into direct contact with the lubricant and its many components, which could also provide a path towards tribochemical film formation, especially under harsh operating conditions <sup>152</sup>. The tribochemical reaction products may form the basis for an improved and more strongly bonded tribofilm that gradually replaces the adsorbed film. Due to the inherently higher chemical reactivity of certain surface functional groups and graphene sheet edges, functionalized graphene derivatives (including graphene oxide) and smaller sheets are likely to be more tribochemically active.

In summary, the high specific surface area of graphene-based nanoadditives allows them to easily adsorb onto the tribosurfaces to form a protective layer. The large lateral size of the deposited 2D nanostructures protects the rubbing surfaces from wear by preventing direct interfacial contact while the friction-reducing performance is attributed to the passivation effect and interlaminar shearing mechanism. However, because the adsorbed graphene sheets are sheared continuously from the beginning of the frictional process, they do not stay intact to the same extent as some adsorbed and rigid 0D carbon nanostructures can do while acting as bearing balls. In the case of CNOs and MWCNTs, pervasive exfoliation and subsequent deposition of individual graphene-like layers was associated with the formation of a third-body material transfer film. It remains undecided whether such a distinction would be appropriate for graphene-based additives or if shearing and lateral displacement of individual graphene sheets should just be considered as an innate part of adsorption films.

However, in addition to shearing, 2D carbon nanostructures may also undergo exfoliation, bending, curling, puckering, rippling, delamination, tearing and rupture depending on the nature and severity of the frictional process<sup>163,202</sup>. Over time such mechanically induced structural changes are likely to compromise the layered and locally ordered structure of the protective film, resulting in deterioration of its ability to reduce friction through interlaminar shearing. Perhaps this transition from an adsorbed layer with lamellar structure to a defect and disordered film, that cannot reduce friction effectively through interlaminar shearing, is a more appropriate way to distinguish adsorption films and material transfer films in the case of 2D carbon nanostructures. That is, of course, if the tribologically transformed layer still do not satisfy the stricter criteria required to qualify as a tribofilm. On the other hand, this transition is likely to be gradual, which may complicate efforts to classify and distinguish different types of protective films. Classification of protective films is also hindered by the fact that surface films are still severely understudied and often insufficiently characterized, as previously established. Hopefully, future research will shed light on the film forming mechanisms and lubrication properties of adsorption films, transfer layers and tribofilms.

### **3.5 CORROSION INHIBITION EFFECT**

Corrosion of metallic surfaces is a possible cause of premature failure in lubricated systems that can be effectively mitigated by the use of appropriate corrosion inhibitor additives<sup>276</sup>. This is particularly important in water-lubricated systems and under boundary lubrication conditions, where the simultaneous action of corrosion and wear may accelerate degradation of the surface in a process known as tribocorrosion<sup>277,278</sup>. However, systems lubricated with hydrocarbon-based lubricants can also suffer corrosion due to water condensation and contamination. Conventional corrosion inhibiting lubricant additives reduce the rate of corrosion by forming a protective barrier on the surface which prevents corrosive species from reaching and interacting with the metal surface<sup>276</sup>, as shown in Figure 3.10<sup>276</sup>. This protective barrier can either be a reaction-type inorganic tribofilm, or the result of physical or

chemical adsorption of organic surfactant molecules that displace adsorbed water molecules from the metal-electrolyte interface <sup>279</sup>. The inhibition efficiency of the resulting inhibitor layer is highly dependent on its coverage of electrochemically active sites and barrier properties.

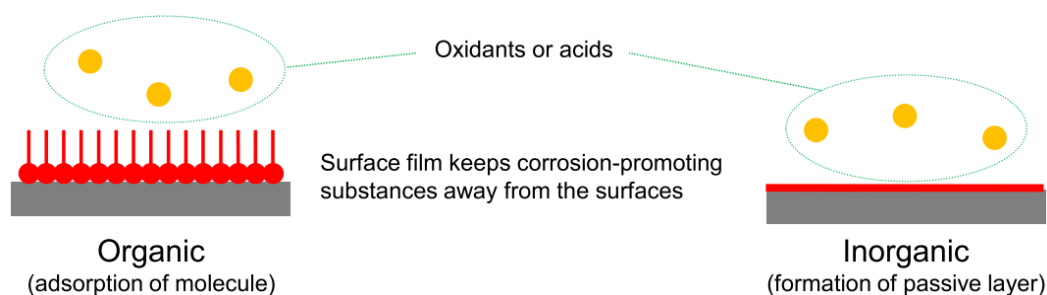


*Figure 3.10: Working principle of organic and inorganic corrosion inhibitors <sup>279</sup>.*

### 3.5.1 0D Carbon Nanostructures

Even though carbon nanostructures are primarily considered to be potential candidates for friction- and wear-reducing additives, recent studies suggest that some 0D carbon nanostructures may have corrosion inhibiting properties as well <sup>78,94,156,249,260</sup>. The adsorbing moiety of conventional organic corrosion inhibiting additives usually contain electronegative heteroatoms (such as oxygen, sulfur, nitrogen or phosphorous), aromatic rings or  $\pi$ -bonds that can adsorb onto the metal surface via the formation of coordinate covalent bonds, or through electrostatic interaction with the metal surface <sup>249</sup>. These are structural features that can also be found on the surface of some CQDs, particularly those synthesized by hydrothermal or solvothermal synthesis of precursors containing heteroatoms.

For instance, Xiao et al. <sup>78</sup> used a one-pot hydrothermal process to prepare sulfur-doped CQDs from sodium citrate and sodium thiosulfate and found that corrosive wear of AISI 52100 steel decreased when the CQDs were added to a water-based lubricant, as made evident by reduced density of corrosive pits and lower oxygen concentration on the worn surface. Similarly, Hu et al. <sup>156</sup> found that the presence of nitrogen-doped CQDs nanoadditives synthesized by thermal carbonization of ammonium citrate not only reduced friction and wear, but also significantly reduced corrosive wear of 316 stainless steel compared to pure water lubrication. The corrosion inhibiting properties of 0.1 mg/mL N-doped CQDs in water were further investigated using a static weight loss method. After soaking for 46 hours, the weight loss of Q235 carbon steel in DI water with CQDs was only 0.0014 g, compared to that of 0.0025 g in pure DI water. In the initial stages, the inhibition efficiency of the CQD nanoadditives was close to 60% before dropping to 27% after 9 hours of immersion, and eventually reaching 44% after 46 hours. The authors attributed these results to the formation of an adsorbed monomolecular layer of CQDs that prevented water and dissolved oxygen from diffusing to the metal surface. The non-bonding lone electron pairs of nitrogen and oxygen atoms in surface functional groups were considered to be excellent candidates for donor-acceptor interactions with the electron-deficient d-orbitals of the surface metal elements, resulting in enhanced chemical adsorption of the inhibitor.

Cui et al. <sup>249,260</sup> used electrochemical techniques to investigate the corrosion inhibiting properties and mechanisms of three different solvothermally synthesized N-doped CQDs on Q235 carbon steel in 1 M HCl solution and concluded that the CQDs were indeed adsorption-type corrosion inhibitors. Both the surface coverage and the corrosion inhibition efficiency were found to increase with increasing concentration and prolonged immersion time before eventually reaching a maximum value when the adsorption process reached equilibrium. In the case of all three N-doped CQDs, the adsorption process obeyed a Langmuir isotherm and the estimated adsorption free energy ( $\Delta G_{ads}^0$ ) indicated that interactions between the CQDs and the steel surface involved a mixture of both physisorption and chemisorption. Besides the chemisorption, owing to the lone electron pairs of heteroatoms on the CQD surface, the N-doped CQDs (synthesized from 4-aminosalicylic acid, o-phenylenediamine and p-phenylenediamine) also exhibited charge transfer character which likely enhanced the adsorption of the inhibitors further <sup>249</sup>.

As an adsorption-type corrosion inhibitor, the inhibition efficiency is highly dependent on the surface coverage of electrochemically active sites. In this regard, achieving a densely packed adsorbed layer with minimal voids between inhibitor molecules is important to prevent corrosive species from reaching the metal surface <sup>276</sup>. For this reason, conventional organic inhibitors often have bulky tail groups, whose spatial extension ensure a tightly packed monolayer above the much smaller adsorbed head groups <sup>276</sup>. Because CQDs are rigid and spherical, nanoparticle size is likely to be a critical parameter for inhibitor efficiency as it controls the size of the void between densely packed spheres. The voids between densely packed spheres of a larger size will inevitably be larger than those between smaller ones. This could be one of the reasons why the corrosion inhibition efficiency of CQDs synthesized from o-phenylenediamine (4-6 nm) was higher than that of those synthesized from p-phenylenediamine (15-20 nm) at the best performing concentration of 200 mg/L. However, it is not unlikely that the additive concentrations required for maximum corrosion inhibition efficiency under static immersion conditions are too high for the dynamic conditions of lubrication and could result in excessive abrasive wear of the very tribosurfaces they were intended to protect. Thus, this is something that would have to be considered when evaluating the applicability of CQDs as corrosion inhibiting additives in boundary lubricating conditions.

All in all, even though the high water dispersibility, good biocompatibility, and low cytotoxicity make CQDs attractive alternatives to conventional corrosion inhibitors, more research is needed to further develop our understanding of their corrosion inhibiting properties and mechanisms, as well as the influence of various operational parameters – particularly under dynamic conditions where adsorbed species are continuously removed from the metal-lubricant interface. In this regard, research into the adsorption kinetics of carbon nanostructures is of utmost importance and should be prioritized as this controls the rate of replenishment of additives at the contact interface. On the one hand, corrosion inhibiting carbon nanostructures may seem like an important step towards multifunctional lubricant

additives (i.e., one additive serving multiple purposes). However, it seems more expedient to regard CQDs primarily as friction- and wear-reducing additives and to consider any corrosion inhibiting properties they may provide as a complementary secondary effect, rather than an exemplary corrosion inhibitor in itself. That is, structural features, properties and concentrations should be optimized with respect to friction and wear performance, rather than corrosion inhibition. However, it might be advantageous to do so in a way that promote tribofilm formation since such a film is also likely to inhibit corrosion by acting a physical barrier between the metal and corrosive species.

### **3.5.2 1D Carbon Nanostructures**

While it is not inconceivable that the third-body material transfer films generated by CNTs could have some barrier properties that can shield the underlying surface from the species in the lubricant and the counter surface, such results have not been reported to date. It could very well be the case that their transfer films are too incomplete or porous to act as a meaningful barrier.

### **3.5.3 2D Carbon Nanostructures**

Despite being only one atom-layer thick, defect-free graphene has been shown to be completely impermeable to all gases and liquids <sup>280,281</sup>. For this reason, graphene-based adsorption layers and tribofilms are believed to be endowed with superior barrier properties that help to minimize the occurrence of chemical attacks by corrosive species from the lubricant system and reduce the rate of corrosion on the tribosurfaces <sup>27,151,153,207,245,282–284</sup>.

For example, Liu et al. <sup>146</sup> observed a significant reduction in the Raman signal originating from iron oxides after water-lubrication with 0.07 wt% polyethyleneimine-functionalized reduced graphene oxide (rGO), compared to the surface lubricated with pure water. This indicated that the presence of the rGO additive had a beneficial effect on reducing the oxidation of 201 stainless steel. The authors attributed this to the nanosheets forming a strong protective film on the surface that served as a solid barrier that stops corrosive species from accessing the metal surfaces of the wear tracks. Contrastingly, under pure water lubrication, the surface oxide film of the stainless steel was constantly destroyed.

Moreover, studies by Upadhyay and Kumar <sup>245</sup> and Xu et al. <sup>285</sup> suggest that graphene not only reduces corrosion of the tribosurfaces, but that it may also limit oxidation of other additives in the lubricant formula. For example, both studies report that oxidation of MoS<sub>2</sub> was restricted in the presence of graphene-based additives. While more research is needed to verify these findings, the preliminary results are intriguing. The potential interplay between carbon nanostructures and other lubricant components will be discussed in greater detail in Chapter 5.

### 3.6 FILLING AND MENDING EFFECT

Due to inherent limitations in conventional manufacturing techniques, the surface of components in industrial machinery are never completely smooth <sup>151</sup>. Instead, surfaces are irregular with numerous micro- and nanosized asperities separated by valleys. When such rough surfaces come into contact with each other under increasing load, the surface asperities are subjected to high localized contact pressure and elastic deformation. Further growth in contact pressure will eventually cause onset of plastic deformation and possibly microwelding of asperities, which are major causes of wear. Another way by which surface asperities contribute to wear is by ploughing or cutting through its countersurface, which is known as abrasive wear. When employed as lubricant additives, nanoparticles can reduce the apparent roughness of the surface by depositing in and filling up the concave areas of the contacting surfaces, as shown in Figure 3.11. This filling effect is also sometimes referred to as a mending or self-healing effect because the same process can be used to compensate for mass loss by filling in and mending wear scars in protective layers or on the tribosurface. In addition, reduced surface roughness due to the filling effect may also help to form a more continuous oil film which further enhances the lubrication performance <sup>152</sup>.

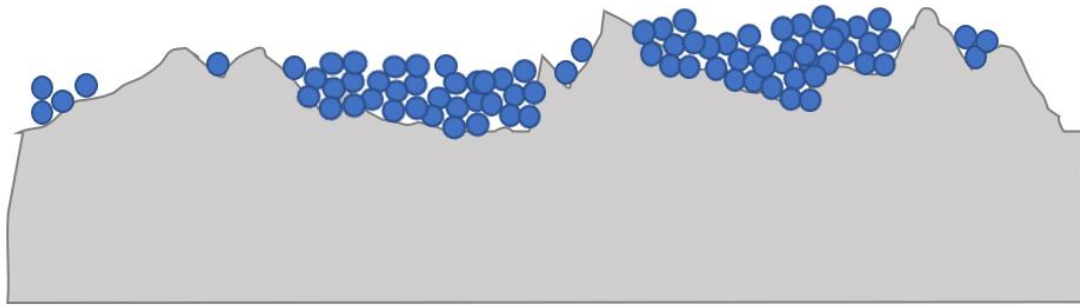


*Figure 3.11: Schematic illustration of the filling effect.*

The most important parameter for the filling and mending effect is arguably the size of nanoparticles or nanoparticle aggregates relative to the surface roughness (i.e., the size of surface valleys). If the nanostructures are small compared to the void into which they are deposited, they may conform more easily to the shape of the valley and allowing more particle to share the load. In contrast, larger particles may be too large to enter the grooves and smoothen the surface. Instead, larger particles may even effectively increase the apparent surface roughness or accelerate abrasive wear by acting as a third-body wear particle.

### 3.6.1 0D Carbon Nanostructures

Owing to their small size in all dimensions, all the 0D carbon nanostructures addressed in Section 2.1 have been credited with the ability to enhance tribological performance through the filling and mending effect when adequately dispersed and used in appropriate concentrations. For example, Tang et al.<sup>77</sup> reported that the mildly aggregated carbon dots formed at low concentrations were able to effectively collect in the nanoscale valleys and reduce wear of an amorphous carbon (a-C) surface. In contrast, the micron-sized aggregates formed at higher additive concentrations were too large to enter the voids, and instead caused excessive ploughing wear on the sliding surfaces of the mated contact. This once again illustrates the importance of nanoadditive dispersibility.

Another aspect worth considering is that reduction of wear caused by the filling effect could befall at the expense of friction performance. This is because the filling effect limits abrasive wear by increasing the interfacial contact area and reducing the high localized contact pressure of surface asperities. While this increased interfacial area is beneficial for wear reduction, it may also increase friction in some cases, as reported by Tang et al.<sup>77</sup>. They found that under extreme boundary conditions where the effect of the liquid lubricant was negligible, the friction was higher in the system where carbon dots had been added to the lubricant due to an increased contact area as a result of the filling effect. This effect was not observed under milder conditions.

### 3.6.2 1D Carbon Nanostructures

Like 0D carbon nanostructures, CNTs have been shown to deposit in cracks, valleys, and wear scars of tribosurfaces, thereby reducing their apparent roughness<sup>117,121</sup>. However, unlike 0D nanostructures that are nanoscale in all dimensions, 1D carbon nanotubes have large aspect ratios. This, along with their tendency to form large bundled aggregates, not only makes it harder for CNTs to enter the contact area, as discussed on Section 3.1 but also the small cracks and valleys on the surface<sup>121</sup>. For this reason, improved dispersion, smaller diameters and shorter lengths are believed to promote filling of the concave areas of the tribosurface and mending of wear scars<sup>121</sup>.

That being said, third-body material transfer films may also exhibit filling and mending properties. For example, Salah et al.<sup>236</sup> concluded that the presence of CNTs could smoothen the surface and minimize its roughness by forming a protective film and filling the concave areas of the tribosurfaces, resulting in reduced and less fluctuating friction values. Using SEM and AFM to characterize the worn surface after tribological testing with SAE 20 mineral base oil containing 0.5 wt% SWCNTs, Cursaru et al.<sup>268</sup> reported that the surface showed few signs of scratching and revealed that the surfaces and valleys were covered and filled with a carbon-based material. These findings show that smoothening effects may also be achieved using larger CNTs that would not otherwise fit in the surface valleys if they undergo structural collapse. In other words, in the case of larger CNTs, the wear debris is likely better suited to fill the voids and bridge the asperities of the tribosurface than intact CNTs.

### 3.6.3 2D Carbon Nanostructures

Despite the larger lateral size of 2D carbon nanostructures, the filling and mending effect have been reported as an important wear-reducing mechanism of graphene-based lubricant additives in several studies<sup>92,152,282,284,286</sup>. As established in Section 3.4.3, graphene and its derivatives are known to form excellent blanketing adsorbed layers and dense tribofilms, that may easily fill wear scars and microvalleys. So, even though the larger 2D sheets may not be able to enter nanoscale valleys like 0D carbon nanostructures can, they may still act to smoothen out nanoroughness by spanning larger areas (i.e., bridging the gaps rather than filling them). This ability of a single 2D nanosheet to smoothen out a significantly larger area than any individual 0D or 1D nanostructure, suggests graphene and its derivatives are significantly more effective at reducing the apparent surface roughness.

## 3.7 POLISHING EFFECT

Another secondary effect of solid nanoadditives is the so-called polishing effect in which surface asperities are removed or smoothened by a nanoparticle abrasion process. Since the main mechanism for material removal is third-body abrasive wear, the polishing effect is highly dependent on the mechanical properties of the nanoparticles, especially their hardness relative to the tribosurfaces<sup>287</sup>. For this reason, the polishing effect is generally only reported for nanodiamonds<sup>19,97,98,159,171,213,218,287</sup>, owing to their high hardness.

Smoothening of the tribosurfaces during the initial stages of the tribological process can reduce the duration of the running-in period and is generally accompanied by a significant drop in friction<sup>19,97,98</sup>. The friction drop is not only attributed to reduced asperity interaction, but also increased fluid film thickness ratio (i.e. ratio of film thickness to surface roughness), causing the system to shift from boundary lubrication conditions towards mixed lubrication conditions<sup>171,287</sup>. Additionally, it has been suggested that the removal of high stress concentrators (e.g. peaks of microscopic ridges) by initial polishing may reduce the occurrence of fatigue wear later on in the tribological process<sup>213</sup>.

However, the polishing effect may also have adverse effects. Firstly, if the abrasion process persists beyond the initial smoothening of the surface roughness, it may significantly increase and accelerate wear<sup>171</sup>. Secondly, the abrasive action of hard nanoparticles could compromise or influence other surface-altering running-in processes, such as the formation of protective tribofilms<sup>171</sup>. Thirdly, under harsh tribological conditions, such as high loads and high sliding velocities, hard nanoparticles could even become embedded in the comparatively softer tribosurfaces<sup>97,98,159,213,218</sup>. In this immobilized state on the surface, they could potentially act as new surface asperities of extreme strength and hardness and damage its countersurface through intensified abrasive wear. According to Ivanov and Shenderova<sup>213</sup>, experimental studies have shown that NDs exhibit a polishing effect and provide a significant reduction of wear in hard-on-soft steel-steel contacts, while they increased wear in a hard-on-hard steel contact. Thus, application of potentially abrasive nanoparticles as lubricant additives should be carefully

considered and evaluated, taking into account the relative hardness and the chemical nature of the surfaces as well as the operating conditions of the mated contact <sup>213</sup>.

### 3.8 WORK HARDENING EFFECT

Machining and tribological action are known to cause structural and chemical changes in the surface layer of metallic components due to extreme contacts stresses, deformation, frictional heat, chemical reactions, and phase transformations <sup>192</sup>. As a result, near-surface regions are endowed with properties that differ from that of the unstressed bulk material. For example, tribological transformed material is characterized by an increasingly fine grain structure closer to the surface, which is associated with increased hardness and yield strength as predicted by the Hall-Petch relationship. Another hardening effect of repeated tribological action and the associated plastic deformation is work hardening (or strain hardening) of the metal surface. In tribology, high surface hardness is often sought as it provides high resistance towards plastic deformation induced by indentation or abrasion, thereby improving resistance towards these types of wear. Obviously, this effect will be most relevant for nanodiamonds and not any other carbon nanostructure because this mechanism requires high strength and hardness. While graphene is generally considered a strong material, its flexibility and lateral size inhibit the contact pressure (load distributed over larger area) necessary to exhibit this behavior. Moreover, as explained earlier, other 0D structures and 1D structures are too fragile.

Experimental studies seem to indicate that the presence of hard nanoparticles at the rubbing interface can enhance the abovementioned hardening processes under boundary lubrication conditions, and several researchers have reported increased hardness and wear resistance on steel tribosurfaces lubricated by nanodiamonds <sup>97-99,158,159</sup>. In these reports, the increased hardness was often attributed often to work hardening and densification effects, brought on by the polishing action of nanodiamonds <sup>98,158,159</sup>, and the effect was shown to increase with increasing nanoparticle concentration in the lubricant <sup>98,99,158</sup>. In addition to enhanced work hardening and grain refining processes, it has been suggested that hard nanoparticles can increase hardness and wear resistance further through dispersion hardening by embedding in comparatively soft tribosurfaces <sup>97,99,159</sup>. Using elemental mapping techniques, Chou and Lee <sup>99</sup> revealed that the atomic carbon concentration inside the wear track was twice that of the unworn surface and attributed this to embedded nanodiamonds in the surface. They also noted that the hardening effect was more prominent in the softer AISI 1025 carbon steel, compared to the initially harder AISI 1045 steel, which could be explained by greater ease of embedding into softer surfaces <sup>99</sup>.

However, hardness and yield strength generally increase at the expense of toughness and ductility <sup>192</sup>. Thus, tribologically hardened surfaces can be quite brittle and potentially more prone to being sheared off to form fine wear debris, depending on the ductility and toughness of surface layers <sup>192</sup>. As a result, increased hardness due to grain refinement, work hardening or embedding of nanoparticles can have widely varying effects depending on the inherent properties of the tribosurface material. For instance,

hard nanoparticles embedded into a relatively soft and yielding material may reduce wear by impeding dislocation motion and limiting crack propagation<sup>98</sup> while the same nanoparticles could act as high stress concentrators and enhance wear in an already hard material<sup>213</sup>. Thus, it is important to consider the material properties of the tribosurface itself, especially in terms of hardness, toughness, and ductility, when evaluating potential benefits and adverse effects of tribologically induced surface hardening.

### 3.9 RHEOLOGICAL EFFECTS

Viscosity is one of the most important physical properties controlling the effectiveness of lubricants; thus, it is important to consider and understand how it may be affected by the addition of solid carbon nanostructures. Different fluids exhibit different viscosities and the thickness of the generated lubricating film in a contact is often proportional to it<sup>177</sup>. On one hand, lubricants should be viscous enough to maintain a sufficiently thick lubricant film to minimize contact and wear of the tribosurfaces. On the other hand, more viscous fluids require more energy to be sheared and is therefore associated with a higher energy loss in the form of friction. Moreover, lubricant viscosity is highly dependent on factors such as shear rate, temperature, and pressure. Fluids whose viscosity is independent of shear rate are called Newtonian, whereas those who exhibit a dependency are termed non-Newtonian. Most conventional liquid lubricants are assumed to behave in a Newtonian manner, however, it is worth noting that severe operating conditions like rapid and extreme pressure variations, extreme temperature variations and high shear rates may cause the fluid to deviate from Newtonian behavior<sup>4</sup>. The viscosity of liquids that are used as lubricants generally increase with increasing pressure and decrease with increasing temperature. In other words, it is important to not only consider how the addition of solid carbon nanostructures can change the viscosity, but also how it may affect the viscosity's dependencies on operational and environmental conditions such as shear rate, temperature, and pressure.

#### 3.9.1 0D Carbon Nanostructures

Numerous studies have found that the addition of nanoparticles can indeed increase the viscosity of various base fluids<sup>172</sup>. However, in the case of 0D carbon nanostructures and the concentration range of interest for application as lubricant additives, the effect of increased viscosity on tribological performance is considered to be low or even negligible<sup>38,39,77,79,210,212</sup>. That is, the slightly increased lubricant viscosity alone is simply not enough to account for the drastic increase in load carrying capacity observed when carbon nanostructures are employed as lubricant additives<sup>212</sup>. Moreover, even the viscosity's dependency on shear rate appears to remain largely unaffected by the addition of 0D carbon nanostructures at low concentrations. This is not entirely unsurprising given the small size and rigidity of 0D carbon nanostructures. To illustrate, the apparent viscosity curves and shear stress curves for deionized water and aqueous dispersions of CQDs (0.1 wt%) and GO (0.1 wt%) for shear rates ranging from 0 to 100 s<sup>-1</sup> is shown in Figure 3.12. Here it can be observed that the apparent viscosity of

deionized water and the CQDs dispersion (0.1 wt%) were considerably close and exhibited a very weak dependency on shear rate, i.e., both fluids exhibit the typical Newtonian behavior<sup>77</sup>. In contrast, the GO dispersion exhibited non-Newtonian behavior and the shear stress-shear rate relationship showed that GO nanosheets could significantly increase the viscous force of water when the shear rate exceeds 10 s<sup>-1</sup>. This difference is likely due to the large lateral size of the 2-dimensional GO nanosheets, which could potentially block or inhibit liquid flow during shear. In contrast, individual CQDs are small, spherical, and rigid, making them less able to inhibit or affect lubricant flow to any significant extent. That being said, poor dispersion stability may lead to the formation of larger aggregates and sediments that may influence rheological properties to a greater extent.

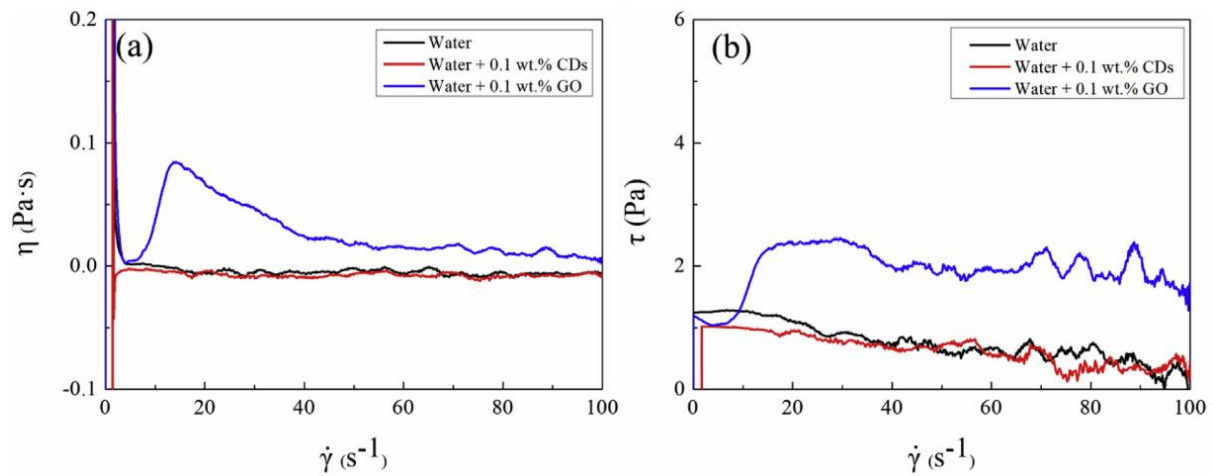


Figure 3.12: The (a) apparent viscosity curves and (b) shear stress curves of deionized water, CDs solution (0.1 wt%), and GO dispersion (0.1 wt%) with increased shear rate<sup>77</sup>.

Many experimental studies investigating how the addition of 0D carbon nanostructures affect the viscosity-temperature relationship of lubricants have concluded that the nanoparticles have little effect<sup>38,39,79,210</sup>. That is, the slight increase in viscosity caused by the nanoadditives is comparable at both low and high temperatures (typically measured at 40°C and 100°C), meaning that the overall viscosity-temperature behavior remains the same. However, even though the viscosity's dependency on temperature is relatively unaffected, the actual temperature of the lubricant in the contact may be altered by the addition of nanoparticles. Firstly, the reduced interfacial contact area caused by the addition of hard spherical nanoparticles is associated with reduced frictional heating of the tribosurfaces and adjacent lubricant layers<sup>218,233</sup>. Secondly, the addition of nanoparticles have been found to influence thermophysical properties of the lubricant, especially the thermal conductivity and specific heat<sup>172,288</sup>. An increase in the thermal conductivity of a lubricant means that heat transfer occurs at a greater rate so that better cooling is achieved<sup>172</sup>. The specific heat also contributes to the heat transfer performance of the lubricant, and may increase or decrease depending on the specific heat of the nanoparticles themselves<sup>288</sup>. The combined effect of these contributions means that the temperature of the lubricant

in the contact may be significantly reduced even though the viscosity-temperature relationship remains unchanged. Hence, under equal lubricating conditions, a lubricant containing nanoparticles is likely to experience an overall lower temperature, thus the viscosity will likely be higher and the fluid film thicker.

Under increased loading or high pressures, another effect of solid nanoadditives in the lubricant becomes evident in the form of significantly increased load carrying capacity. Ku et al.<sup>39</sup> added 0.1 vol% fullerene nanoparticles to five different naphthalene mineral oils with varying viscosity grades, and evaluated the extreme pressure properties of the lubricants using a four-ball tester. They observed that the weld points (i.e., the lowest applied load at which the rotating ball either seizes and welds to the three stationary balls, or at which point extreme scoring of the three balls occurs) of the oils with and without fullerene nanoparticles increased with increasing viscosity and viscosity grade. The weld points of the lubricant containing nanoparticles were always significantly higher than those of the pure base oil. The relative increase in weld point due to the addition of fullerene was found to be more significant at lower lubricant viscosities, indicating that fullerene played a more prominent role at low viscosities. The authors attributed this to increased load carrying capacity owing to the mechanically separating effect of fullerene nanoparticles between the surfaces. However, while this is likely to be the main cause of the enhanced load carrying capacity of the lubricant, the possible contribution of increased lubricant viscosity due to pressure in the heavily loaded and non-conformal contact was not considered. Since the viscosity generally increases with increasing loads, it is therefore of practical importance to assess and quantify the pressure-viscosity behavior of any lubricant in order to assess its effectiveness inside the system under varying degrees of operating pressures.

Hu et al.<sup>289</sup> performed molecular dynamics simulations to investigate the interactions between nanoparticles and the base fluid and reveal the effect of nanoparticles on the frictional behavior of lubricant films under shear stresses and loading. They found that both the base fluid and the nano-formulated fluid underwent a liquid-solid transition under high loads, however, the transition pressure of the nano-formulated fluid was considerably higher than that of the pure base fluid. This was mainly attributed to the volume effect of nanoparticles, which increases the load carrying capacity of the lubricant film by increasing its compressive strength and preventing excessive film thickness reduction under heavy load, and the micromotion of the nanoparticles. In agreement with previous studies<sup>290,291</sup>, Hu et al.<sup>289</sup> found that, besides the main flow, the nanoparticles have rotations and translations that could strengthen the partial flowing in the fluids containing nanoparticles. In other words, when the load is high, the random micromotions of the nanoparticles are believed to enhance the liquidity of the lubricant film and prevent early solidification. In this way, nanoparticles could potentially enhance the flow properties of lubricants under higher loads and increase the operating window of the lubricant in terms of pressure. Furthermore, given a constant volume concentration, the number of nanoparticles would increase drastically with decreasing nanoparticle radius, and the combined effect of nanoparticle

micromotions would be stronger. Therefore, the transition pressure and load carrying capacity is likely to increase with decreasing nanoparticle size.

In summary, even though the slight increase in viscosity caused by individual 0D nanoparticles is not considered to be particularly significant, the combined effect of enhanced thermal transport properties and increased load carrying capacity help to stabilize the rheological characteristics of the lubricating film across a wider range of operating conditions<sup>98,265</sup>. It is also worth noting that increased load carrying capacity without an accompanying increase in viscosity is of great interest as it may allow for improved antiwear performance without the increased energy losses associated with higher viscosity<sup>39</sup>.

### 3.9.2 1D Carbon Nanostructures

Like in the case of 0D carbon nanostructures, the change in viscosity caused by the addition of CNT additives is generally small enough to be considered negligible in the concentration range suitable for lubrication purposes<sup>236</sup>. Neither does the addition of CNT additives affect the viscosity-temperature relationship of the lubricant to any significant extent<sup>236,266,292–294</sup>. In response to shear rate, however, the rheological behavior of various CNT-based lubricants have been shown to vary. These variations are not entirely unsurprising and can likely be explained in terms of CNT aspect ratio, state of dispersion and the nature of functionalization. Firstly, due to the high aspect ratios, individual CNTs are likely to provide varying resistance towards lubricant flow depending on their relative orientation with respect to the flow field<sup>295</sup>. However, when subjected to shear, the CNTs may eventually rearrange themselves to accommodate the applied flow, resulting in the formation of nematic phases of reduced viscosity<sup>296</sup>. For this reason, dispersions of CNT tend to exhibit non-Newtonian shear thinning behavior<sup>294,297</sup>, particularly at high concentrations<sup>296</sup>. Breakup of larger aggregates under the influence of shear could also contribute to shear thinning behavior<sup>295</sup>. In addition to CNT length, the viscosity of dilute CNT dispersions have been found to correlate with the degree of bundling<sup>296</sup>. This is because, larger particles and aggregates are more likely to cause disturbances in the lubricant flow field. Similarly, electrostatic or steric repulsion between functionalized particles define an excluded volume that is not accessible to other particles, which also increases the effective particle volume and hence its influence on lubricant viscosity<sup>297</sup>. As an example, Lijesh et al. reported that the viscosity of a lubricant containing surfactant dispersed MWCNTs was the highest among all samples analyzed<sup>13</sup>.

Alirezaie et al.<sup>292</sup> investigated the rheological behavior of 50SAE engine oil containing a hybrid nanoadditive comprised of carboxylated MWCNTs and MgO nanoparticles in a 10:90 ratio in response to temperature, shear rate and nanoparticle concentration. Herein, the MWCNTs had a diameter of 10–30 nm and a length of 10  $\mu\text{m}$ , and the dispersion was reported to remain stable for more than 6 days. At low temperatures and higher concentrations, the nano-formulated fluids exhibited slight non-Newtonian behavior in the form of shear thinning. However, the effect was not very drastic, and the behavior was reported to become entirely Newtonian at higher temperatures. In contrast, Cornelio et al.<sup>266</sup> found that

oil containing carboxylic acid-functionalized MWCNTs and SWCNTs exhibited shear thickening behavior up to shear rates of  $30 \text{ s}^{-1}$  before establishing Newtonian behavior at higher shear rates. Herein, the shear thickening effect at lower shear rates was attributed to rearrangements in the distribution of CNTs in the fluid. In this case, it was also observed that the viscosity was independent of time for all the samples analyzed.

Wang et al.<sup>293</sup> covalently functionalized MWCNTs with an imidazolium-based ionic liquid to enable stable dispersion in 1-butyl-3-methylimidazolium hexafluorophosphate. Herein, the diameter and length of the MWCNTs were 20-40 nm and 5-15  $\mu$ , respectively, and the rheological behavior of the resulting lubricant was similar to that of surfactant worm-like micelle systems. The authors attributed this to the high aspect ratio and flexibility of the CNTs, as well as their ability to form a transient network through nanotube-nanotube interactions and nanotube-matrix interactions. At rather low concentrations ( $<0.04 \text{ wt}\%$ ) the lubricants exhibited shear thinning behavior at low shear rates and Newtonian behavior at higher shear rates. This reflects the characteristics of the pure ionic liquid base fluid, which could be described as a structured liquid of polymeric hydrogen-bonded supramolecules. At higher concentrations (0.06-0.1 wt%), the shear thinning properties of the lubricant extended over a wider shear rate range, indicating the formation of a transient network, before eventually exhibiting shear thickening behavior above a critical shear rate. Here, the different behavior at high and low shear rates were attributed to aggregation and entanglement of MWCNTs at low shear rates, and deformation and alignment at shear rates. From these examples, it should be evident that the viscosity-shear rate behavior of CNT-containing lubricants can vary widely depending on CNT properties, dispersibility, surface chemistry and base fluid properties.

As mentioned in Section 3.9.1, reducing lubricant temperature in the contact can enhance the lubricant film thickness by increasing the viscosity of the oil. Since the thermal conductivity of fluids is conspicuously higher than that of the pure base fluid<sup>250,294</sup>, the addition of nanoparticles can improve the tribological performance of the lubricant by promoting dissipation of frictional heat<sup>298</sup>. CNTs are believed to be particularly suited for this due to their extraordinarily high thermal conductivity<sup>299</sup>. Choi et al.<sup>300</sup> dispersed up to 1 vol% MWCNTs with a mean diameter of  $\sim 25 \text{ nm}$  and a length of  $\sim 50 \mu\text{m}$  in synthetic polyalphaolefin oil and reported that the thermal conductivity was not only anomalously greater than theoretical predictions, but also non-linear with nanotube loading. Ettefaghi et al.<sup>301</sup> reported that both the viscosity and thermal conductivity of SAE20W50 engine oil were directly correlated to the MWCNT concentration, and that the addition of just 0.5 wt% increased the thermal conductivity of the oil by 22.7%. However, it was also noted that such high concentrations led to deterioration of the biological properties due to excessive agglomeration of MWCNTs in the lubricant. While it is evident that the addition of CNT-based nanoadditives can improve the thermal transport properties of lubricants, it is also worth noting that while use of stabilizing surfactants solve the problem

of aggregation, it has also been shown to reduce the thermal conductivity and efficiency of nanoparticle-containing fluids <sup>163,292,302</sup>.

### 3.9.3 2D Carbon Nanostructures

Due to the large lateral size, 2D carbon nanostructures can influence the flow field and hence the viscosity of the lubricant to a greater extent than 0D and 1D carbon nanostructures <sup>77,162,163</sup>. For this reason, the concentration, sheet size and shape of 2D carbon nanostructures have been identified as critical parameters determining the rheological properties of lubricants containing graphene or its derivatives <sup>163</sup>. For instance, Park and Kim <sup>303</sup> found that the viscosity increase caused by the addition of 0.01 vol% graphene with an average particle diameter of 15  $\mu\text{m}$  was about 16% at room temperature, which was 1.2 times higher than that graphene with a smaller average particle diameter of 5  $\mu\text{m}$ . As for the temperature dependency of viscosity, lubricant fluids containing graphene and its derivatives show a downward trend with increasing temperature, just like their base fluids <sup>162</sup>. However, in terms of the relative viscosity, which was defined as the ratio between the viscosity of the nanoparticle-containing fluid and the corresponding base fluid at the same temperature, Hamze et al. <sup>162</sup> reported that varying effects of temperature have been observed (i.e., the relative viscosity has been observed increase, decrease or remain unchanged with increasing temperature). These variations can likely be contributed to the different rheological properties of the base fluid as well as differences in graphene properties such as sheet size, number of layers, interlayer distance and surface chemistry.

As with 1D carbon nanostructures, the higher dimensionality of 2D carbon nanostructures can give rise to non-Newtonian behavior in response to shear. Specifically, nano-formulated fluids of graphene and its derivatives tend to exhibit shear-thinning behavior at low shear rates and the effect becomes more evident at higher nanoparticle concentrations <sup>162</sup>. The shear-thinning behavior is generally attributed to the gradual alignment of the 2D nanostructure within the flow field with increasing shear, which results in decreased momentum transfer between adjacent fluid layers and lower viscosity <sup>152,163</sup>. It has also been speculated whether viscous drag force could be sufficient to facilitate shearing of the lamellar structure of layered 2D carbon nanostructures during lubrication (i.e, taking advantage of the self-lubricating properties and interlaminar shear mechanism of graphene and its derivatives), and whether this may contribute to the observed shear-thinning behavior <sup>145,304</sup>. At an optimized concentration of 0.2 mg/mL reduced graphene oxide (rGO) in PEG, Gupta et al. <sup>145</sup> achieved a low friction coefficient of 0.06 and a wear reduction of about 50% without the formation of a deposited graphene-based surface film in the contact region. Instead, the excellent lubrication performance was attributed to a freely suspended network of PEG intercalated and aligned rGO sheets, as shown in Figure 3.13. The rGO were believed to interact with PEG molecules through hydrogen bonding and reduce friction through interlaminar sheets. This effect was lost at higher concentrations, as illustrated in Figure 3.13(c), due to agglomeration and subsequent loss of alignment.

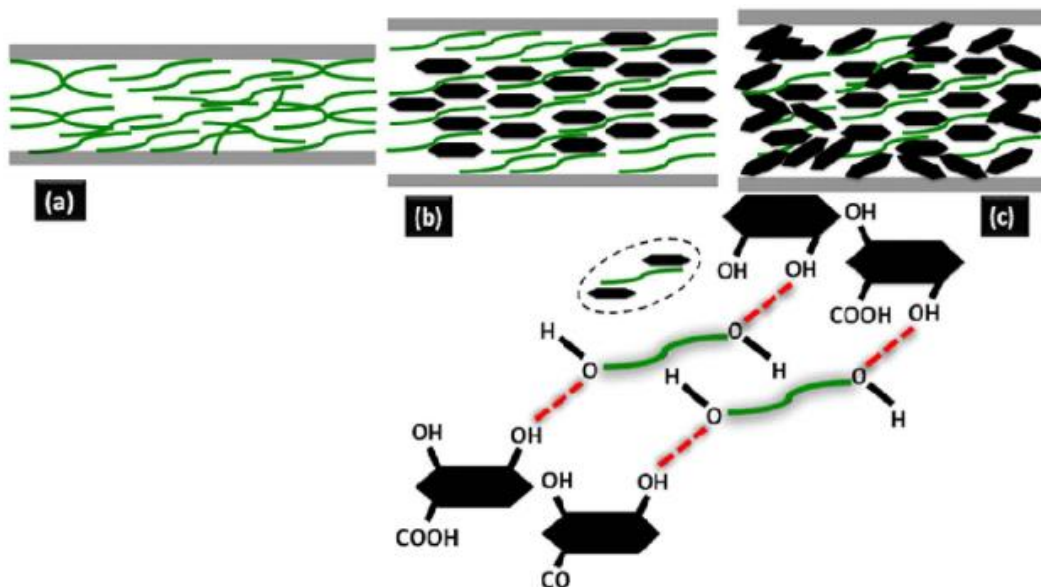


Figure 3.13: Lubrication mechanism of a steel-steel contact lubricated by (a) pure PEG, (b) 0.2 mg/mL rGO in PEG, and (c) 1.0 mg/mL rGO in PEG <sup>145</sup>.

Stable and homogeneous dispersion of solid carbon nanostructures is generally achieved through covalent or non-covalent functionalization, as will be addressed in greater detail in Chapter 4. However, it is worth noting that surface functionalization or use of surfactants will also influence the rheological behavior of nano-formulated fluids <sup>162</sup>. As mentioned in Section 3.9.2, stabilizing functional groups or dispersing agents increases the effective nanoparticle volume by defining a volume from which neighboring nanoparticles are excluded, which in turn increases viscosity further by providing more resistance to flow. Hamze et al. <sup>162</sup> reported that comparable concentrations of different surfactants could provide varying degrees of viscosity enhancement, or cause changes in the Newtonian or non-Newtonian behavior of the dispersions. Sarsam et al. <sup>305</sup> found that the shear-thinning tendency of water-based graphene fluids could be considerably reduced through use of an appropriate amount of surfactant. Moreover, since surface chemistry of 2D carbon nanostructures dictate interactions with surrounding lubricant molecules, the presence of chemically active surface functional groups may influence their mobility, and hence the apparent viscosity of the lubricant. One example of this is the aforementioned study by Gupta et al. <sup>145</sup> in which the reduced graphene oxide interacted with the surrounding PEG molecules by hydrogen bonding. Another example is a study by Park and Kim <sup>303</sup> who reported that viscosity increase caused by the addition of 0.01 vol% oxidized graphene was about 60% lower than that of non-oxidized graphene with the same average particle diameter (5  $\mu\text{m}$ ).

As with 0D and 1D carbon nanostructures, graphene and its derivatives have been shown to significantly improve the thermal transfer properties of the fluids into which they are dispersed <sup>162,163,296</sup>, however, graphene-containing fluids generally exhibit better thermal conductivity than CNTs at equal volume concentrations <sup>163</sup>. The thermal transfer properties of both graphene and graphene oxide nanofluids have

been shown to increase with increasing nanoparticle concentration <sup>163,306</sup>, however, the nanoadditive concentration should likely be optimized with respect to friction- and wear performance rather than thermal conductivity. Research into the influence of sheet size and surface functionalization on the thermal transport properties of nano-formulated lubricants have yielded conflicting results <sup>163</sup>. Thus, future developments in this area could provide better insights into the effects of nanoparticle size and surface chemistry on the coolant properties of nanoparticle-containing lubricants. It is also vital to investigate the effect of surfactants on the thermal transport properties of such fluids since various studies have shown diverse effects of surfactants <sup>163</sup>.

It is possible to argue that the small changes in viscosity and deviation from Newtonian behavior caused by the addition of carbon-based nanoadditives are likely not of great concern under boundary lubrication conditions where the influence of lubricant viscosity is less significant. However, it illustrates that even though carbon nanostructures are primarily considered to be a surface-active friction- and wear reducing additive for applications in boundary lubrication, they may also influence hydrodynamic lubrication in which viscosity is the dominating factor in the friction force and load-bearing capacity of the lubricant <sup>152</sup>. Moreover, even though changes in rheological behavior are not considered to be of great importance under boundary lubrication conditions, the effect of enhanced thermal transfer properties could be significant. Hence, efforts that improve our understanding of how the morphological and chemical characteristics of carbon nanostructures affect the cooling properties of lubricants are welcomed.

### **3.10 CHAPTER SUMMARY AND COMPARISON**

By now it should be evident that carbon nanostructures are a very big family of materials with widely different properties, and that this influences the mechanisms by which they can reduce friction and wear when employed as lubricant additives. A prerequisite for all additives in a lubricated system is that they are present in the interfacial contact area. However, how they reduce friction and wear once inside the contact mostly depends on the structural morphology as well as the mechanical and chemical properties of the additives. Generally, carbon nanostructures can be divided into two main groups depending on whether or not they have a planar and lamellar structure that can undergo interlaminar shear. This first group includes the 2D carbon nanostructures and 0D graphene quantum dots (GQDs). The second group of non-lamellar structures can also be divided into two subgroups depending on whether their mechanical and chemical properties are likely to allow nanoparticle rolling between the tribosurfaces or not. The carbon nanostructures that cannot roll tend to undergo structural collapse and form surface films with various properties instead. The following paragraphs aim to briefly summarize some key aspects of the lubrication performance of each type of carbon nanostructure reviewed for this thesis. Lastly, some general remarks about how these differences are likely to influence suitability for various lubrication applications will follow.

Even though  $C_{60}$  fullerene have been shown to reduce both friction and wear, most studies on fullerene tend to highlight the high load-carrying capacity and increased weld load of fullerene-enriched lubricants<sup>35–37,39</sup>. However, since few studies have attempted to characterize the state of fullerene after tribological testing, there is little experimental evidence on ability of fullerenes to retain their structure. Even though some MD simulations have shown that fullerene rolling is theoretically possible between certain surfaces under very low loads, it is more likely that  $C_{60}$  undergoes structural degradation. This is because its small radius of curvature imposes a certain structural strain, which makes  $C_{60}$  prone to bond-rearrangement as a means of strain reduction under compressive loads. This tendency for interfacial bonding with the tribosurfaces is believed to lower mobility and make it susceptible to further friction-induced degradation. This type of behavior has also been confirmed by MD simulations. In other words, it is considered likely that the observed friction and wear reduction, and especially the increased weld load, is attributable to the presence of fullerene wear debris rather than intact spherical nanoparticles.

The ball bearing abilities of CNOs are supported by MD simulations as well as the presence of intact CNOs after tribological testing in certain experimental studies. However, CNOs have also been shown to undergo varying degrees of structural degradation under higher loads. Depending on the operating conditions, descriptions of tribologically transformed CNOs in the literature range from mostly intact and slightly deformed<sup>53</sup>, to ‘smashed’<sup>55</sup>, graphene-like or amorphous<sup>307</sup>. However, what kind of friction and wear behavior corresponds to what kind of structural state remains unknown, i.e., whether intact CNOs or CNO-based transfer material most beneficial to improve tribological performance. In some instances, the onset of steady-state low friction seems to coincide with structural degradation and the formation of a transfer film at higher loads<sup>55</sup>, but this is something that requires further investigation. It is also worth mentioning that knowledge of the lubrication performance of CNOs is likely to be somewhat swayed by the fact that most studies on the matter have been done by the same group using the same CNOs, in the same base oil, in the same tribosystem, and under the same operating conditions<sup>52–55</sup>. Thus, examining the behavior of CNOs in response to changes in these parameters would be of interest. Moreover, there are still no studies available in which CNO additives have been functionalized in any way, and the dispersion stability of pristine CNOs in the already-published studies is rarely disclosed. This is a gap in our understanding of CNO additives that should be filled.

Despite being one of the most recently discovered carbon nanostructures, CQDs have attracted considerable interest and have been shown to perform excellently as a lubricant additive. While many studies attribute its tribological performance to the ball bearing mechanism, there is still no theoretical or experimental evidence to support this claim. That is not to say it is not possible, but rather that this is something that should be explored further. Compared to many of the other carbon nanostructures, as-prepared CQDs generally have a considerable amount of surface functional groups. This not only improves dispersibility in the lubricant but is also believed to promote adsorption of CQD additives

onto the tribosurfaces. This is believed to contribute to the formation of a more extensive and strongly bonded adsorbed layer. The more chemically reactive surface functional groups also lend themselves excellently to further chemical modification and are believed to increase the likelihood of tribofilm formation. In this regard, a better understanding of the nature of tribofilm formation and how the adsorption process influence lubrication behavior is likely to be of great benefit in future research on CQD lubricant additives. Either way, the excellent preliminary results and highly tunable surface chemistry makes CQDs a very promising candidate for future lubricant additives.

Already back in 1996, it was established that nanodiamonds can have excellent friction-reducing, antiwear and load-bearing capacity<sup>97</sup>. The outstanding load-carrying capacity can in large be explained in terms of the superior mechanical strength of nanodiamonds. However, this high hardness also presents one of the biggest challenges in using nanodiamonds as lubricant additives. That is, under harsh tribological conditions, in terms of load and sliding speed, the tribosurfaces are more likely to yield than the nanodiamonds. In some cases, this may contribute with beneficial secondary effects such as work hardening or polishing during the running in period. However, in other cases, it may also severely aggravate abrasive wear, or cause either indentation or embedding. Some studies have also suggested that the abrasive nature of nanodiamonds may negatively impact other beneficial running-in processes, while others have claimed positive effects. Either way, the nature of the abrasion process has been found to be highly sensitive to small changes in concentration and operating conditions which may pose a problem for real life applications. More studies are needed to discern the unintended consequences of nanodiamond abrasion and the factors that promote it.

The lubrication performance of CNTs is routinely attributed to the rolling bearing mechanism. However, based on the mechanical properties of CNTs, their poor dispersibility, characterization after tribological testing, and the few fundamental studies available, this is deemed to be highly unlikely. CNTs have been shown to deform even under the influence of weak van der Waals forces<sup>244</sup> and is unlikely to bear any considerable weight in its intact tubular state. At best, CNTs may be able to move similarly to a bulldozer belt, as described by Ni and Sinnott<sup>240</sup> and illustrated in Figure 3.14, for a very short while before cross-linking and undergoing structural degradation. The resulting wear debris may deposit on the surface to form a transfer film of significantly varying performance – depending on properties such as adhesive and cohesive strength, roughness, and structural morphology. Some graphene-like wear debris have been observed among the degraded nanostructures in the case of MWCNTs, but their potential contribution to lubrication remains largely unexplored. Based on the difficulty of dispersing CNTs, their tendency to degrade, and the very inconsistent tribological performance of the resulting transfer material, it is possible to argue that CNTs are a less versatile additive than some of the other carbon nanostructures. This is probably the reason why research interest in CNTs has dissipated in the last decade. The same can arguably be said for fullerenes and CNOs as well.

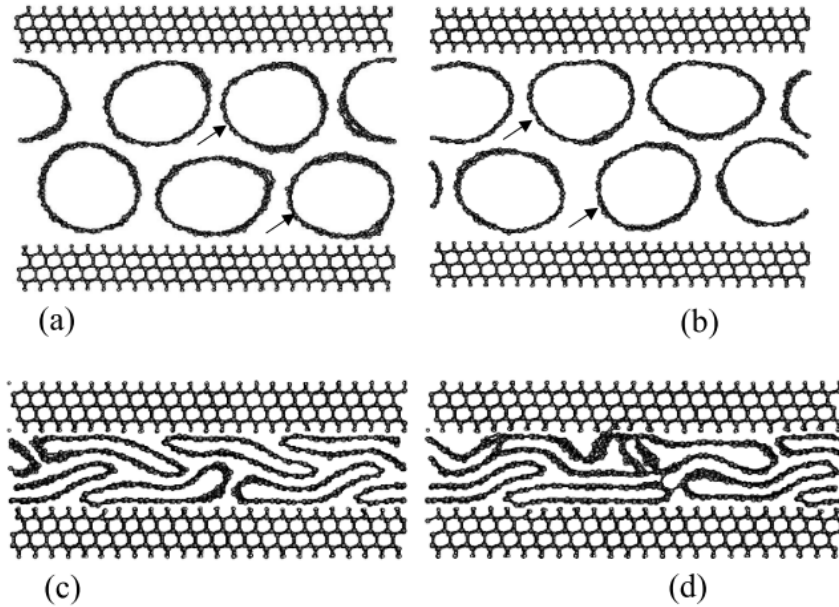


Figure 3.14: Snapshots from simulations that examine the sliding of the topmost diamond surface on horizontally arranged nanotubes at different at different compressional loads: (a) and (b) are at a pressure of 0 GPa; the arrows act as markers showing how the positions of two of the nanotubes changes as they slide; (c) and (d) are with a pressure of 13.7 GPa<sup>240</sup>.

As mentioned in Section 2.1.4, research into 0D graphene quantum dots (GQDs) as lubricant additives is severely limited. Nevertheless, their preliminary results are promising and warrants further research. Meanwhile, 2D graphene-based lubricant additives and their interlayer shearing mechanisms are arguably the most extensively studied. There are several studies, both theoretical and experimental, that have systematically investigated the influence of parameters such as degree of exfoliation, sheets size and surface chemistry. However, there are still quite a few aspects of graphene-based lubrication that remain uncertain. For example, the friction- and wear reducing contribution from each mechanism and the interplay among mechanisms is still not fully understood. For instance, on the one hand, we know that dangling bonds, defects, and certain surface functional groups are factors that can reduce the mechanical strength and wear resistance of graphene-based adsorption films and make them more prone to friction-induced damage during lubrication. On the other hand, such structural features are also associated with enhanced adsorption which may promote the formation of a more adhesive protective film. They may also increase tribochemical activity and the likelihood of tribofilm formation. Thus, the potential benefits and drawbacks caused by the inclusion of such structural elements is likely something that would have to be outweighed, balanced, and considered, depending on the application.

Understanding how the different types of carbon nanostructures work and which lubrication mechanisms are active or dominant under various conditions is likely to be an important step towards evaluating their suitability for various applications or lubrication scenarios. For example, experimental studies have shown that the friction of CNTs tend to increase with increasing loads<sup>117,182</sup>, indicating

that CNT additives are more effective at low loads. In contrast, graphene-based additives generally exhibit the opposite trend (i.e., decreasing friction with increasing loads) <sup>145,182</sup>. This observation is supported by Sun et al. <sup>308</sup> who, by means of first-principle calculations, showed that the sliding friction of a graphene-graphene system can decrease with increasing normal load and drop to nearly zero at a critical point. This unusual drop in friction was attributed to an abnormal transition of the sliding potential energy surface from corrugated, to substantially flattened, and eventually to counter-corrugated states. In other words, various lubrication mechanisms are active under different conditions and respond differently to changes in conditions.

For example, carbon nanostructures whose lubrication performance is highly dependent on strong adhesion to the tribosurfaces may not be appropriate for tribosystems with relatively inert surfaces. Tang et al. <sup>77</sup> attributed the relatively poor lubrication performance of water-dispersed graphene oxide (GO) to insufficient adhesion to the inert amorphous carbon (a-C) tribosurfaces. Because of the low adhesive strength, the GO nanosheets could not remain stably on the surfaces and were instead pushed out of the contact region, as illustrated in Figure 3.8. The ejected GO nanosheets accumulated along the wear track edges, which resulted in increased friction over time due to restricted lubricant flow. In contrast, the ball bearing mechanism of 0D nanostructures would likely benefit from the low adhesive strength and high mobility on more inert surfaces.

Based on preliminary results, it is also possible to argue that self-lubricating structures such as graphene are likely to be more suitable for applications and systems where dry friction or sustained periods of dry friction are more likely to occur. Since the interlayer shearing mechanism of graphene has been shown to remain active even in dry, inert and vacuum environments <sup>27</sup>, graphene-based lubricant additives can perform excellently even in when the lubricant has been completely squeezed out of the contact <sup>245</sup>. This is unlike non-lamellar materials that are generally dependent on lubricant wedge films to facilitate nanoparticle motion or prevent structural deterioration in the contact area <sup>245</sup>.

## 4 FUNCTIONALIZATION OF CARBON NANOSTRUCTURES

---

For lubricating nanostructures to be effectively transported into the contact area, they need to be homogeneously and stably dispersed in the base fluid. However, as established in Section 3.1, this is made challenging by their tendency to agglomerate in most base fluids, especially when subjected to changes in temperature and pressure<sup>13</sup>. This does not only render them too large to enter the contact area, but is also associated with a higher sedimentation rate, which further compromises the dispersion stability<sup>174</sup>. Thus, surface functionalization of carbon nanostructures in order to achieve stable dispersion and ensure homogeneous distribution of additives in the lubricant base fluid is critical for their application as lubricant additives. In this context, carbon nanostructures with inherent oxygen moieties, like graphene oxide (GO), can be considered as an already functionalized derivative of a pristine structure with appreciable affinity and dispersibility in several polar base fluids, including water.

Surface functionalization of carbon nanostructures can be classified as either covalent or non-covalent, depending on the nature of the bond between the nanostructure and the functional group<sup>131,309,310</sup>. Covalent functionalization is characterized by a formation of a strong covalent bond, while non-covalent functionalization is based on weaker interactions, such as electrostatic interactions or  $\pi$  effects<sup>310</sup>. For applications where the electronic structure of the material is important, the non-covalent approach is attractive because it preserves the original bonding and hybridization of the nanostructure, whereas the formation of a covalent bond is accompanied by rehybridization. In graphene, for instance, this entails a transition from  $sp^2$  to  $sp^3$  hybridization. Another advantage of non-covalent functionalization is the dynamic nature of bonding, which could potentially allow for continuous detachment and spontaneous re-adsorption of functional groups during the tribological process. Moreover, given sufficient availability of spontaneously adsorbing surfactants in the lubricant, the nanostructure could theoretically be re-functionalized *in situ* which is especially beneficial under harsh tribological conditions where ligands may be damaged or degraded. Covalently bonded functional groups, on the other hand, are generally grafted onto the nanostructure during synthesis without the possibility of replenishment during the tribological process. Both covalent and non-covalent approaches are found in recent literature, and there are numerous examples of surface functionalized carbon nanostructures improving the tribological performance of various lubricants. The investigated functional groups range from simple oxygen functional groups (e.g. graphene oxide) to large polymeric moieties (e.g. hyperbranched polyamine ester<sup>311</sup> and polymeric aryl phosphates<sup>312</sup>).

While the primary focus of functionalization for a long time has been to enable and enhance the dispersibility of nanoadditives, the extensive research on the topic in the last years has led to the identification of several other potential benefits of surface modification. For instance, surface modification is inevitably accompanied by a change in the nanoparticle's ability to interact with its

surrounding environment, most often in the form of reduced chemical inertness and increased chemical reactivity. Since the interactivity of a nanoadditive is closely related to its affinity and ability to adsorb on the friction surfaces, this will also influence the performance of the nanostructure as a friction-reducing and antiwear additive. In addition to changes in adsorptivity, surface functionalization of an additive can influence the overall wettability of the lubricant on the moving surfaces, which in turn may affect the lubrication regime of the tribosystem. Consequently, through considerate selection of functional groups, it is possible to synthesize carbon-based nanoadditives with more favorable adsorption and wetting characteristics, which may improve the tribological performance of the lubricant beyond the contribution of the carbon nanostructure alone.

Moreover, it has been found that friction-induced degradation of functional groups under harsh tribological conditions may allow certain functional groups to undergo tribochemical reactions, resulting in tribofilms with better friction and wear characteristics than what would have been produced in the absence of these chemical species. Another interesting approach for improving the performance of carbon-based friction-modifying and antiwear additives involves combining nanostructures of different dimensionality to obtain a hybrid nanostructure that make use of the characteristic lubrication mechanisms of its components. Lastly, the great potential of carbon nanostructures to act as carrier materials have led some researchers to functionalize carbon-based nanoadditives with structures that provide additional properties, such as antioxidative moieties, which is an important step towards deliberate development of multifunctional additives. With greater understanding of the underlying lubrication mechanisms of carbon nanostructures, these findings could possibly be exploited to develop the lubricant additives of the future. The following sections use relevant examples from recent experimental literature to elaborate on the abovementioned ways by which surface functionalization can contribute to the improvement of tribological properties.

#### **4.1 ACHIEVING DISPERSIBILITY AND ENHANCING ADSORPTIVITY**

There are two main mechanisms through which surface functionalization of nanostructures can enhance dispersion stability and inhibit agglomeration, namely steric stabilization and electrostatic stabilization<sup>98</sup>. The latter involves functionalizing the nanostructures with electrostatically repulsing surface functional groups such as ionogenic groups or adsorbed ions. Their presence increases the apparent surface charge of the structure and the thickness of its electrical double layer, such that if two particles are brought into proximity, the enhanced electrostatic repulsion between them may counteract the attractive van der Waals forces. Steric stabilization, on the other hand, prevent agglomeration due to the spatial extension of long functional groups, typically polymers, on the surface of the nanostructure. Together, these polymeric functional groups form a brush-like layer which shields the particles from attractive interactions and provides a repulsive force due to pure steric effect. The steric repulsion can be attributed to energetically unfavourable loss of configurational entropy as the brush-like layers

penetrate in close proximity. Electrostatic and steric stabilization mechanisms can also be combined in a so-called electrosteric approach by selecting large sterically hindering groups with functional terminations that repel each other, such as a polyelectrolyte <sup>98</sup>.

The improved dispersibility of functionalized nanostructures in a lubricant medium can also be understood as providing the nanostructure with functional groups that have appreciable affinity to the surrounding liquid, meaning it is more energetically favorable for the nanostructure to be dispersed and surrounded by liquid rather than aggregated and sedimented. This enhanced affinity towards the liquid is generally accompanied an increase in general chemical activity, also towards the tribosurfaces. This is generally sought in friction-reducing and antiwear additives whose working principle is dependent on being present on the tribosurface interface. Moreover, the enhanced affinity has been found to have a positive effect on the protective film formation process as the associated increase in adsorptivity has the potential to shorten the running-in period, due to faster establishment of a physical adsorption film, in addition to providing a denser and more cohesive film with better adhesion to the substrate.

For instance, Hu et al. <sup>201</sup> covalently grafted amino-containing polyethylene glycol (PEG) onto the surface of carboxylated graphene nanosheets through facile amidation under mild conditions to enable stable dispersion. Based on UV-vis adsorption spectroscopy results, it was estimated that functionalization with PEG increased the dispersibility of carboxylated graphene from 0.201 mg/mL to 0.326 mg/mL. At the optimal concentration of 0.05 wt%, the friction and wear rate of the tribopair consisting of a Si disc and an Al<sub>2</sub>O<sub>3</sub> ball was reduced by 38.5% and 81.23%, respectively, compared to pure water. Moreover, the functionalized graphene dispersion consistently outperformed dispersions of unfunctionalized carboxylated graphene. The superior friction-reducing and antiwear performance was attributed to the enhanced dispersibility due to the amino-containing PEG groups forming a brush-like layer which provided resistance towards aggregation. In addition, the PEG moieties had significant affinity towards the tribosurfaces, thereby promoting the formation of an adsorbed protective film on the tribosurfaces.

Lee et al. <sup>159</sup> modified the surface of hydrophilic nanodiamonds (NDs) with oleic acid to enhance dispersion stability and avoid severe aggregation in oil. The oleic acid was found to be chemisorbed to the NDs as a carboxylate ion and its presence rendered the nanodiamond surface hydrophobic enough to be stably dispersed in commercial Shell Helix HX7 oil for more than 10 days. Due to the spatial extension and weak repulsion among the functional groups, this surface modification reduced the average particle size of NDs in the oil from 268.6 nm to 20.1 nm by breaking down large aggregates of primary nanoparticles into smaller ones. The addition of 0.05 wt% modified NDs was found to reduce friction by 23% compared to the pure lubricant and the tribosurface barely exhibited any wear. The lower friction coefficient was attributed to the excellent intrinsic tribological properties of the NDs, the smaller average particle size of 20.1 nm, and the superior dispersion stability of the oleic acid-treated NDs in the base oil. It was also noted that friction decreased over time, indicating improved friction-

reduction over longer sliding distances. The drastic reduction in wear could in part be explained by increased surface toughness by a work hardening effect due to the embedding of the NDs, as explained in Section 3.8.

Wang et al. <sup>173</sup> non-covalently enhanced the hydrophobicity of graphene oxide through electrostatic adsorption of oleylamine in a simple phase transfer method. This allowed for graphene oxide to be dispersed in hexadecane. As shown in Figure 4.1, the addition of just 10 mg/L functionalized graphene oxide drastically reduced the wear rate during tribological testing compared to pure hexadecane oil. This was largely because the GO additive ensured a lower and more stable friction from the beginning, by rapidly depositing on the sliding surfaces, whereas the pure hexadecane experienced long running-in periods. The authors proposed three active anti-friction mechanisms to explain the low and stable friction behavior. Firstly, once the nanosheets had deposited onto the sliding surfaces and formed a physisorbed film, the molecular chains of oleylamine were thought to weakly repel each other and ensure easy relative slip in a manner similar to the organic friction modifiers presented in Chapter 1. Secondly, the low interlaminar shear strength of the graphene oxide was believed to an important role in reducing friction whenever asperities on the countersurfaces come into contact. Lastly, the low flow shear stress of hexadecane aided in keeping friction steady throughout the sliding process.

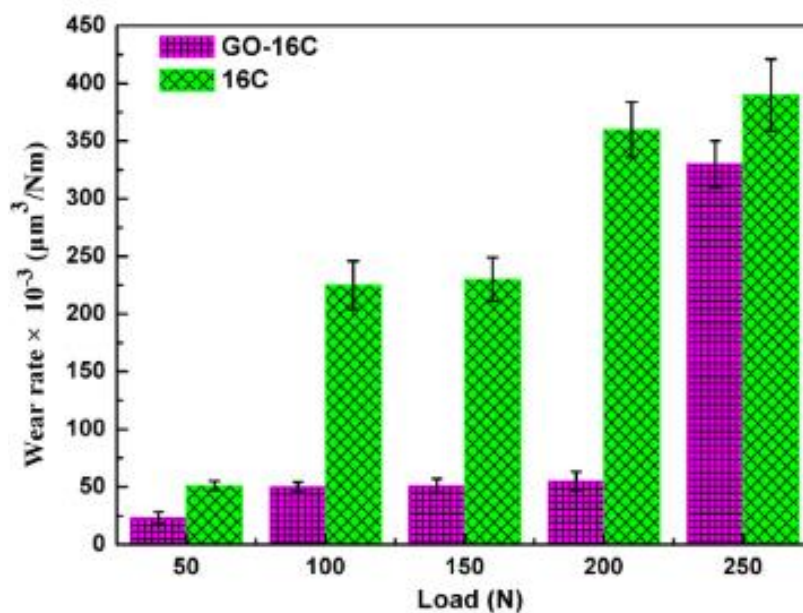


Figure 4.1: Comparison of wear rates on 52100 bearing steel with pure hexadecane oil (16C) and hexadecane oil containing 10 mg/L oleylamine-functionalized graphene oxide (GO-16C) under various loads <sup>173</sup>.

Tang et al.<sup>153</sup> improved the dispersion stability of graphene oxide in an aqueous solution of triethanolamine (2 wt%) by functionalizing with an amino-terminated imidazole-based ionic liquid (IL) after activating the carboxylic groups of GO by  $\text{SOCl}_2$ , as shown in Figure 4.2. The IL groups were covalently grafted onto the sheet edges of the GO by amidation under relatively mild conditions, as well as non-covalently attached through cation- $\pi$  stacking between imidazolium cations of the IL and the graphitic domains of the GO basal plane. While the abundant oxygen-groups on unfunctionalized GO provided some short-term dispersibility in the aqueous base liquid, significant amounts of GO sedimented after only 2 weeks. In contrast, the IL-functionalized GO exhibited long-term dispersion stability in the base liquid due to the electrostatic repulsion between the grafted IL groups on the sheets. For comparison, the authors also reported on the very poor dispersibility of an unreacted mixture of GO and IL in the same base fluid. At an optimal concentration of 0.02 wt%, the IL-functionalized GO resulted in a 57% and 76% reduction of friction and wear, respectively, compared the pure base liquid under the same test conditions. The excellent tribological performance was largely ascribed to the enhanced dispersion stability and improved adsorptivity. The latter was not only thought to enhance the embedded stability of the IL-functionalized GO on the rubbing surfaces, but also promote the formation of a boundary tribofilm through tribochemical reactions. This tribofilm greatly reduced friction and wear by preventing direct contact between the countersurfaces.

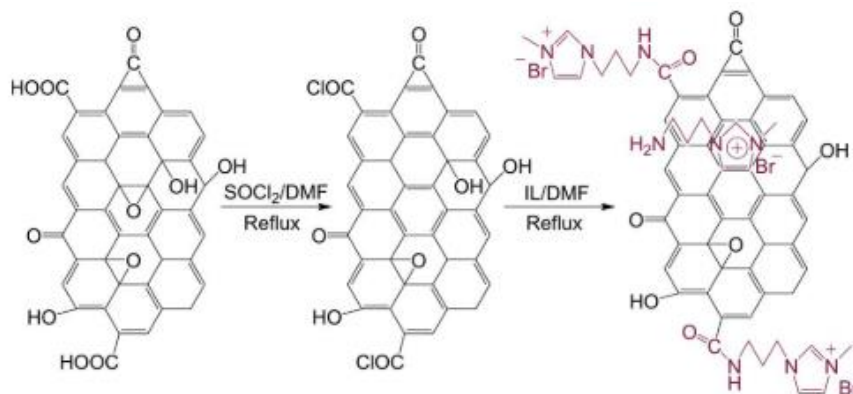


Figure 4.2: Schematic illustration of the synthesis procedures of IL-functionalized GO<sup>153</sup>.

Chouhan et al.<sup>283</sup> investigated the lubrication potential of GO that had been simultaneously reduced and functionalized with 3,5-di-tert-butyl-4-hydroxybenzaldehyde (DtBHBA) by using (3-aminopropyl)-trimethoxysilane (APTMS) as a chemical linker in a two-step process, as schematically illustrated in Figure 4.3. The resulting structure (rGO-DtBHBA) had appreciable dispersibility and stability in the SN-150 mineral base oil thanks to van der Waals interaction between the tertiary-butyl group of the additive and the hydrocarbon chains of the base oil. Using the rGO-DtBHBA as an additive improved both the friction and wear characteristics of a steel-steel rotating contact in the boundary lubrication regime. At a concentration of 0.2 mg/mL, the friction and wear were reduced by ~40% and ~16%, respectively. Moreover, the friction at this concentration also remained low and fairly stable over

time, unlike that of the pure base oil which increased over time. The wear scars of samples lubricated by rGO-DtBHBA were significantly smoother due to the formation of a thin lubricating film of functionalized nanosheets on the interfaces. Raman mapping showed that the graphene lamellae were not uniformly distributed in the wear scar, which the authors attributed to uneven load distribution and surface roughness.

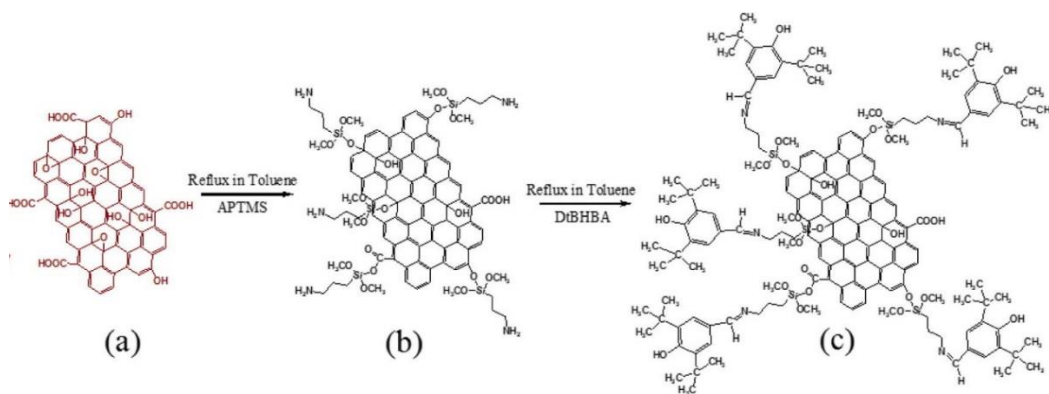


Figure 4.3: (a) Representative structure for GO. (b) APTMS was grafted onto GO targeting oxygen functionalities. Simultaneously several oxygen functionalities are eliminated during reflux reaction. (c) The DtBHBA was covalently grafted on amino sites of APTMS-functionalized graphene <sup>283</sup>.

Shang et al. <sup>165</sup> tuned the hydrophilicity and hydrophobicity of nitrogen-doped carbon dots to achieve long-term dispersion stability of the nanoadditives in both polar and non-polar base oils. Hydrophilic CQDs were prepared by a low temperature solid phase method with urea and citric acid, and the presence of multiple oxygenated and nitrous functional groups on the surface of the resulting structure enabled excellent dispersibility in polar synthetic polyethylene glycol (PEG) base oil. The hydrophobic CQDs were synthesized through covalent grafting of oleylamine on the surface of the as-prepared hydrophilic CQDs. An ideal mass fraction of oleyl amine on CQDs of 87.9 wt% allowed the hydrophobic CQDs to be directly dispersed in apolar synthetic polyalphaolefin (PAO) base oil with long-term stability. Both the additives significantly enhanced the friction-reducing and antiwear properties of their respective base fluids under boundary lubrication. The addition of 1.0 wt% of hydrophilic CQDs to PEG reduced friction and wear by 75.9% and 82.8%, respectively, while 1.0 wt% of hydrophobic CQDs in PAO provided a reduction of 47.1% and 90.5%. Interestingly, the friction and wear of PAO with hydrophobic CQDs were also lower than that of PAO with 1.0 wt% ZDDP. The tribological properties of a fully formulated commercial 5W-30 oil were also significantly improved by the addition of 1.0 wt% hydrophobic CQDs, indicating good compatibility with the other additives in the given formulation. Surface analysis of the wear scar lubricated by novel hydrophobic CQDs in PAO led the author to propose a lubrication mechanism in which CQDs adsorb onto the sliding surfaces and act as bearing balls. The CQDs were also found to fill the valleys on the tribosurface, thereby providing a mending effect. Under prolonged or rigorous sliding, tribochemical reactions may occur, leading to the formation of a tribofilm.

At first glance it may seem as if enhanced dispersion stability and adsorptivity is automatically accompanied by better lubrication and tribological properties, however, that is not necessarily the case. For instance, a functionalized nanoadditive which provide excellent friction reduction in one base oil, may have no friction-reducing capabilities in another oil. For example, Ye et al. <sup>79</sup> used a one-step pyrolysis method to prepare nitrogen-doped CQDs with covalently grafted diphenylamine (DPA) on the surface, and tested it in polyethylene glycol (PEG) under boundary lubrication. A year later, the same group reported on the tribological performance of the same additive under identical lubrication conditions, but this time in a bio-based castor oil <sup>211</sup>. The evolution of friction over time for different additive concentrations in the two cases are shown in Figure 4.4. By adding 1 wt% of the functionalized CQDs to PEG friction and wear were reduced by 75% and 82%, respectively. In contrast, the same CQD additive increased friction when added to castor oil. These differences can be attributed to differences in the inherent lubricating properties of the two base oils.

Specifically, from Figure 4.4 it is clear that castor oil without any additives exhibits a significantly lower friction than PEG under the same conditions. This is because the polar groups and long hydrocarbon chains of castor oil can adsorb onto the tribosurfaces and act similarly to an organic friction modifier. In contrast, the linear polyether PEG does not self-assemble onto the tribosurfaces to the same extent. Thus, when the functionalized CQDs are added to PEG, they aid lubrication through their respective lubrication mechanisms. When the functionalized CQDs are added to castor oil, on the other hand, the polar additive is believed to compete with oil molecules for available surface adsorption sites on the metal surface, thereby preventing the self-assembly of castor oil. Therefore, the media into which the nanoadditive is introduced also plays a very important role in the tribological performance. Ideally, the lubrication mechanism of the selected nanostructure should not compromise the lubrication mechanism of the base fluid or other lubricant components. Interactions between lubricant constituents will be addressed further in Section 5.

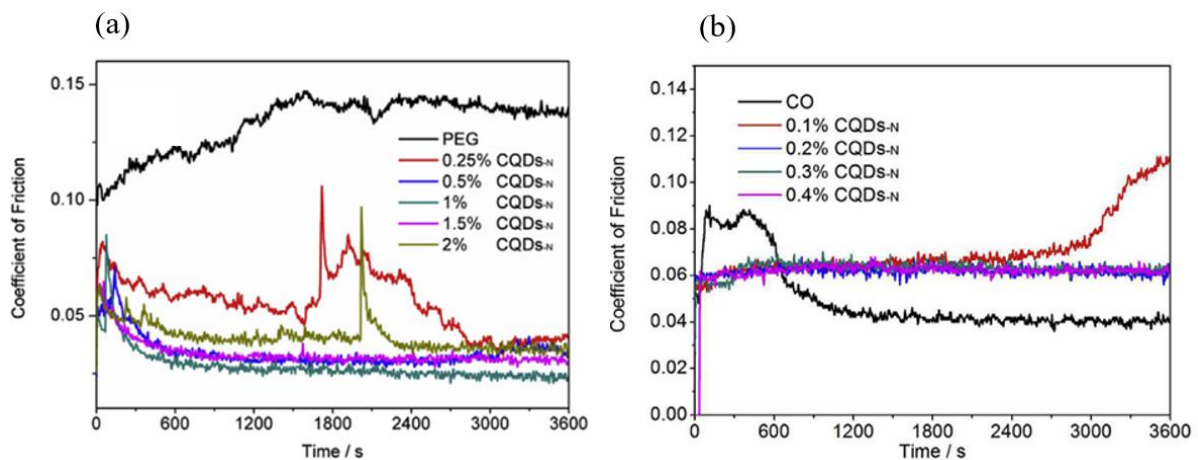


Figure 4.4: Friction curves from nitrogen-doped CQDs in (a) PEG <sup>79</sup> and (b) castor oil <sup>211</sup> at various concentrations.

To summarize, improved dispersibility as a result of surface functionalization is often accompanied by an increase in general chemical reactivity and adsorptivity, which in turn may affect the lubrication performance of the nanoadditives. In the case of graphene-based nanoadditives that rely on interlaminar shearing as one of its primary lubrication mechanisms, increased adsorptivity and high adsorption strength is likely to be of great benefit, as established in Section 3.2.3 and 3.4.3. In contrast, if a given tribosystem would benefit from having the ball bearing mechanism of 0D carbon nanostructures as one of its primary lubrication mechanisms, then a very high adsorption strength may not be desirable. This is because the rolling motion of 0D nanoadditives may be inhibited if the particle is too strongly associated with the underlying substrate, as discussed in Section 3.3.1. Hence, preserving the rolling capability of the 0D nanoadditives requires a more mindful approach. Their affinity to the surface should be strong enough to allow dispersion and ensure their presence on the interface, yet the interaction should not be so strong as to limit their movement on the tribosurface as this could deteriorate their friction and wear characteristics. All in all, overcoming the problem of nanoadditives aggregation whilst preserving the lubrication mechanisms of the nanostructure is an important aspect that should be considered in the development of carbon-based nanoadditives for liquid lubrication. Navigating this matter requires a fundamental understanding of each lubrication mechanism, and how a prospective functional group may affect it.

## 4.2 ENHANCING WETTABILITY

Change in the surface chemistry of a nanoadditive as a result of surface functionalization also has the potential to affect the wettability of the lubricant on the friction surfaces. In this context, the term wettability refers to the ability of a liquid lubricant to maintain contact with a solid surface. The wettability of a liquid is the result of a force balance between the cohesive forces within the liquid and adhesive forces between the liquid and the underlying surface. The cohesive force promotes the liquid droplet to bead up and avoid contact with the underlying surface whilst the adhesive force encourages spreading of the liquid across the surface. In tribology and lubrication, the wettability of a certain lubricant on a given surface is an important parameter especially in the boundary and mixed lubrication regimes due to the expected solid-solid contact of the moving surfaces. In these regimes, enhanced wettability can improve lubricant coverage and reduce the occurrence of undesirable dry friction between the solid surfaces.

Hu et al.<sup>200</sup> used a non-covalent approach to modify reduced graphene oxide (rGO) with  $\beta$ -lactoglobulin (BLG), in order to improve dispersibility in water.  $\beta$ -lactoglobulin is a highly stable amphiphilic biopolymer that can adhere strongly to rGO through hydrophobic and  $\pi$ - $\pi$  interactions, meanwhile hydrophilic groups are oriented out towards the aqueous phase, resulting in aqueous dispersions that remained stable for more than 8 months. Tribological testing of these dispersions showed that friction and wear rate could be reduced by 37% and 45%, respectively, compared to water alone. The water

wettability was characterized using contact angle measurements equipped with video capture technology, which revealed that the BLG-rGO dispersion had better wettability on the friction surfaces than pure water and aqueous dispersions of GO or rGO (see Figure 4.5). Since the friction testing was performed in the mixed lubrication regime and the surface wettability is closely related to the stability of the generated boundary lubricant film, the improved wettability resulted in improved lubricant coverage and tribological performance compared to GO and rGO. Moreover, TEM and Raman spectroscopy revealed the presence of a stable 5-6 nm tribofilm with graphene stacked together in different orientations. The authors suggested that the random stacking could facilitate the sliding path to occasionally switch from a commensurate state to the highly lubricating incommensurate state. In summary, the friction- and wear-reducing properties of BLG-rGO were attributed to enhanced boundary lubrication effect in the mixed lubrication regime and the formation of a protective low-shear lamellar tribofilm.

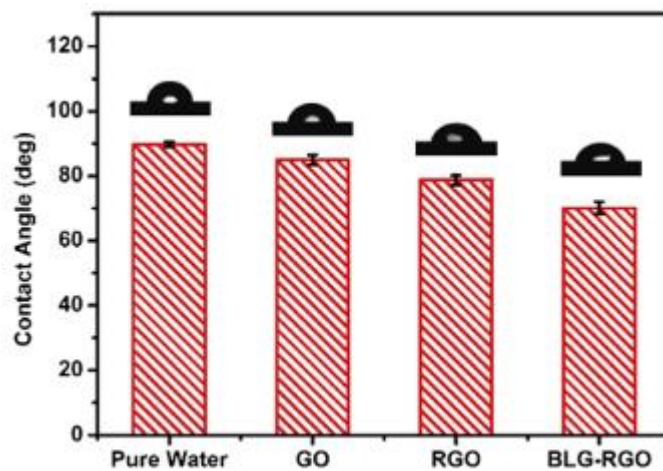


Figure 4.5: Contact angles of pure water, GO, rGO and BLG-rGO dispersion on the 316 stainless steel<sup>200</sup>.

Gan et al.<sup>313</sup> improved the dispersibility and lubricity of graphene oxide (GO) in water by ionic liquid (IL) functionalization. A simple liquid phase method was used to interlaminar multi-layered GO with a hydroxyl-terminated ionic liquid, which adsorbed onto the sheets through strong hydrogen bond interactions between the terminal hydroxyl groups of the ILs and oxygen-containing groups on the GO. The IL functional groups were believed to act as a bridging agent between GO and water which significantly improved the dispersibility of functionalized additive. While both unfunctionalized multilayer GO and GO-IL were able to enter the contact region and reduce friction during water lubrication, it was the GO-IL additive that really stood out in terms of friction-reducing and antiwear performance. The authors attributed this to the high negative zeta potential of GO-IL which prevented aggregation and allowed the additive to electrostatically adsorb onto the positively charged friction surfaces, thus promoting the formation of an integrated and dense deposition film. In fact, Raman mapping revealed a 3-4 times increase in the average G band intensity in the GO-IL deposition film

compared to that produced by unfunctionalized GO. Moreover, while the average sheet size is reduced and defect concentration is increased during sliding in the case of the GO deposition film, the  $I_D/I_G$  ratio of the GO-IL deposition film remained almost unchanged. This suggests continuous and dynamic deposition of fresh GO-IL through electrostatic adsorption interaction, meaning that self-healing functions are realized. Furthermore, it was found that the ILCAs-GO deposition film had significantly better wettability with water than the bare steel or GO deposition film. Not only does this improved friction surface wettability reduce the chances of dry rubbing, but it also results in a thicker adhesive layer of aqueous lubricant to further improve friction and wear characteristics.

Liu et al.<sup>146</sup> covalently modified graphene oxide (GO) with polyethyleneimine (PEI) and investigated its tribological properties as an aqueous lubricant additive. The nucleophilic addition of reactive amine sites from PEI onto the epoxy groups of GO, reduced GO to rGO and improved the dispersion stability of the layered PEI-rGO nanocomposite in water. It was found that an addition of 0.05 wt% PEI-rGO could reduce friction and wear rate by as much as 55% and 45%, respectively. Friction was found to decrease with increasing sliding frequency, suggesting operation in the boundary and mixed lubrication regime, in which high sliding frequency can facilitate dispersion of additives so that more additives can be brought into the contact area to reduce friction and wear. The mean coefficient of friction was also found to decrease with increasing normal loads, indicating shear-thinning of the lubricant layer and decrease in intermolecular friction in the confined volume. The authors proposed that the presence of hydrophilic amino groups of PEI-rGO enhanced the surface wettability and the adsorptivity of the nanoadditive, as shown in Figure 4.6, which promoted the formation of a protective lubricant film on the wear surface. Moreover, in addition to enhancing the antiwear performance of the lubricant, the PEI-rGO nanosheets also seemed to provide an anti-corrosion effect. The authors attributed this to the cohesive PEI-rGO protective film acting as a solid barrier stopping oxygen from accessing the exposed surface of the wear track. This is a highly desirable feature in water-lubrication where continuous disruption of the oxide film on the steel surface and subsequent exposure to aerated water is a common problem.

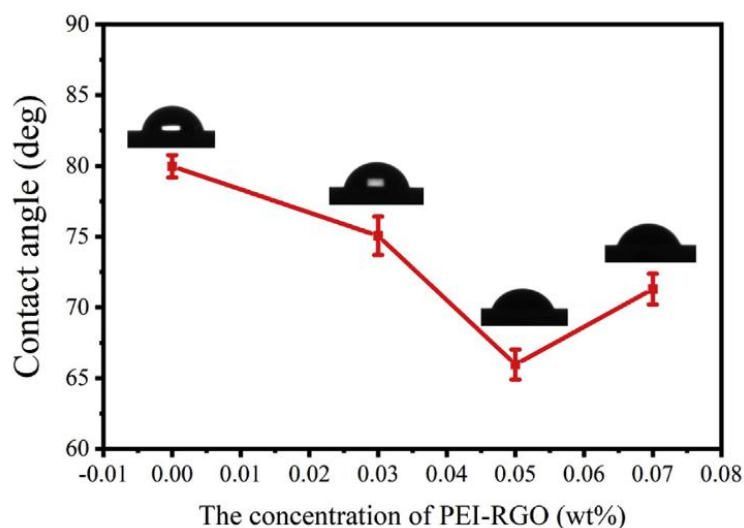


Figure 4.6: Contact angles of pure water and PEI-RGO dispersion on the 201 stainless steel <sup>146</sup>.

In short, improving the wetting characteristics of lubricants through chemical modification of additives can increase the thickness of the lubricant layer and minimize the occurrence of undesirable dry friction and solid-solid contact in the boundary and mixed lubrication regimes. Awareness and exploitation of this phenomenon could be especially advantageous in the development of aqueous environmentally acceptable lubricants where the inherent viscosity characteristics are generally quite poor compared to conventional hydrocarbon-based base fluids.

### 4.3 EXPLOITING TRIBOCHEMICAL INTERACTIONS

The tendency of larger molecular ligands to degrade under harsh tribological conditions have led some researchers to argue that self-dispersed particles without the need for surfactants or large grafted groups are more advantageous <sup>13</sup>. Such a category would for instance include graphene oxide with its many small hydroxyl, carbonyl and epoxide functional groups. However, while it is true that these small oxygen functional groups are sufficient to ensure the dispersibility of graphene oxide in several polar solvents, larger molecular ligands can provide several additional benefits beyond improved dispersion stability. For instance, a more extensive layer of functional groups can provide a cushioning effect to protect the internal nanostructure from direct contact with the sliding surfaces, which is especially beneficial under high loads or at high pressure <sup>13,314</sup>. Furthermore, when involved in tribochemical reactions under severe operating conditions, a more elaborate molecular functional group can potentially act as a precursor for the formation of a more complex tribofilm with improved friction-reducing and antiwear characteristics. In such a case, the degradation of the functional group can be considered beneficial. In theory, the tribofilm properties could potentially be tuned to ensure optimal lubricating conditions through clever use of chemistry and thoughtful selection of surface functionalities that are designed to intentionally undergo tribochemical reactions. However, such a deliberate approach

would likely require a more comprehensive understanding of tribochemical film formation than what is available at present day. Nevertheless, several recent papers have reported on instances of tribofilm formation after tribological testing of various functionalized nanostructures, and several tribochemically active functional groups have been identified.

For instance, literature on the tribological properties of ionic liquids (ILs) have demonstrated that certain hexafluorophosphate and tetrafluoroborate anions can readily decompose and react with metal species on the friction surfaces to form a lubricating and protective tribofilms composed of more scratch resistant compounds like fluorides, phosphates and borides <sup>251,263,315–318</sup>. This has been shown to have a positive effect on the friction-reducing and antiwear capabilities of the tribofilm. For instance, Fan and Wang <sup>264</sup> prepared two ionic liquid gels by grinding multi-walled carbon nanotubes (MWCNTs) into two kinds of imidazolium ILs (with tetrafluoroborate and hexafluorophosphate anions, respectively) at room temperature and investigated their tribological properties. The MWCNTs bundles were gently exfoliated and modified through van der Waals and  $\pi$ - $\pi$  interactions with the ILs, resulting in more relaxed bundles without undesired disruption of the CNT structure. While the worn surface was not extensively characterized, X-ray photoelectron spectroscopy (XPS) analysis of the worn surfaces indicated presence of fluoride, likely in the form of  $\text{FeF}_2$ , which is known to provide good scratch resistance. However, due to environmental regulations, fluorine-based additives are likely to be phased out in the coming years.

Other functional groups, besides ILs, have also been shown to undergo tribochemical reactions and improve the tribological properties of surface films. Zhang et al. <sup>142</sup> found that covalently functionalizing graphene oxide with long alkyl chains containing sulfur elements resulted in a tribofilm with improved tribological properties, especially in terms of antiwear capabilities, supposedly due to the formation of iron (II) sulphate ( $\text{FeSO}_4$ ). The concentration of sulfuric compounds in the tribofilm was found to increase with increasing additive concentration above 0.4 wt% and increasing load and contact temperature due to tribochemical activation. Gong et al. <sup>312</sup> grafted polymeric aryl phosphates (PAPs) onto the surface of multiwalled carbon nanotubes (MWCNTs) to prepare MWCNT-PAPs nanocomposites. The PAPs were found to be covalently attached to the convex surfaces of MWCNTs at a weight ratio of about 23%, which improved the dispersibility of MWCNTs in polyalkylene glycol (PAG) base oil. XPS analysis of the worn surface indicated the formation of a protective tribochemical surface film containing various iron oxides and  $\text{FePO}_4$ , which contributed to the low friction and high wear resistance of MWCNT-PAPs in PAG at elevated temperature. The role and contribution of the CNTs themselves to the lubrication performance was not investigated.

Shang et al. <sup>81</sup> covalently grafted a tetrahedral chelated orthoborate IL onto the surface of carbon quantum dots (CQDs) for use as a lubricant additive in polyethylene glycol (PEG) under boundary lubrication. The resulting structure showed excellent long-term dispersion stability without the use of any dispersants and significantly reduced friction and wear when employed as a lubricant additive.

While friction remained low and stable during lubrication with the IL-functionalized CQDs, the use of individual IL, CQDs, or their unreacted blend in the same base fluid exhibited large friction fluctuations over time. The authors proposed that the combined effect of covalent interaction and electrostatic force between the hybrid additive and the positive surface enhanced the adsorption capacity of the hybrid compared to the individual ionic liquid and CQDs, which in turn promotes the formation of a stable physical adsorption film, as discussed in Section 4.1. They proceeded to suggest that, at high loads, the CDQs were inclined to degrade into a more ordered structure while the IL moiety could undergo complex tribochemical reactions during sliding to form products such as  $\text{Fe}_2\text{O}_3$ ,  $\text{B}_2\text{O}_3$ , organic and/or inorganic carbon, and/or organic amines. From here, these products could potentially be mixed with the adsorbed additives to form an even stronger hybrid protective tribochemical thin film with C, B and N elements. The C, B and N content on the wear surface was found to increase with increasing load and sliding duration, which ensured excellent performance at high loads and improved the functional duration of the additive.

As discussed in Section 3.4, the tribofilm formation and the underlying reaction mechanisms are still a topic of great debate among researchers. The interplay of chemical species, environmental conditions and mechanical agitation remains elusive. Moreover, analysis of the tribochemical products after tribological events is generally insufficient to provide a comprehensive understanding of the nature and origin of the chemical reactions<sup>9</sup>. However, as the field progresses and the nature of tribofilm formation is better understood, it is possible to imagine how tribochemical interactions can be exploited in the design and development of additives that are able to undergo intentional tribochemical reactions to produce tribochemical surface films with tailored tribological properties. That being said, many of the surface functional groups that have been identified as tribochemically active (e.g., sulfur, phosphorous and chlorine) are often also recognized for their environmental toxicity and propensity for bioaccumulation<sup>121</sup>. Thus, efforts to identify new pathways to tribofilm formation in absence of such species are recommended moving forward.

In 2016, Erdemir et al.<sup>319</sup> reported on the *in operando* formation of carbon-based tribofilm via dissociative extraction from base-oil molecules on catalytically active sliding surfaces. I.e., the PAO base oil not only provided the liquid lubrication, but also the solid tribofilm. Structurally, the resulting tribofilms were similar to diamond-like carbon (DLC) and, in ball-on-disk tests at contact pressures of 1.3 GPa, they nearly eliminated wear and provided lower friction than the tribofilms formed by ZDDP. Reactive *ab initio* MD simulations suggested that the catalytic action of the surfaces facilitated dehydrogenation of linear olefins of the lubricating oil, as well as random scission of their carbon-carbon backbones, before the products recombined to nucleate and grow a compact amorphous tribofilm. Even though more research is needed to understand and verify this mechanism, it is possible to envision how a better understanding of such catalytic interactions could potentially contribute to future research and development of tribochemically active lubricant additives. In this regard, it might

be worth exploring the potential influence of trace impurities in carbon nanostructures (e.g., graphene and CNTs) grown on catalytic surfaces. Perhaps extensive purification processes to remove such impurities will not be necessary for use in future tribological applications, which can ultimately reduce the cost of deploying these nanostructures as additives for liquid lubrication.

#### 4.4 NANOCOMPOSITES OF MIXED DIMENSIONALITY

This approach is based on the idea of combining nanostructures with different dimensionality, to form hybrid structures that can make use of a larger number of lubrication mechanisms, either simultaneously or under different operating conditions. For example, since the ball bearing mechanism of 0D nanostructures is effective primarily under low loads while the shearing mechanism of graphene remains active at higher loads, a hybrid structure of the two may enhance tribological performance under a wider range of operating conditions. Alternatively, the simultaneous rolling action of 0D nanostructures and shearing of 2D nanostructures could potentially outperform that of either mechanism on its own.

Min et al.<sup>320</sup> synthesized a hybrid structure of graphene oxide (GO) nanosheets and carboxyl-functionalized multi-walled carbon nanotubes (MWCNTs-COOH) and investigated its tribological properties as an additive for water-based lubricants. A condensation reaction between the carboxyl groups of MWCNTs-COOH and the hydroxyl and epoxy groups of GO firmly attached the nanotubes to the graphene oxide sheets, and due to the interconnected network structure of the hybrid, the GO sheets did not readily stick together. It was found that the introduction of GO in the hybrid structure was able to improve the dispersibility of MWCNTs-COOH in water, possibly due to  $\pi$ - $\pi$  interactions between the MWCNTs-COOH and  $\pi$  regions in the GO basal plane. The hybrid additive was found to be a better friction modifier than both GO and MWCNTs-COOH at concentrations above 0.5 wt% and the authors proposed a lubrication mechanism in which the non-covalent  $\pi$ - $\pi$  bonding between MWCNTs-COOH and  $\pi$  regions in GO were overcome by strong shear forces during sliding, resulting in GO nanosheets being transferred to the rubbing surfaces. Once on the surfaces, GO could improve friction and wear by increasing the load carrying capacity and prevent direct contact between the surfaces. Meanwhile, the MWCNTs-COOH components of the hybrid were believed to contribute to lubrication performance by enhancing the load carrying and through the ball bearing mechanism. However, no evidence was provided to support their proposed mechanism and, as established in Section 3.3.2, the roller bearing mechanism of MWCNTs is highly questionable. Instead, it is conceivable that the reported increased dispersibility played a larger role in the improved tribological performance than anticipated.

Zhang et al. <sup>212</sup> investigated the possibility of using CQDs as exfoliation stabilizing agents in liquid phase exfoliation of hexagonal boron nitride (h-BN), MoS<sub>2</sub>, MoSe<sub>2</sub>, WS<sub>2</sub> and graphene. After ultrasonic processing and subsequent centrifugation, the spherical CQDs with an average diameter of 3 nm had effectively exfoliated the laminar bulk materials and were uniformly attached and interspersed on the exfoliated monolayered and few-layered 2D nanosheets, which improved the dispersibility of the 2D nanostructures in water. The different hybrid structures were utilized as aqueous lubricant additives and exhibited significantly improved friction and wear characteristics, both compared to pure water and pure water with just CQDs. As illustrated in Figure 4.7, the authors suggested that individually adsorbed CQDs tend to be squeezed out of the contact at increased loads, whereas the assembled nanoadditives are harder to squeeze out due to their larger lateral surface area. They also suggested that, once inside the interfacial contact area, the composite additive could reduce friction and wear through the interlayer shearing mechanisms of the 2D structure and the ball bearing mechanism of the CQDs. However, it is also possible that the friction-reduction could be attributed to lower resistance to interlaminar shear due to increased interlaminar distance, rather than the combined action of both interlaminar shearing and rolling. It would be interesting to explore this further in future investigations.

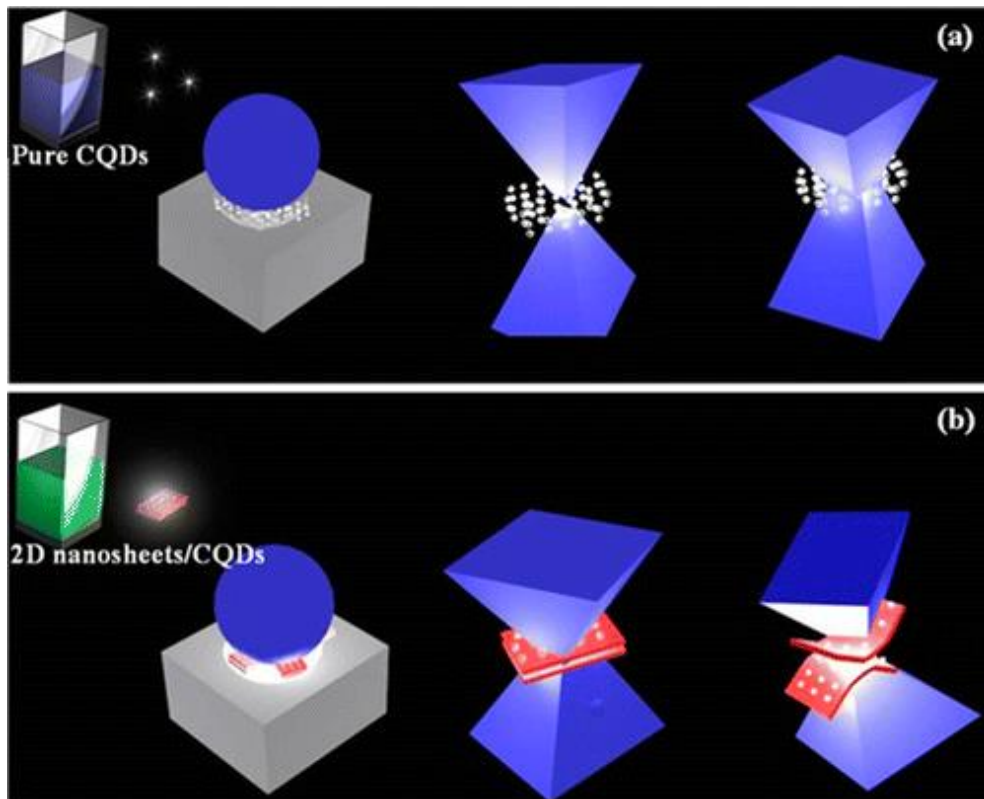


Figure 4.7: Proposed lubrication model for aqueous dispersions of (a) pure CQDs and (b) 2D nanosheets decorated by CQD <sup>212</sup>.

Wang et al. <sup>26</sup> used a facile and fast one-step laser irradiation method to prepare a silver (Ag) and graphene oxide (GO) nanocomposite in which the layered structure of GO was preserved, and the GO sheets were uniformly decorated with interlaminar spherical Ag nanoparticles. Silver nanoparticles were chosen owing to their good ductility and low melting point, which makes them excellent solid lubricants <sup>321,322</sup> and promising lubricant additives. The tribological performance of the nanocomposite in liquid paraffin was compared to that of various other additives, including GO, raw Ag, Ag spheres, and a pre-irradiation blend of Ag and GO. Just 0.1 wt% of the nanocomposite additive not only outperformed all these dispersions, but also three commercial additives zinc dialkyl dithiophosphates (ZDDP), triethanolamine borate (TAB), and phosphate esters (PPE). The authors attributed the outstanding performance to the synergistic combination of a self-lubricating lamellar structure and the load-carrying and ball bearing action of the interlaminar Ag nanospheres. Lastly, residual Ag nanoparticles were found to deposit into wear grooves on the surface in a self-repairing process that reduced apparent surface roughness of the sliding surfaces.

In this regard, it is worth mentioning that the ball bearing ability of Ag nanoparticles under such loads has yet to be confirmed. Moreover, given the high ductility and low melting point of silver, it is conceivable that a softening or melting behavior, followed by spreading on the tribosurface, is a more likely course of events. Such behavior was reported by Meng et al. <sup>323</sup>, who also used Ag nanoparticles, in this case to uniformly decorate multi-walled carbon nanotubes (MWCNTs) through a simple aldehyde reduction of inorganic salts in supercritical CO<sub>2</sub> medium. The tribological properties of the resulting Ag/MWCNT nanocomposite as a lubricant additive in commercial 10w40 engine oil was investigated after a simple surface modification process using oleyl amine. At an optimal concentration of 0.18 wt%, the nanocomposite was found to reduce the friction and wear rate by 36.4% and 32.4%, respectively, compared to that of pure engine oil. In this case, the contribution of the Ag nanoparticles was attributed to softening and spreading as well as improved thermal conductivity. The latter allows for more effective decentralization of frictional heat, which helped to maintain oil viscosity and fluid film thickness.

Luo et al. <sup>324</sup> used a one-step laser irradiation method to prepare a laminated composite structure comprised of ultrasoft MoS<sub>2</sub> sub-micron spheres embedded within multiple layers of reduced graphene oxide (rGO). Scanning electron microscopy (SEM) micrographs of the resulting structure are presented in Figure 4.8. The nanocomposite was claimed to effectively combine the advantages of 0D nanospheres and 2D nanosheets when used as a lubricant additive in 10w40 engine oil. The presence of interfacial bonds between the quasi-fullerene-like MoS<sub>2</sub> and the surrounding graphene were believed to stabilize the sulfide particles on the graphene support, thus preventing undesired agglomeration of the additive in the base oil. Compared to individual rGO nanosheets, MoS<sub>2</sub> nanoflakes, spherical MoS<sub>2</sub> particles and an unreacted blend of GO and MoS<sub>2</sub> spheres, 0.2 wt% of the synthesized nanocomposite in the base oil exhibited superior dispersion stability as well as friction-reducing, friction-stabilizing

and antiwear capabilities. Surface analysis of the wear scar indicated the formation of a tribofilm on the sliding surfaces lubricated by the nanocomposite additive. The large specific surface area of graphene was believed to promote deposition onto the sliding surfaces during the tribological test, where it prevented wear by acting as a spacer and reducing direct metal-to-metal contact. The authors also proposed that the MoS<sub>2</sub> spheres between the graphene layers could contribute to lubrication by acting as miniature ball bearings that convert sliding friction into rolling friction under strong shear force. However, once again, it remains unverified whether interlaminar 0D nanoparticles actually contribute to friction reduction due to the ball bearing mechanism, or whether they just promote the interlaminar sliding mechanism by increasing the interlayer distance.

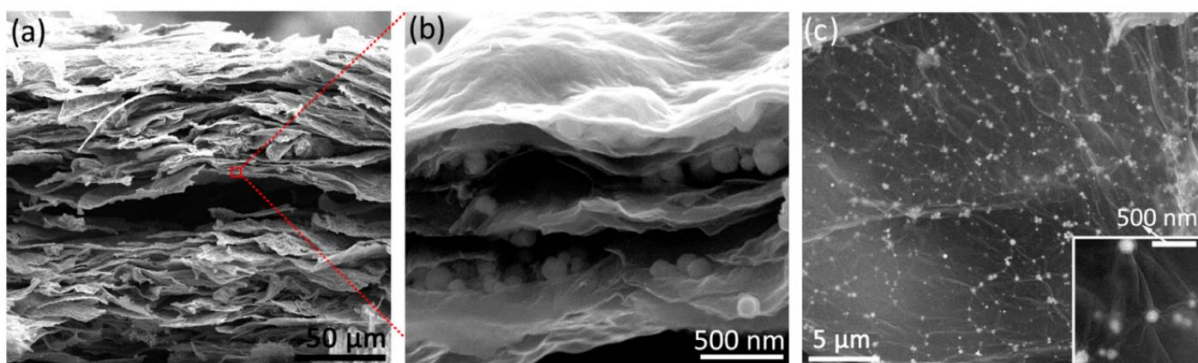


Figure 4.8: SEM micrographs of the rGO/MoS<sub>2</sub> composite structure: (a)(b) cross-sectional and (c) top view<sup>324</sup>.

In summary, combining nanostructures of different dimensionality have been shown to improve tribological performance in several instances. In most cases, the experimental researchers have attributed this to the combined action (i.e., lubrication mechanisms) of the composite constituents. While this idea and approach is certainly novel, its validity remains unexplored. Indeed, it could be that the superior tribological performance of the composite additives is instead attributable to secondary effect such as improved dispersibility, adsorptivity or thermal conductivity. Thus, more research is needed to better our understanding of how the individual components of composite additives contribute to lubrication performance. Either way, the findings presented in this section have highlighted another attractive concept. Specifically, an advantage of composite or hybrid structures is that they are all transported to the contact region as one cohesive unit. As a result, the presence of all the components is ensured at the interfacial contact – regardless of competing adsorption processes. This potential strategy and the importance of considering competing adsorption processes of surface-active additives in lubricant additives will be addressed further in Chapter 5.

## 4.5 INTRODUCING ADDITIONAL ADDITIVE FUNCTIONALITY

Having one additive serving more than one function in a lubricant could potentially allow for the total number of additives in a formula to be reduced. This is an attractive prospect as a higher number of additives increases the likelihood of unintended interactions among lubricant constituents, as will be discussed in greater detail in Chapter 5. Carbon nanostructures are excellent candidates for the development of multifunctional additives due to their excellent properties as carrier materials combined with the rich and well-established chemistry of carbon. This has inspired some researchers to equip carbon nanostructures with functional groups that provide the nanoadditive with supplementary functionality, beyond its inherent friction-reducing and antiwear capabilities.

Ye et al.<sup>79</sup> synthesized N-doped CQDs and covalently functionalized them with diphenylamine (DPA) in a one-pot pyrolysis method, and investigated their potential as a multifunctional lubricant additive in polyethylene glycol (PEG). The small photoluminescent particles had excellent dispersion stability in PEG and were shown to provide antioxidative properties in addition to impressive antiwear and friction-reducing properties. The authors proposed an antioxidant mechanism in which the diphenylamine (DPA) structure acts as a radical scavenger, as shown in Figure 4.9. It is well known that the autoxidative degradation of an organic hydrocarbon base oil (RH) is a free-radical chain reaction in which RH undergoes a chain initiation reaction when exposed to light or heat to produce an alkyl radical ( $R\cdot$ ). The  $R\cdot$  may react further with  $O_2$  to produce an alkyl peroxy radical ( $ROO\cdot$ ), which is an especially pernicious radical as it will attack and further degrade the base oil (RH) to produce another  $R\cdot$  and hydroperoxide (ROOH). Herein, the N-H bond of the DPA groups donates its hydrogen atom to an alkyl peroxy radical ( $ROO\cdot$ ), thereby preventing it from further attacking RH. Depending on the antioxidative proficiency of the PDA functional groups, the CQDs<sub>S-N</sub> additive could potentially eliminate the need for a separate antioxidant additive in the final lubricant formulation, thus reducing the number of lubricant components and the possibility of undesirable interactions among them.

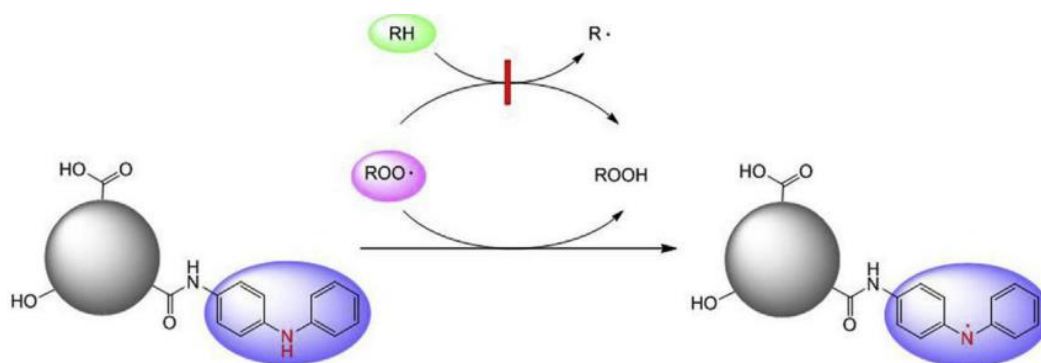


Figure 4.9: Possible antioxidant mechanism of DPA- functionalized and nitrogen-doped CQDs in PEG<sup>79</sup>.

Zhang et al.<sup>311</sup> also synthesized an additive that could potentially eliminate the need for other lubricant components, in this case, the base fluid itself. The authors functionalized reduced graphene oxide (rGO) with hyperbranched polyamine ester (HBPE), as schematically illustrated Figure 4.10, and the result was a homogenous viscous graphene liquid (rGO-HBPE) that could spontaneously flow and form a uniform adsorbed film without the use of any solvent. The soft polymeric HBPE provided fluidity and acted as a base oil that is covalently bonded to the reduced graphene oxide additive, resulting in a self-suspended lubrication system. The tribological behavior of liquid-like RGO-HBPE was compared to that of an unreduced equivalent (GO-HBPE), which was a solid-like phase at room temperature due to strong adsorption and substantial crosslinking of oxygen and polar functional groups in the polymeric chain regions. The solid-like GO-HBPE did not spread efficiently on the surface and had a tendency to squeeze out of the contact, resulting in overall poor lubrication properties, even though small amounts could be compacted and exhibit behavior in a manner similar to a solid lubricant. In contrast, rGO-HBPE was able to spread and form a uniformly adsorbed lubrication film that could be ordered by the directional movement of the shear, resulting in a low coefficient of friction. Furthermore, under high loads, the fluidity of rGO-HBPE allowed filling of the friction-induced wear tracks to provide a mending effect. Therefore, functionalizing reduced graphene oxide with this specific polymer resulted in a self-suspended hybrid with liquid-like properties that eliminated the need for any solvent. While these findings are certainly intriguing, such an approach would likely be too expensive for most practical applications. Here, a comparison to ionic liquids can be made. ILs were initially proposed as alternative base fluids, however, due to the expensive nature of the approach they are now being explored as lubricant additives. Perhaps such an approach could be considered for rGO-HBPE and similar structures as well.

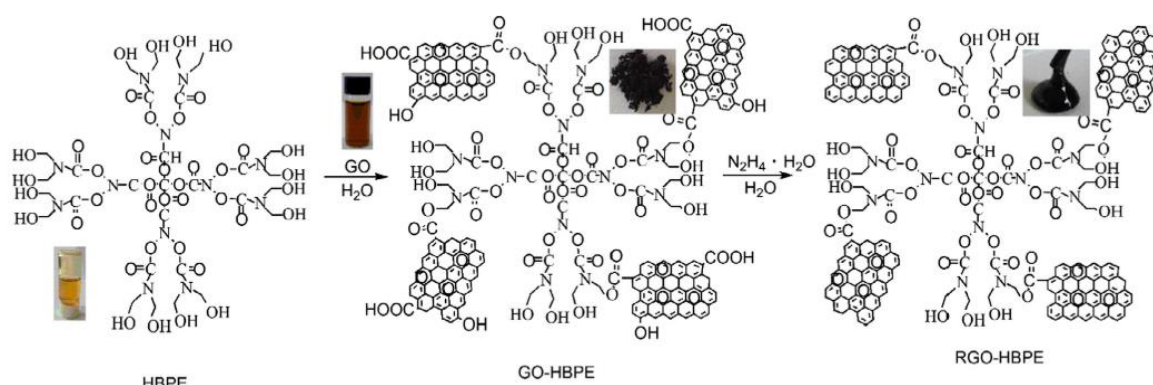


Figure 4.10: Synthetic schematic of rGO-HBPE<sup>311</sup>.

One possible approach in the development of multifunctional carbon-based nanoadditives could be to combine carbon nanostructures with already known lubricant additives. For instance, polymethyl methacrylate (PMMA) is a transparent thermoplastic polymer and a well-established viscosity index (VI) improver. For this reason, Sarno et al. <sup>210</sup> investigated whether a nanocomposite comprised of CQDs and PMMA would be able to act as a multifunctional additive with viscosity index improving capabilities in addition to the inherent friction-reducing and antiwear properties of CQDs. The CQDs were encapsulated in an extremely thin layer of PMMA by thermal expansion of the PMMA molecular chains and subsequent cooling, as schematically illustrated in Figure 4.11. The resulting PMMA/CQD nanocomposite had a size distribution centered around 4 nm and a hydrodynamic diameter within a range of 3-10 nm. The tribological properties of the PMMA/CQDs composite as a lubricant additive in commercial VG 220 mineral base oil was compared to that of treated PMMA and pure base oil, in both boundary and mixed lubrication regime. The untreated CQDs showed insufficient dispersibility in the base oil. The PMMA/CQDs additive was found to provide the best friction-reducing and antiwear properties in addition to increased load carrying capacity. The author attributed these improvements to the steady release of entrapped CQDs from the polymer matrix during lubrication, and the ball bearing action of the released CQDs. Unfortunately, multifunctionality beyond friction-reducing and antiwear properties of CQDs was not achieved, most likely because the addition of just 0.1 wt% PMMA/CQDs was too small to cause any significant changes in viscosity. However, according to the authors, an improvement in the viscosity index could be expected by increasing the PMMA content of the additive. And, since the PMMA is effectively the dispersing agent of CQDs, such an increase is expected to positively affect the CQD dispersion.

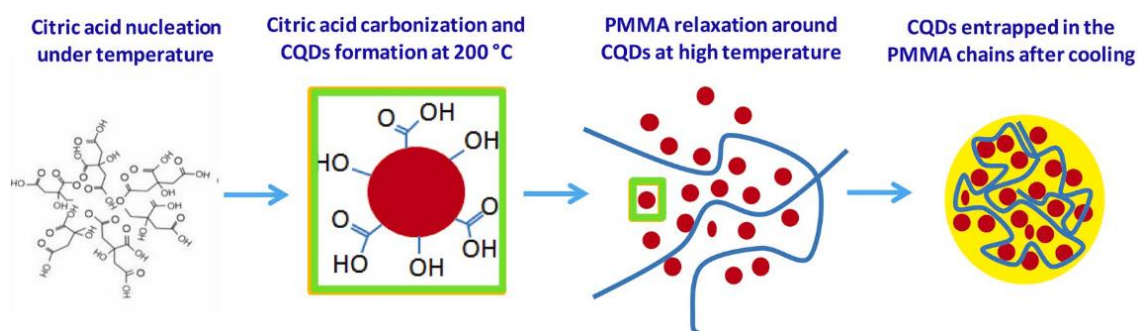


Figure 4.11: Illustrative representation of formation and entrapment of CQDs within PMMA structure <sup>210</sup>.

All in all, studies attempting to provide carbon nanostructures with functional groups that impart new additive functionalities are still incredibly scarce owing to the novelty of the strategy. However, based on the excellent properties of carbon nanostructures as carrier materials and the endless opportunities for structural modification and additional functionalization, the approach is believed to show great promise.

## 5 INTERACTIONS WITH OTHER LUBRICANT ADDITIVES

---

Lubricants are used in a wide range of applications, each requiring a different formulation to meet specified performance criteria<sup>8</sup>. For this reason, most modern lubricants are complex chemical systems comprised of a base fluid and a variety of carefully selected additives. The base fluid provides the main properties to the lubricant, whereas the additives provide the base fluid with the necessary functionalities for each targeted application. Since ecological and environmental considerations have gained importance in the recent years, the lubrication industry must adapt in order to comply with increasingly stricter regulations. The less environmentally friendly nature of certain conventional lubricant components (such as those based in halogens and heavy metals) means that a move towards more environmentally acceptable lubricants (EALs) will inevitably include having to find new alternatives for both base fluids and lubricant additives.

Moreover, as established in Chapter 1, the shift towards E-mobility (i.e., transition from internal combustion engines (ICE) to electrical vehicles (EVs)) is predicted to be accompanied by a radical and fundamental shift in lubrication focus from hydrodynamic to boundary lubrication mechanisms, likely by switching to base fluids of lower viscosity<sup>23</sup>. Lowering the lubricant viscosity to reduce hydrodynamic friction is an approach that should ideally be combined with friction-reducing additives that minimize boundary friction<sup>24</sup>. In addition to friction-reducing, antiwear and extreme pressure additives, future base fluids are likely to require a whole series of other additives to compensate for other base fluid deficiencies (e.g., corrosion inhibitors, viscosity modifiers etc.) and meet the required performance criteria for different applications and components in tribosystems. The high number of additives in modern lubricants presents a real challenge in lubricant development and formulation because each additive package is a unique blend of numerous components whose combination produces a complex chemistry. In other words, a large number of lubricant additives increases the likelihood of unintentional interactions among additives. As postulated in Chapter 4, this is why having one additive serving more than one function in the lubricant (i.e., multifunctionality) is an attractive prospect. These interactions can have both positive and negative implications and are often referred to as *synergies* and *antagonisms*<sup>8</sup>.

In relation to lubricant additives, a synergy is defined as occurring when a combination of two additives gives better performance than both of the individual additives alone when the latter are used at a concentration which is the sum of the concentrations of the two additives employed in the combination<sup>24</sup>. Antagonism is less formally defined but is generally considered to occur when an additive in combination with another additive performs worse than when used alone at the same concentration<sup>24</sup>.

In 1989, Spikes<sup>325</sup> identified four main mechanisms by which synergisms and antagonisms can arise:

1. Direct interactions in the liquid phase
2. Direct interactions on the surfaces
3. Complementary or exclusory effects
4. Graded response

The first group of potential additive interactions involve direct physical or chemical interaction between additives in the liquid phase and can be either beneficial or harmful to lubricant performance. A well-known example of such an interaction is the antagonistic relationship between aminic dispersants and the surface active antiwear additive ZDDP, which is believed to be the result of complex formation in the solution that reduce the chemical activity and adsorptivity of ZDDP<sup>24</sup>. The second group involves interactions between additives or the reaction products of additives on the tribosurfaces. This group would include both instances where two additive molecules interact directly with each other on the metal surface, and instances where the one additive interacts with the chemical by-product of another additive on the tribosurface. For example, it has been found that some friction modifying additives adsorb more strongly onto metal sulfides formed by some extreme pressure additives than on the bare metal alone, thereby providing a synergistic effect<sup>325</sup>. Complementary effects can for instance refer to situations where different additives of the same class can each contribute to a beneficial effect whose sum is greater than its parts. For instance, the combination of two different antioxidants can potentially be more effective than either additive separately because they tackle different stages of the hydrocarbon autoxidation cycle. In contrast, some corrosion inhibitors have been found to have an antagonistic exclusory effect on the performance of friction modifiers and extreme pressure additives due to competing occupancy of surface sites<sup>11</sup>. Lastly, the term graded response is used to describe the complementary additive action over a range of operating conditions. By employing a combination of additives that are each active under slightly different operating conditions, the range of superior performance can be extended, which is especially beneficial for applications where conditions change throughout operation<sup>325</sup>.

Because lubricant additives tend to perform quite differently in a blend with other additives than they do on their own, it is important to investigate how carbon nanoadditives may interact with other lubricant additives. While studies addressing the interaction between carbon nanoadditives and other classes of additives are still scarce, a few papers have reported on the performance of carbon nanostructures when used in combination with another type of carbon nanostructure<sup>19,100,245</sup>. Wu et al.<sup>100</sup> studied the synergistic behavior of graphene oxide (GO) and nanodiamonds (NDs) in water lubrication. Although both individual GO and individual NDs significantly improved the lubrication performance of pure water, a combination of both additives resulted in very low friction coefficient (i.e., 0.03) when the concentrations of GO and NDs were 0.1 wt% and 0.5 wt%, respectively. This was 2.7 times lower than that of 0.1 wt% GO and 2.3 times lower than that obtained with 0.5 wt% NDs

alone. This blend also outperformed the individual additives at a concentration equal to the sum of concentrations in the blend (0.6 wt%), demonstrating that the two additives had a synergistic friction-reducing effect. While the origin and mechanism of this effect remains unverified, the authors hypothesized that it could potentially be due to the combined action of interlayer shearing in GO and the ball bearing effect of NDs.

A few studies have also reported on the performance of carbon nanostructures when used alongside other types of friction-reducing or antiwear additives <sup>245,285</sup>. Similarly to graphite, molybdenum disulfide (MoS<sub>2</sub>) is a well-established solid lubricant that owes its lubricating properties to its easily sheared lamellar structure of molybdenum atoms sandwiched between planes of sulfide ions. The lubricating properties of MoS<sub>2</sub> have also been utilized in liquid lubricants by adding either solid MoS<sub>2</sub> particles or oil soluble organomolybdenum additives that can react to form MoS<sub>2</sub> nanocrystals under extreme tribological conditions such as high loads. Xu et al. <sup>285</sup> investigated the interplay between graphene and MoS<sub>2</sub> when used as additives in esterified bio-oil for boundary lubrication in mated steel contacts. When used together, in an optimal ratio of 0.2 wt% MoS<sub>2</sub> and 0.3 wt% graphene, the friction- and wear-reducing performance outperformed that of either additive alone at any concentration. When used on their own, graphene was generally ground into small defective particles while the MoS<sub>2</sub> additive was both ground into smaller particles and oxidized to MoO<sub>3</sub> during the frictional process. When used together, graphene and MoS<sub>2</sub> formed a thicker adsorbed film containing both additives and organics from the base oil. Herein, the MoS<sub>2</sub> supposedly protected the graphene from being crushed into small defective platelets, thereby retaining graphene's excellent lubricating properties. Meanwhile, graphene was credited for enhancing the durability and retention of the MoS<sub>2</sub> surface films as well as prevent oxidation of MoS<sub>2</sub>. The proposed ability of graphene to inhibit oxidation of other lubricant additives have also been supported by Upadhyay and Kumar <sup>245</sup>.

While both abovementioned examples demonstrate alleged synergistic interactions, it is conceivable that carbon nanostructures are particularly susceptible to antagonistic interactions during operation due to the prevalence of antagonistic mechanisms involving the mated metal surfaces and the likely prospect of other surface-active additives being present in the formula. That is, phenomena such as competing adsorption processes and interactions with other surface-active additives (e.g., corrosion inhibitors, dispersants, or detergents) are likely to occur. For example, it has been suggested that the abrasive polishing action of NDs could potentially inhibit other beneficial running-in processes, such as the establishment of a protective tribofilm <sup>171</sup>. Such behavior has been reported for the combination of ZDDP additives and carbonaceous soot or carbon black <sup>326,327</sup>. Herein, the soot is believed to continually abrade the relatively soft ferrous sulfide- and/or phosphate-based films formed by initial reaction between the anti-wear additive and the mated surfaces, resulting in a tribocorrosion wear mechanism <sup>327</sup>.

Another proposed antagonistic interaction between soot and ZDDP is a decrease in surface coverage rate by ZDDP molecules due to competing physical adsorption of carbon black on the surface<sup>328</sup>. Similarly, Nunn et al.<sup>19</sup> suggested that the deteriorated performance of sp<sup>2</sup>-hybridized carbon nanostructures when used alongside an oil-soluble organic molybdenum additive containing sulfur and phosphorus (MoDDP) could potentially be due to competing adsorption and film-forming processes on the surface. Even though additives ZDDP and MoDDP are likely to be phased out over the coming years due to their questionable environmentally friendliness, the principle remains the same: application of carbon nanostructures as lubricant additives requires careful consideration and investigation of potential antagonistic interactions with other additives in the lubricant formula. The presence of carbon nanostructures should not hinder or limit the performance of other lubricant additives, and other lubricant components should not impede the functioning of the carbon-based nanoadditives. In this regard, competing adsorption processes are believed to be a particularly important consideration. Thus, as previously recommended, the adsorption behavior of carbon nanoadditives should be characterized and reported in future experimental studies.

However, one potential approach for mitigating the issue of competing adsorption processes among surface-active additives can be envisioned based on the functionalization strategies presented in Chapter 4. By exploiting the excellent carrier material properties of carbon nanomaterials, it might be possible to combine certain additives into one cohesive hybrid structure. This way, the delivery of both surface-active components to the interfacial contact area is ensured, which may potentially reduce the antagonistic effect of competing adsorption processes. For instance, in the case where graphene adsorbs preferentially onto available surface sites, another antiwear additive such as MoS<sub>2</sub> might not have sufficient presence on the metal surfaces to properly partake in wear protection. However, when combining the additive constituents rather than adding them separately, graphene could potentially act as a vessel or carrier structure to deliver MoS<sub>2</sub> to the contact area. Moreover, the ability to tune the relative proportion of the two components in the hybrid structure may offer more control over the relative ratio of the two additives on the mated surfaces compared to the situation where their presence is left up to individual adsorption processes. There are couple of experimental studies that indicate that this could potentially be a viable approach.

For example, Song et al.<sup>329</sup> used a facile and effective chemical vapor deposition method to grow 5-7 layers of MoS<sub>2</sub> on the surface of strongly oxidized carbon nanotubes (CNTs) to produce a nanocomposite, and investigated its tribological performance as an additive in dibutyl phthalate (DBP). The nanocomposite outperformed corresponding dispersions of individual CNTs, MoS<sub>2</sub> and a mixture of the two, both in terms of friction-reducing and antiwear capabilities. A nanocomposite concentration of 0.02 wt% reduced the coefficient of friction and wear scar diameter by 58% and 19%, respectively, and the resulting wear scar was significantly smoother than that of all other additives tested. Based on surface analysis of the wear scar after friction testing, the authors suggested a lubrication mechanism in

which the composite additive is deposited on the metal surface to form a protective physisorbed film before gradually undergoing tribochemical reactions to produce a protective tribochemical film, mainly consisting of  $\text{Fe}_2\text{O}_3$ ,  $\text{Cr}_2\text{O}_3$  and  $\text{MoO}_3$ . In contrast, when the surfaces were lubricated by an unreacted mixture of CNTs and  $\text{MoS}_2$ , only  $\text{MoS}_2$  remained adsorbed on the surface while CNTs were gradually detached. In other words, the nanocomposite approach ensured the presence of both additives on the sliding surfaces.

The same researches have also anchored  $\text{MoS}_2$  to the surface of graphene nanosheets to prepare two nanocomposites with different morphologies<sup>330</sup>. As shown in Figure 5.1, a hydrothermal process was used to dot  $\text{MoS}_2$  nanoflowers (NFs) on the graphene nanosheet surface to make up the nanocomposite denoted as GNS/ $\text{MoS}_2$ -NFs, and a chemical vapor deposition method was used to uniformly attach  $\text{MoS}_2$  nanoplatelets (NPs) on the graphene nanosheets to form the nanocomposite labelled as GNS/ $\text{MoS}_2$ -NPs. Both nanocomposites improved the friction and wear characteristics of dibutyl phthalate (DBP), but the GNS/ $\text{MoS}_2$ -NFs almost invariably exhibited better tribological performance than GNS/ $\text{MoS}_2$ -NPs. This was attributed to the stronger interfacial bonding between graphene and  $\text{MoS}_2$  nanoflowers which allowed the nanoflowers to remain attached to the nanosheets during operation. In contrast,  $\text{MoS}_2$  nanoplatelets on GNS/ $\text{MoS}_2$ -NPs would become partially or completely detached and the additive removed from the contact area. These findings indicate that hybrid structure cohesion could be an important parameter governing the success of this nanocomposite approach.

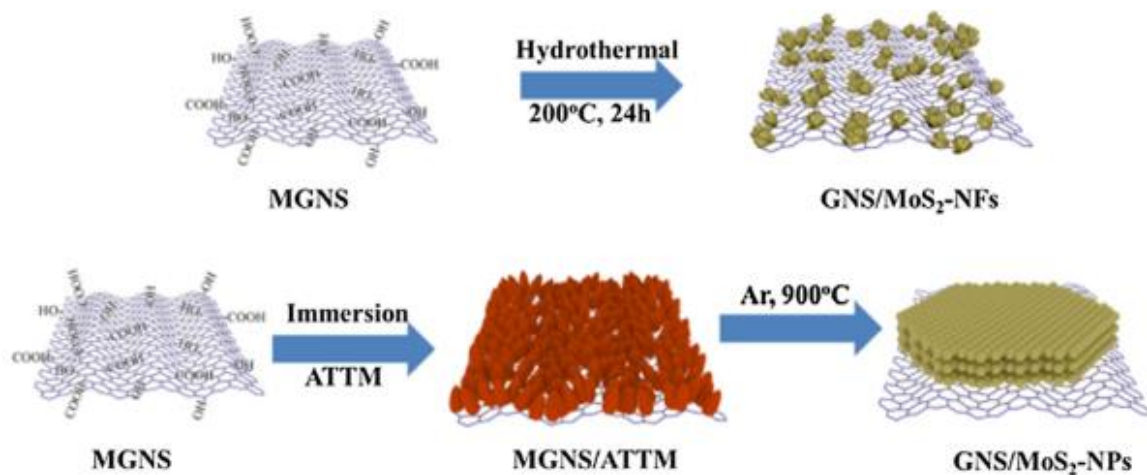


Figure 5.1: The schematic illustration of the synthesis procedure of GNS/ $\text{MoS}_2$ -NFs and GNS/ $\text{MoS}_2$ -NPs<sup>330</sup>.

Lastly, Zhang et al.<sup>212</sup> observed that intercalating lamellar materials such as hexagonal boron nitride (h-BN),  $\text{MoS}_2$ ,  $\text{MoSe}_2$ ,  $\text{WS}_2$ , and graphene with spherical CQDs with an average diameter of 3 nm significantly improved their friction and wear characteristics during tribological testing. When used on their own, individual CQDs tend to adsorb onto the friction surfaces to form a lubricating adsorbed

layer on the asperities, but under increased loads, individual CQDs tend to be squeezed out of the contact. When the CQDs were attached onto the 2D nanosheets, on the other hand, the assembled nanoadditives were harder to squeeze out of the contact due to their larger lateral surface area. In other words, combining CQDs with 2D nanostructures, improved the retention of CQDs on the surface during higher loads. Even though a lot more research is necessary to evaluate the feasibility of this strategy as a way to mitigate the antagonistic effect competing adsorption processes, these preliminary results further validate the claim made in Chapter 4, i.e., exploiting the excellent properties of carbon nanostructures as carrier materials is something that should be explored further moving forward.

All in all, the prevalence of synergistic and antagonistic interaction among additives makes lubricant development and formulation a challenging and time-consuming endeavor. As new additives emerge, and a larger number of additives may be required to compensate for the deficiencies of new base fluid alternatives, the task of identifying and controlling interactions among additives is expected to become even more challenging in the coming years. This is why the prospect of developing multifunctional additives is an attractive concept. However, a lot of work will still be required to investigate the compatibility of carbon nanoadditives with other kinds of lubricant components. Studies on the interactions of carbon-based additives with other classes of additives are still scarce, but it is conceivable that carbon nanostructures are particularly susceptible to antagonistic interactions with other surface-active additives. Inspired by the functionalization practices discussed in Chapter 4, a potential strategy for mitigating the effect of certain competing adsorption processes was presented.

## 6 SUMMARY AND OUTLOOK

---

Carbon nanostructures make up a very big family of materials with a wide range of properties, and this influences the mechanisms by which they can reduce friction and wear when employed as lubricant additives. Dispersibility, mechanical properties and chemical interactions have been identified as critical factors governing the tribological behavior of carbon nanostructures. Generally, carbon nanostructures can be divided into two main groups depending on whether they have a planar and lamellar structure that can undergo interlaminar shear or not. The first group includes 2D carbon nanostructures and 0D graphene quantum dots (GQDs). The second group of non-lamellar structures can further be divided into two subgroups depending on whether their mechanical and chemical properties are likely to allow nanoparticle rolling between the tribosurfaces or not. The carbon nanostructures that are unlikely to roll (e.g. CNTs, CNOs and fullerenes) tend to undergo structural collapse and form surface films with various properties instead. Whether solid lubricant nanoadditives should adhere to surface and shear, be mobile and roll around, or simply deposit on the surface depends on the tribosystem. However, one thing is clear – the working principles of certain carbon nanostructures are fundamentally different.

Yet, carbon nanostructures are often treated as a rather homogeneous group of materials in most tribology literature. Overall, many researchers seem largely unaware of the wide range of structures and properties within this class of materials, and it is often not recognized that certain lubrication mechanisms (e.g., interlayer shearing or rolling) only pertain to certain structures. In some cases, this generalization is even extended to include other types of nanoparticles such as metal, metal oxide, and ceramic nanoparticles. Such assumptions of analogous behavior among nanostructures are an unfortunate source of confusion, albeit commonplace when dealing with such a novel class of materials, that serve to perpetuate inaccuracies in tribological literature.

Furthermore, even among carbon nanostructures of a given dimensionality (e.g., 0D, 1D or 2D), or within a specific type of carbon nanostructure (e.g., graphene) there can be large variations in properties that influence tribological behavior. For instance, not only is pristine graphene different from graphene oxide, but even among pristine graphene samples there are numerous parameters such as sheet size, number of layers, interlayer spacing, and edge morphology that can influence tribological performance. All in all, the apparent unawareness of the diversity among carbon nanostructures means that material properties such as these are often insufficiently characterized and reported, and that these parameters tend to be poorly controlled in many experimental studies. This, in turn, makes systematic study and evaluation of lubrication properties difficult and can lead to inconsistent and seemingly random results. Thus, the tribology community could benefit from increased awareness and better understanding of the fact that ‘carbon is not just carbon’ and that choice of carbon nanostructure matters.

As established in Section 3.10, different lubrication mechanisms are active under different conditions and are influenced by varying parameters. Thus, different carbon nanostructures are likely to be suitable for different applications. For example, carbon nanostructures whose lubrication performance is highly dependent on strong adhesion to the tribosurfaces (e.g., 2D carbon nanostructures) may not be appropriate for tribosystems with relatively inert surfaces. Hence, a better understanding of the factors that influence the various lubrication mechanisms may help elucidate why a certain lubricant additive performed better in a given system compared to another. Therefore, the choice of carbon nanostructure should be carefully considered based on desired properties and working principle for the application in question.

Chapter 3 also revealed certain discrepancies between the lubrication mechanisms that are routinely being postulated in experimental studies and the findings of more fundamental or theoretical studies on nanoparticle behavior. For example, in experimental literature, the roller bearing mechanism is consistently being presented as the primary lubrication mechanisms of carbon nanotubes (CNTs). However, based on the fundamental studies available at present date, the roller bearing mechanism of CNTs is highly questionable. Firstly, even in absence of compressional forces, both theoretical and experimental studies on the nanoscale motion of CNTs suggest that rolling of individual CNTs is only attainable under very specific and idealized conditions that are unlikely to be met on real tribosurfaces with roughness and complex surface chemistries, especially in the presence of liquid media<sup>238,239,242,243</sup>. Secondly, owing to their low Young's modulus perpendicular to their tubular axis, CNTs have been reported to undergo significant radial deformation under just adhesive interactions or van der Waals forces<sup>244,331</sup>. Thus, the likelihood of CNTs being able to sustain any significant load, nevertheless while rolling, is deemed to be extremely low. Yet, the vast majority of experimental studies seem to be unaware of this.

Another contradiction between statements made in experimental literature and the findings of fundamental studies is related to the nature of rolling friction versus sliding friction on the nanoscale. On the macroscale, rolling friction is typically several orders of magnitude smaller than the sliding friction on the same surface<sup>209</sup>. However, there are several reports suggesting that this does not seem to be the case on the nanoscale<sup>171,223,238,242,243</sup>. So, even though there is theoretical support for the ball bearing ability of certain 0D carbon nanostructures, it is uncertain whether this contributes to reducing the interfacial friction between tribosurfaces under low loads. This is something that should be subjected to further research and that has yet to be acknowledged in most experimental literature.

The origin of both these discrepancies are likely to be rooted in a larger problem within research on the tribological performance of carbon nanostructures – namely, the very limited amount of fundamental and systematic research into the various lubrication mechanisms. To date, most experimental studies on the tribological behavior of carbon nanostructures have been primarily concerned with reporting on the observed friction and wear behavior, without going into greater detail about the origin of the observed

behavior. Instead, they habitually reiterate previously proposed lubrication mechanisms even though very little attention and research has been dedicated to systematically investigate or verify these mechanisms. Over time, these speculative mechanisms have become accepted as consensus based on unsatisfactory theoretical support and evidence. Thus, now that the friction- and wear-reducing potential of carbon nanostructures has been thoroughly established, more resources and focus should be dedicated to systematically investigate and evaluate the merit and validity of the already proposed lubrication mechanisms.

In particular, research into the nature of tribofilm formation and the role of adsorption should be prioritized, for reasons previously discussed. Moreover, many tribologists have a tendency to explain lubrication performance based on a primarily mechanical approach, such as the physical separation effect of solid nanoparticles, while far fewer seem to recognize the contribution and influence of chemical interaction, such as the passivation effect. This is something that should also be addressed in future research. All in all, a more substantial body of fundamental research is believed to help efforts to consolidate discrepancies between experimental and theoretical research and provide a strong theoretical framework for future development of carbon-based nanoadditives.

Our understanding of the carbon nanostructures and their lubrication mechanisms should also inform the choice of surface functionalization. To date, carbon nanostructures are primarily functionalized to enhance dispersion stability with seemingly little regard for how the choice of functional group may influence the various lubrication mechanisms of the additive. However, as identified in Chapter 4, surface functionalization can also be used as a tool to promote, tune, or inhibit different lubrication mechanisms, for instance by enhancing adsorptivity or tribochemical activity. In other words, choice of functionalization matters.

Knowing which mechanism to promote or inhibit requires a comprehensive understanding of how and to which extent each lubrication mechanism contributes to the overall performance, as well as the interplay among them. For example, if rheological effects of carbon nanoadditives turns out to be of little importance for applications under boundary lubrication conditions, then efforts to promote rheological influence should not be prioritized. Similarly, if the ball bearing action of 0D carbon nanostructures is found to be more effective for friction- or wear-reduction than tribofilm formation, then functionalization should aim to promote and extend the durability and robustness of this mechanism rather than the tribofilm formation. Either way, the rich chemistry of carbon and practices of organic chemistry offer endless possibilities in terms of functionalization, potentially allowing tribologists to tailor the additive properties to meet specific requirements in terms of dispersibility, adsorptivity and wettability, as well as general compatibility with the sliding surfaces, base fluid, and other additives. In other words, functionalization can be used for more than achieving dispersibility and the tribology community could benefit greatly from a more conscious approach to functionalization and chemistry in general.

Chapter 4 also explored the possibility of combining nanoparticles with different dimensionalities in an effort to make use of several lubrication mechanisms, either simultaneously or under different operating conditions. For example, since the ball bearing mechanism of 0D nanostructures is effective primarily under low loads while the shearing mechanism of graphene remains active at higher loads, a hybrid structure of the two may enhance tribological performance under a wider range of operating conditions. Alternatively, the simultaneous rolling action of 0D nanostructures and shearing of 2D nanostructures could potentially outperform that of either mechanism on its own. While this is a good example of a more conscious approach to functionalization, the validity and viability of this approach has yet to be confirmed. For instance, it is possible that improved friction obtained using a 0D intercalated 2D structure could be the result of lower shear strength due to increased interlaminar distance rather than the combined action of the ball bearing and interlaminar shearing mechanisms. Thus, more research is required to evaluate this strategy.

Although a significant amount of literature on the lubricating potential of carbon nanostructures has accumulated in the last couple of decades, this has not yet been translated in to practical use in commercial liquid lubricants <sup>11</sup>. Besides the issues discussed above, this can likely be attributed to a few different reasons. Firstly, most established industries are hesitant to invest in new materials that have a high risk of failure <sup>332</sup>. Overcoming this issue will require the scientific community to demonstrate convincing concepts for scalable products. As previously established, researchers are currently in the process of conceptualizing and verifying the working principles of carbon nanostructures as lubricant additives. This corresponds to a technology readiness level (TRL) between 2 and 3 according to the definitions presented in Table 2. TRL is a way of estimating and evaluating the maturity of a technology that was developed by NASA in the 1970s, and the definitions presented in Table 2 were adopted by the EU Horizon 2020 program in 2014. However, even though carbon-based nanoadditives are not yet ready for commercialization, increasing environmental concern and emerging trends are believed to incentivize and expedite the development process going forward.

*Table 2: Technology readiness levels (TRLs) adopted by the EU Horizon 2020 program in 2014* <sup>333</sup>.

<b>TRL 1</b>	Basic principles observed
<b>TRL 2</b>	Technology concept formulated
<b>TRL 3</b>	Experimental proof of concept
<b>TRL 4</b>	Technology validated in the lab
<b>TRL 5</b>	Technology validated in relevant environment (industrially relevant environment in the case of key enabling technologies)
<b>TRL 6</b>	Technology demonstrated in relevant environment (industrially relevant environment in the case of key enabling technologies)
<b>TRL 7</b>	System prototype demonstration in operational environment
<b>TRL 8</b>	System complete and qualified
<b>TRL 9</b>	Actual system proven in operational environment (competitive manufacturing in the case of key enabling technologies; or in space)

As presented in Chapter 1, increasingly strict environmental protection regulations and the shift towards e-mobility concretize two of the main future and disruptive trends that will inevitably impact the future development of high-performance lubricants. A move towards more environmentally acceptable lubricants involves finding alternatives for both base fluids and additives, and the following aspects of the value chain of lubricant production and requirements must be considered and met in the near future:

- Availability of raw materials,
- New sources and synthesis pathways,
- Independency from mineral oil or fossil fuel sources,
- Reduction of CO<sub>2</sub> footprint,
- Environmental acceptability of base fluids and additives,
- Impact on the industrial and automotive markets,
- New performance requirements for lubricants (i.e., temperature, materials compatibility, electrical conductivity, etc).

If carbon-based lubricant additives are found to satisfy these criteria, the industry would be incentivized to invest resources in their continued development. Thus far, carbon nanostructures have shown promise in several aspects. Firstly, carbon element is incredibly abundant, and there are methods that allow carbon nanostructures to be synthesized from biomass or through so-called *green synthesis* methods<sup>210,334–336</sup>. Moreover, the well-established and rich chemistry of carbon is predicted to offer great control and allow selective tuning of chemical properties to ensure compatibility with both new and exciting base fluids, as well as a wide range of operating conditions. However, one very important paucity that has still not been adequately addressed or considered is the potentially adverse biological or environmental impact of carbon nanostructures.

In the literature reviewed for this master's thesis, carbon nanostructures are generally celebrated for their biocompatibility and non-toxicity. These beliefs are generally rooted in the idea of carbon nanostructures being 'just carbon' and the similarity to harmless 3D carbon allotropes such as graphite or diamond<sup>337</sup>. However, nanomaterials differ from their 3D counterparts in that their small size may allow them to penetrate physiological barriers and cellular structures by several administration routes and means of exposure, which may result in toxicity *in vivo* and *in vitro*<sup>338</sup>. At present, there is insufficient literature to draw any conclusions about the potential hazards of carbon nanostructures, but two opposing opinions have begun to emerge: some studies on biotechnical and biomedical applications have indicated that carbon nanostructures have excellent biocompatibility<sup>334,339,340</sup>, while others have reported adverse biological responses like carcinogenic and toxic effects, such as cytotoxicity and genotoxicity<sup>338,341,342</sup>. The potential toxicity of carbon nanostructures is likely to depend on administration method, exposure time and concentration. How this potential risk will influence the

suitability of application as lubricant additives remains to be seen. Nevertheless, it is something that warrants caution and further research.

Another reason why widespread commercial interest in carbon nanostructures as lubricant additives is still pending could be that there is still no clear cost benefit from introducing such additives. In general, the penetration of carbon nanostructures, particularly graphene, into the market has been hindered by relatively high cost, immature manufacturing processes, and inconsistent material quality, compared to that of incumbent material technologies<sup>343</sup>. Fortunately, there has been a steady trend of steep price reduction. For example, the price of graphene nanoplatelets decreased by an order of magnitude from US\$250 pr. kg to US\$20 pr. kg within four years after 2011<sup>332</sup>. As a result, the first commercial products with graphene technologies have begun to emerge<sup>332</sup>, and the global graphene market is predicted to exceed £150 million by 2022<sup>343</sup>. A potentially redeeming prospect of using carbon nanostructures as lubricant additives is that certain defects and trace impurities from synthesis may actually benefit tribological performance<sup>120,235,236,319</sup>. This is very promising as extensive purification processes to remove trace impurities (such as catalyst materials) from the synthesized structure greatly adds to the cost of production<sup>344</sup>. Hopefully, future advances in synthesis and production will make carbon nanostructure additives an economically feasible option for commercial lubricants.

A third reason why research on the lubricating potential of carbon nanostructures still has not translated into commercial use is likely because there are still no clear performance benefits of doing so. As stated by Spikes<sup>11</sup>, it is possible that such additives will only become widely used if they can address problems that the current soluble additives cannot. In this regard, the author of this thesis would argue that carbon nanostructures offer several advantages compared to both conventional molecular additives and other classes of nanoparticles (e.g., metal, metal oxide etc.). Firstly, carbon nanostructures are already multifunctional in that they can act as both friction-modifying and antiwear additives. Secondly, their excellent properties as carrier materials, combined with the well-established and copious chemistry of carbon, offer several routes for functionalization. Deliberate and selective tuning of chemical properties through functionalization have the potential to enhance the inherent lubrication mechanisms of the nanostructures and enable dispersion in both polar and non-polar base fluids. Lastly, strategic functionalization of carbon nanostructures could potentially enable development of multifunctional additives. Such an approach could for instance include chemical grafting of a surface functional group that can impart new functionality, such as antioxidant properties.

Having one additive serving multiple functions in a lubricant may allow lubricant developers to reduce the total number of additives in the formula, which in turn reduces complexity and the likelihood of antagonistic interactions among lubricant constituents. For example, in Chapter 5 it was suggested that antagonistic interactions among surface-active additives could potentially be mitigated by synthesizing a hybrid structure which ensures delivery of both additives to the interfacial contact area, despite competing adsorption processes. Even though some work would still be required to investigate the

compatibility with other additive package constituents, this approach shows potential as an enabling technology that could possibly make lubricant formulation easier.

As for which carbon nanostructures should be prioritized in this endeavor, both graphene-based nanostructures and carbon quantum dots (CQDs) have demonstrated some particularly attractive qualities. Specifically, graphene-based structures, including graphene quantum dots (GQDs), are believed to be especially promising due to their self-lubricating lamellar structure, excellent film forming abilities, and wide operating range. However, it remains to be seen how the robustness and durability of the interlayer shearing mechanism is affected by extensive functionalization and disruption of the hexagonal lattice. In contrast, CQDs may not have self-lubricating properties, but they make up for this deficiency by having tunable and inherently richer surface chemistry. The surface functional groups of as-prepared CQDs are not only attractive sites for chemical grafting and further functionalization but are also believed to make them better candidates for tribochemical interactions during lubrication.

Fullerenes, carbon nano-onions (CNOs), and carbon nanotubes (CNTs), are not believed to be particularly promising candidates as their main contribution seem to be structural collapse and formation of third-body material transfer films with rather unreliable tribological performance. Nanodiamonds (NDs) have excellent mechanical properties, however, their application is made challenging by their abrasive nature. These are likely to be contributing reasons to why research interest in fullerenes, CNOs, CNTs and NDs as lubricant additives have dissipated in later years.



## 7 CONCLUDING REMARKS

---

This master's thesis has critically reviewed and systematized the large body of literature on the lubricating performance of carbon nanostructures and contributed to the future establishment of better guidelines for further research and development on the subject. Firstly, it was established that carbon nanostructures can have widely different properties, and that this influences the mechanisms by which they can reduce friction and wear when employed as lubricant additives. Herein, dimensionality, mechanical properties, and the nature of chemical interactions were identified as particularly important parameters governing the tribological behavior of carbon nanostructures. Thus, it was concluded that the tribology community could benefit from increased awareness about the diversity within this class of materials as well as a more comprehensive understanding of how different properties influence tribological behavior.

Secondly, after critically examining the theoretical basis for the lubrication mechanisms that have been proposed in experimental literature, it was concluded that some of the mechanisms are still quite poorly understood while others are speculative at best. For this reason, more resources and focus should be dedicated to systematically investigate and evaluate the merit and validity of the proposed lubrication mechanisms. A more substantial body of fundamental research should help to consolidate discrepancies between experimental and theoretical research and provide a stronger theoretical framework for future development of carbon-based nanoadditives.

By reviewing recent experimental literature, it was also identified that the choice of surface functionalization matters beyond improving dispersibility. Specifically, it was recognized that surface functionalization has the potential to both promote and inhibit certain lubrication mechanisms. In many cases, the change in lubricating behavior could be attributed to a general increase in adsorptivity or tribochemical activity. Thus, efforts to improve our understanding of the influence and nature of these phenomena are recommended moving forward. In this regard, an important first step would be to characterize and report on the adsorption strength and kinetics of newly synthesized additives and conduct more extensive analysis of potential material on the worn surface after tribological testing.

Lastly, it was discovered that a more conscious and deliberate approach to functionalization of carbon nanostructures could potentially pave the way for future development of multifunctional lubricant additives. This strategy shows great promise as an enabling technology that could potentially make lubricant formulation both easier and cheaper by reducing the total number of additives in a formula and provide better control over interactions among the lubricant constituents.

All in all, despite certain ambiguities at the conceptual level, it can be concluded that certain carbon nanostructures are promising candidates for a new generation of lubricant additives. Specifically, lamellar graphene-based structures and carbon quantum dots were identified as particularly promising

owing to their interlayer shearing mechanisms and tribochemical activity, respectively. Moving forward, it might be beneficial to regard these carbon nanostructures as blank canvases, with a certain set of inherent friction- and wear-reducing properties, onto which surfactants or surface functional groups can be attached to further customize properties or provide additional additive functionality. The well-established and copious chemistry of carbon combined with the excellent properties of carbon nanostructures as carrier materials, offer several routes for functionalization and endless opportunities for tailoring.

## BIBLIOGRAPHY

---

1. Stachowiak, G. & Batchelor, A. W. *Engineering Tribology*. (Elsevier Science & Technology, 2013).
2. Holmberg, K. & Erdemir, A. Influence of tribology on global energy consumption, costs and emissions. *Friction* **5**, 263–284 (2017).
3. Marinescu, I. D., Rowe, W. B., Dimitrov, B. & Ohmori, H. 16 - Tribochemistry of abrasive machining. in (eds. Marinescu, I. D., Rowe, W. B., Dimitrov, B. & Ohmori, H. B. T.-T. of A. M. P. (Second E.) 483–517 (William Andrew Publishing, 2013). doi:<https://doi.org/10.1016/B978-1-4377-3467-6.00016-1>
4. Hamrock, B. J., Schmid, S. R. & Jacobson, B. O. *Fundamentals of Fluid Film Lubrication*. (Marcel Dekker, Inc., 2004).
5. Carnes, K., Gresham, R. M., Canter, N. & Anderson, M. The ten greatest events in tribology history. *Tribol. Lubr. Technol.* **61**, 38–47 (2005).
6. Lindemann, D. L. Future Challenges of the Lubricants Industry. in *FUCHS Capital Market Day 2018* (2018).
7. Braun, J. Additives. in *Lubricants and Lubrication: Second Edition* (eds. Mang, T. & Dresel, W.) 88–118 (WILEY-VCH Verlag, 2006). doi:10.1002/9783527610341
8. Sniderman, D. The chemistry and function of lubricant additives. *Tribol. Lubr. Technol.* **73**, 18–28 (2017).
9. Hsu, S. M., Zhang, J. & Yin, Z. The nature and origin of tribochemistry. *Tribol. Lett.* **13**, 131–139 (2002).
10. Spikes, H. The history and mechanisms of ZDDP. *Tribol. Lett.* **17**, 469–489 (2004).
11. Spikes, H. Friction Modifier Additives. *Tribol. Lett.* **60**, 1–26 (2015).
12. Cheng, X. *Nanostructures: Fabrication and applications. Nanolithography: The Art of Fabricating Nanoelectronic and Nanophotonic Devices and Systems* (Woodhead Publishing Limited, 2013). doi:10.1533/9780857098757.348
13. Ali, I. *et al.* Advances in carbon nanomaterials as lubricants modifiers. *J. Mol. Liq.* **279**, 251–266 (2019).
14. Padgurskas, J., Rukuiza, R., Prosyčėvas, I. & Kreivaitis, R. Tribological properties of lubricant additives of Fe, Cu and Co nanoparticles. *Tribol. Int.* **60**, 224–232 (2013).
15. Choi, Y. *et al.* Tribological behavior of copper nanoparticles as additives in oil. *Curr. Appl. Phys.* **9**, e124–e127 (2009).
16. Uflyand, I. E., Zhinzhiro, V. A. & Burlakova, V. E. Metal-containing nanomaterials as lubricant additives: State-of-the-art and future development. *Friction* **7**, 93–116 (2019).
17. Laad, M. & Jatti, V. K. S. Titanium oxide nanoparticles as additives in engine oil. *J. King Saud Univ. - Eng. Sci.* **30**, 116–122 (2018).
18. Gupta, B. K. & Bhushan, B. Fullerence particles as an additive to liquid lubricants and greases for low friction and wear. (1994).
19. Nunn, N. *et al.* Tribological properties of polyalphaolefin oil modified with nanocarbon

- additives. *Diam. Relat. Mater.* **54**, 97–102 (2015).
20. 2005/360/EC: Commission Decision of 26 April 2005 establishing ecological criteria and the related assessment and verification requirements for the award of the Community eco-label to lubricants. *Official Journal of the European Union* (2005). Available at: <https://eur-lex.europa.eu/eli/dec/2005/360/oj>. (Accessed: 21st March 2021)
  21. Commission Decision (EU) 2018/1702 of 8 November 2018 establishing the EU Ecolabel criteria for lubricants. *Official Journal of the European Union* (2018). Available at: <https://eur-lex.europa.eu/eli/dec/2018/1702/oj>. (Accessed: 22nd March 2021)
  22. Executive Summary. in *STLE 2020 Report on Emerging Issues and Trends in Tribology and Lubrication Engineering* (Society of Tribologist and Lubrication Engineers, 2020).
  23. Rensselaar, J. Van. Lubrication and tribology trends and challenges in electric vehicles. *Society of Tribologists and Lubrication Engineers* (2020). Available at: [https://www.stle.org/files/TLTArchives/2020/07\\_July/Webinars.aspx?WebsiteKey=a70334df-8659-42fd-a3bd-be406b5b83e5#.Xx\\_cfX-cpiM.linkedin](https://www.stle.org/files/TLTArchives/2020/07_July/Webinars.aspx?WebsiteKey=a70334df-8659-42fd-a3bd-be406b5b83e5#.Xx_cfX-cpiM.linkedin).
  24. Guegan, J., Southby, M. & Spikes, H. Friction Modifier Additives, Synergies and Antagonisms. *Tribol. Lett.* **67**, 1–12 (2019).
  25. Shang, W., Cai, T., Zhang, Y., Liu, D. & Liu, S. Facile one pot pyrolysis synthesis of carbon quantum dots and graphene oxide nanomaterials: All carbon hybrids as eco-environmental lubricants for low friction and remarkable wear-resistance. *Tribol. Int.* **118**, 373–380 (2018).
  26. Wang, L., Gong, P., Li, W., Luo, T. & Cao, B. Mono-dispersed Ag/Graphene nanocomposite as lubricant additive to reduce friction and wear. *Tribol. Int.* **146**, 106228 (2020).
  27. Berman, D., Erdemir, A. & Sumant, A. V. Graphene: a new emerging lubricant. *Mater. Today* **17**, 31–42 (2014).
  28. Georgakilas, V., Perman, J. A., Tucek, J. & Zboril, R. Broad Family of Carbon Nanoallotropes: Classification, Chemistry, and Applications of Fullerenes, Carbon Dots, Nanotubes, Graphene, Nanodiamonds, and Combined Superstructures. *Chem. Rev.* **115**, 4744–4822 (2015).
  29. Kroto, H. W., Heath, J. R., O'Brien, C., Curl, R. F. & Smalley, R. E. C<sub>60</sub>: Buckminsterfullerene. *Nature* **318**, 162–163 (1985).
  30. Krätschmer, W., Lamb, L. D., Fostiropoulos, K. & Huffman, D. R. Solid C<sub>60</sub>: a new form of carbon. *Nature* **347**, 354–358 (1990).
  31. Ruoff, R. S., Tse, D. S., Malhotra, R. & Lorents, D. C. Solubility of C<sub>60</sub> in a variety of solvents. *J. Phys. Chem.* **97**, 3379–3383 (1993).
  32. Howard, J. B., McKinnon, J. T., Makarovskiy, Y., Lafleur, A. L. & Johnson, M. E. Fullerenes C<sub>60</sub> and C<sub>70</sub> in flames. *Nature* **352**, 139–141 (1991).
  33. Lamb, L. D. & Huffman, D. R. Fullerene production. *J. Phys. Chem. Solids* **54**, 1635–1643 (1993).
  34. Xing, M., Wang, R. & Yu, J. Application of fullerene C<sub>60</sub> nano-oil for performance enhancement of domestic refrigerator compressors. *Int. J. Refrig.* **40**, 398–403 (2014).
  35. Ginzburg, B. M. *et al.* Antiwear effect of fullerene C<sub>60</sub> additives to lubricating oils. *Russ. J. Appl. Chem.* **75**, 1330–1335 (2002).
  36. Jiang, G., Guan, W. & Zheng, Q. A study on fullerene-acrylamide copolymer nanoball - A new type of water-based lubrication additive. *Wear* **258**, 1625–1629 (2005).
  37. Lei, H., Guan, W. & Luo, J. Tribological behavior of fullerene-styrene sulfonic acid copolymer

- as water-based lubricant additive. *Wear* **252**, 345–350 (2002).
38. Lee, J., Cho, S., Hwang, Y., Lee, C. & Kim, S. H. Enhancement of lubrication properties of nano-oil by controlling the amount of fullerene nanoparticle additives. *Tribol. Lett.* **28**, 203–208 (2007).
  39. Ku, B. C. *et al.* Tribological effects of fullerene (C60) nanoparticles added in mineral lubricants according to its viscosity. *Int. J. Precis. Eng. Manuf.* **11**, 607–611 (2010).
  40. Liu, Y. H., Liu, P. X., Che, L., Shu, C. Y. & Lu, X. C. Tunable tribological properties in water-based lubrication of water-soluble fullerene derivatives via varying terminal groups. *Chinese Sci. Bull.* **57**, 4641–4645 (2012).
  41. Liu, B. & Li, H. Alkylated fullerene as lubricant additive in paraffin oil for steel/steel contacts. *Fullerenes Nanotub. Carbon Nanostructures* **24**, 712–719 (2016).
  42. Ugarte, D. Curling and closure of graphitic networks under electron-beam irradiation. *Nature* **359**, 707–709 (1992).
  43. Alexandrou, I., Wang, H., Sano, N. & Amaratunga, G. A. J. Structure of carbon onions and nanotubes formed by arc in liquids. *J. Chem. Phys.* **120**, 1055–1058 (2004).
  44. Sano, N., Wang, H., Chhowalla, M., Alexandrou, I. & Amaratunga, G. A. Synthesis of carbon ‘onions’ in water. *Nature* **414**, 506–507 (2001).
  45. Imasaka, K., Kanatake, Y., Ohshiro, Y., Suehiro, J. & Hara, M. Production of carbon nanoonions and nanotubes using an intermittent arc discharge in water. *Thin Solid Films* **506–507**, 250–254 (2006).
  46. Yao, Y., Wang, X., Guo, J., Yang, X. & Xu, B. Tribological property of onion-like fullerenes as lubricant additive. *Mater. Lett.* **62**, 2524–2527 (2008).
  47. Hu, S., Bai, P., Tian, F., Cao, S. & Sun, J. Hydrophilic carbon onions synthesized by millisecond pulsed laser irradiation. *Carbon N. Y.* **47**, 876–883 (2009).
  48. Kuznetsov, V. L., Chuvilin, A. L., Butenko, Y. V., Mal’kov, I. Y. & Titov, V. M. Onion-like carbon from ultra-disperse diamond. *Chem. Phys. Lett.* **222**, 343–348 (1994).
  49. Zhang, C. *et al.* The efficient synthesis of carbon nano-onions using chemical vapor deposition on an unsupported Ni–Fe alloy catalyst. *Carbon N. Y.* **49**, 1151–1158 (2011).
  50. Bogdanov, K. *et al.* Annealing-induced structural changes of carbon onions: High-resolution transmission electron microscopy and Raman studies. *Carbon N. Y.* **73**, 78–86 (2014).
  51. Krishnamurthy, S., Butenko, Y. V., Dhanak, V. R., Hunt, M. R. C. & Šiller, L. In situ formation of onion-like carbon from the evaporation of ultra-dispersed nanodiamonds. *Carbon N. Y.* **52**, 145–149 (2013).
  52. Joly-Pottuz, L. *et al.* Diamond-derived carbon onions as lubricant additives. *Tribol. Int.* **41**, 69–78 (2008).
  53. Joly-Pottuz, L. *et al.* Friction properties of carbon nano-onions from experiment and computer simulations. *Tribol. Lett.* **37**, 75–81 (2010).
  54. Joly-Pottuz, L., Vacher, B., Ohmae, N., Martin, J. M. & Epicier, T. Anti-wear and friction reducing mechanisms of carbon nano-onions as lubricant additives. *Tribol. Lett.* **30**, 69–80 (2008).
  55. Matsumoto, N., Joly-Pottuz, L., Kinoshita, H. & Ohmae, N. Application of onion-like carbon to micro and nanotribology. *Diam. Relat. Mater.* **16**, 1227–1230 (2007).
  56. Luo, N., Xiang, J. X., Shen, T., Liang, H. L. & Xin, S. One-step gas-liquid detonation synthesis

- of carbon nano-onions and their tribological performance as lubricant additives. *Diam. Relat. Mater.* **97**, 107448 (2019).
57. Xu, X. *et al.* Electrophoretic Analysis and Purification of Fluorescent Single-Walled Carbon Nanotube Fragments. *J. Am. Chem. Soc.* **126**, 12736–12737 (2004).
  58. Li, H., Kang, Z., Liu, Y. & Lee, S. T. Carbon nanodots: Synthesis, properties and applications. *J. Mater. Chem.* **22**, 24230–24253 (2012).
  59. Lu, J. *et al.* One-Pot Synthesis of Fluorescent Carbon Nanoribbons, Nanoparticles, and Graphene by the Exfoliation of Graphite in Ionic Liquids. *ACS Nano* **3**, 2367–2375 (2009).
  60. Zheng, L., Chi, Y., Dong, Y., Lin, J. & Wang, B. Electrochemiluminescence of Water-Soluble Carbon Nanocrystals Released Electrochemically from Graphite. *J. Am. Chem. Soc.* **131**, 4564–4565 (2009).
  61. Zhou, J. *et al.* An Electrochemical Avenue to Blue Luminescent Nanocrystals from Multiwalled Carbon Nanotubes (MWCNTs). *J. Am. Chem. Soc.* **129**, 744–745 (2007).
  62. Bourlinos, A. B. *et al.* Photoluminescent Carbogenic Dots. *Chem. Mater.* **20**, 4539–4541 (2008).
  63. Pan, D., Zhang, J., Li, Z. & Wu, M. Hydrothermal Route for Cutting Graphene Sheets into Blue-Luminescent Graphene Quantum Dots. *Adv. Mater.* **22**, 734–738 (2010).
  64. Tian, L. *et al.* Nanosized Carbon Particles From Natural Gas Soot. *Chem. Mater.* **21**, 2803–2809 (2009).
  65. Liu, R. *et al.* An aqueous route to multicolor photoluminescent carbon dots using silica spheres as carriers. *Angew. Chem. Int. Ed. Engl.* **48**, 4598–4601 (2009).
  66. Zong, J., Zhu, Y., Yang, X., Shen, J. & Li, C. Synthesis of photoluminescent carbogenic dots using mesoporous silica spheres as nanoreactors. *Chem. Commun.* **47**, 764–766 (2011).
  67. Choi, Y. *et al.* Microwave-assisted synthesis of luminescent and biocompatible lysine-based carbon quantum dots. *J. Ind. Eng. Chem.* **47**, 329–335 (2017).
  68. Jiang, J., He, Y., Li, S. & Cui, H. Amino acids as the source for producing carbon nanodots: microwave assisted one-step synthesis, intrinsic photoluminescence property and intense chemiluminescence enhancement. *Chem. Commun.* **48**, 9634–9636 (2012).
  69. Li, H. *et al.* One-step ultrasonic synthesis of water-soluble carbon nanoparticles with excellent photoluminescent properties. *Carbon N. Y.* **49**, 605–609 (2011).
  70. Yan, X., Cui, X. & Li, L. Synthesis of Large, Stable Colloidal Graphene Quantum Dots with Tunable Size. *J. Am. Chem. Soc.* **132**, 5944–5945 (2010).
  71. Hess, S. C. *et al.* Direct synthesis of carbon quantum dots in aqueous polymer solution: one-pot reaction and preparation of transparent UV-blocking films. *J. Mater. Chem. A* **5**, 5187–5194 (2017).
  72. Ma, X. *et al.* Synthesis of luminescent carbon quantum dots by microplasma process. *Chem. Eng. Process. - Process Intensif.* **140**, 29–35 (2019).
  73. Wang, C., Li, D., Lu, Z., Song, M. & Xia, W. Synthesis of carbon nanoparticles in a non-thermal plasma process. *Chem. Eng. Sci.* **227**, 115921 (2020).
  74. Cui, L., Ren, X., Wang, J. & Sun, M. Synthesis of homogeneous carbon quantum dots by ultrafast dual-beam pulsed laser ablation for bioimaging. *Mater. Today Nano* **12**, 100091 (2020).
  75. Li, X. *et al.* Preparation of carbon quantum dots with tunable photoluminescence by rapid laser passivation in ordinary organic solvents. *Chem. Commun.* **47**, 932–934 (2011).

76. Calabro, R. L., Yang, D.-S. & Kim, D. Y. Liquid-phase laser ablation synthesis of graphene quantum dots from carbon nano-onions: Comparison with chemical oxidation. *J. Colloid Interface Sci.* **527**, 132–140 (2018).
77. Tang, J. *et al.* Carbon dots as an additive for improving performance in water-based lubricants for amorphous carbon (a-C) coatings. *Carbon N. Y.* **156**, 272–281 (2020).
78. Xiao, H. P., Liu, S. H., Xu, Q. & Zhang, H. Carbon quantum dots: An innovative additive for water lubrication. *Sci. China Technol. Sci.* **62**, 587–596 (2019).
79. Ye, M. *et al.* Friction-induced transfer of carbon quantum dots on the interface: Microscopic and spectroscopic studies on the role of inorganic–organic hybrid nanoparticles as multifunctional additive for enhanced lubrication. *Tribol. Int.* **127**, 557–567 (2018).
80. Ma, W. *et al.* Superlubricity achieved by carbon quantum dots in ionic liquid. *Mater. Lett.* **195**, 220–223 (2017).
81. Shang, W. *et al.* Covalent grafting of chelated othoborate ionic liquid on carbon quantum dot towards high performance additives: Synthesis, characterization and tribological evaluation. *Tribol. Int.* **121**, 302–309 (2018).
82. Ponomarenko, L. A. *et al.* Chaotic dirac billiard in graphene quantum dots. *Science (80-. ).* **320**, 356–358 (2008).
83. Tian, P., Tang, L., Teng, K. S. & Lau, S. P. Graphene quantum dots from chemistry to applications. *Mater. Today Chem.* **10**, 221–258 (2018).
84. Wang, C.-C. & Lu, S.-Y. Carbon black-derived graphene quantum dots composited with carbon aerogel as a highly efficient and stable reduction catalyst for the iodide/tri-iodide couple. *Nanoscale* **7**, 1209–1215 (2015).
85. Dong, Y. *et al.* One-step and high yield simultaneous preparation of single- and multi-layer graphene quantum dots from CX-72 carbon black. *J. Mater. Chem.* **22**, 8764–8766 (2012).
86. Ye, R. *et al.* Coal as an abundant source of graphene quantum dots. *Nat. Commun.* **4**, 2943 (2013).
87. Shinde, D. B. & Pillai, V. K. Electrochemical preparation of luminescent graphene quantum dots from multiwalled carbon nanotubes. *Chemistry* **18**, 12522–12528 (2012).
88. Dong, Y. *et al.* Etching single-wall carbon nanotubes into green and yellow single-layer graphene quantum dots. *Carbon N. Y.* **64**, 245–251 (2013).
89. Sarkar, S. *et al.* Graphene quantum dots from graphite by liquid exfoliation showing excitation-independent emission, fluorescence upconversion and delayed fluorescence. *Phys. Chem. Chem. Phys.* **18**, 21278–21287 (2016).
90. Habiba, K. *et al.* Luminescent graphene quantum dots fabricated by pulsed laser synthesis. *Carbon N. Y.* **64**, 341–350 (2013).
91. Tang, L. *et al.* Deep Ultraviolet to Near-Infrared Emission and Photoresponse in Layered N-Doped Graphene Quantum Dots. *ACS Nano* **8**, 6312–6320 (2014).
92. He, C., Yan, H., Wang, X. & Bai, M. Graphene quantum dots prepared by gaseous detonation toward excellent friction-reducing and antiwear additives. *Diam. Relat. Mater.* **89**, 293–300 (2018).
93. Qiang, R., Hu, L., Hou, K., Wang, J. & Yang, S. Water-Soluble Graphene Quantum Dots as High-Performance Water-Based Lubricant Additive for Steel/Steel Contact. *Tribol. Lett.* **67**, 1–9 (2019).

94. Wolk, A. *et al.* A Novel Lubricant Based on Covalent Functionalized Graphene Oxide Quantum Dots. *Sci. Rep.* **8**, 1–9 (2018).
95. Yin, X. *et al.* Tribochemical mechanism of superlubricity in graphene quantum dots modified DLC films under high contact pressure. *Carbon N. Y.* **173**, 329–338 (2021).
96. Williams, O. A. Nanocrystalline diamond. *Diam. Relat. Mater.* **20**, 621–640 (2011).
97. Tao, X., Jiazheng, Z. & Kang, X. The ball-bearing effect of diamond nanoparticles as an oil additive. *J. Phys. D. Appl. Phys.* **29**, 2932–2937 (1996).
98. Ivanov, M. G. & Ivanov, D. M. *Nanodiamond nanoparticles as additives to lubricants. Ultrananocrystalline Diamond* (Elsevier Inc., 2012). doi:10.1016/B978-1-4377-3465-2.00014-1
99. Chou, C.-C. & Lee, S.-H. Tribological behavior of nanodiamond-dispersed lubricants on carbon steels and aluminum alloy. *Wear* **269**, 757–762 (2010).
100. Wu, P., Chen, X., Zhang, C. & Luo, J. Synergistic tribological behaviors of graphene oxide and nanodiamond as lubricating additives in water. *Tribol. Int.* **132**, 177–184 (2019).
101. Iijima, S. Helical microtubules of graphitic carbon. *Nature* **354**, 56–58 (1991).
102. Iijima, S. & Ichihashi, T. Single-shell carbon nanotubes of 1-nm diameter. *Nature* **363**, 603–605 (1993).
103. Bethune, D. S. *et al.* Cobalt-catalysed growth of carbon nanotubes with single-atomic-layer walls. *Nature* **363**, 605–607 (1993).
104. Karousis, N., Tagmatarchis, N. & Tasis, D. Current progress on the chemical modification of carbon nanotubes. *Chem. Rev.* **110**, 5366–5397 (2010).
105. Baughman, R. H., Zakhidov, A. A. & De Heer, W. A. Carbon nanotubes - The route toward applications. *Science (80-. )*. **297**, 787–792 (2002).
106. Biercuk, M. J. *et al.* Carbon nanotube composites for thermal management. *Appl. Phys. Lett.* **80**, 2767–2769 (2002).
107. Harris, P. J. F. Carbon nanotube composites. *Int. Mater. Rev.* **49**, 31–43 (2004).
108. Javey, A., Guo, J., Wang, Q., Lundstrom, M. & Dai, H. Ballistic carbon nanotube field-effect transistors. *Nature* **424**, 654–657 (2003).
109. Martel, R., Schmidt, T., Shea, H. R., Hertel, T. & Avouris, P. Single- and multi-wall carbon nanotube field- effect transistors. *Appl. Phys. Lett.* **73**, 2447 (1998).
110. Liu, C. *et al.* Hydrogen Storage in Single-Walled Carbon Nanotubes at Room Temperature. *Science (80-. )*. **286**, 1127 LP – 1129 (1999).
111. Cheng, H.-M., Yang, Q.-H. & Liu, C. Hydrogen storage in carbon nanotubes. *Carbon N. Y.* **39**, 1447–1454 (2001).
112. Coustel, N. *et al.* Application of Carbon Nanotubes as Supports in Heterogeneous Catalysis. *J. Am. Chem. Soc.* **116**, 7935–7936 (1994).
113. Tavasoli, A. *et al.* Cobalt supported on carbon nanotubes — A promising novel Fischer–Tropsch synthesis catalyst. *Fuel Process. Technol.* **89**, 491–498 (2008).
114. Dai, H., Hafner, J. H., Rinzler, A. G., Colbert, D. T. & Smalley, R. E. Nanotubes as nanoprobe in scanning probe microscopy. *Nature* **384**, 147–150 (1996).
115. Kong, J. *et al.* Nanotube Molecular Wires as Chemical Sensors. *Science (80-. )*. **287**, 622 LP –

- 625 (2000).
116. Popov, V. N. Carbon nanotubes: properties and application. *Mater. Sci. Eng. R Reports* **43**, 61–102 (2004).
  117. Peng, Y., Hu, Y. & Wang, H. Tribological behaviors of surfactant-functionalized carbon nanotubes as lubricant additive in water. *Tribol. Lett.* **25**, 247–253 (2007).
  118. Min, C., He, Z., Liu, D., Zhang, K. & Dong, C. Urea modified fluorinated carbon nanotubes: unique self-dispersed characteristic in water and high tribological performance as water-based lubricant additives. *New J. Chem.* **43**, 14684–14693 (2019).
  119. Joly-Pottuz, L., Dassenoy, F., Vacher, B., Martin, J. M. & Mieno, T. Ultralow friction and wear behaviour of Ni/Y-based single wall carbon nanotubes (SWNTs). *Tribol. Int.* **37**, 1013–1018 (2004).
  120. Joly-pottuz, L. & Ohmae, N. Carbon-Based Nanolubricants. in *Nanolubricants* (eds. Martin, J.-M. & Ohmae, N.) 93–147 (Wiley, 2008). doi:<https://doi.org/10.1002/9780470987711.ch3>
  121. Ye, X., E, S. & Fan, M. The influences of functionalized carbon nanotubes as lubricating additives: Length and diameter. *Diam. Relat. Mater.* **100**, 107548 (2019).
  122. Wallace, P. R. The Band Theory of Graphite. *Phys. Rev.* **71**, 622–634 (1947).
  123. Boehm, H. P., Clauss, A., Fischer, G. O. & Hofmann, U. Das Adsorptionsverhalten sehr dünner Kohlenstoff-Folien. *Zeitschrift für Anorg. und Allg. Chemie* **316**, 119–127 (1962).
  124. Novoselov, K. S. *et al.* Electric Field Effect in Atomically Thin Carbon Films. *Science (80-. )*. **306**, 666–669 (2004).
  125. McNaught, A. D. & Wilkinson, A. Compendium of Chemical Terminology, 2nd ed. (the ‘Gold Book’). *IUPAC* (1997).
  126. Bhuyan, M. S. A., Uddin, M. N., Islam, M. M., Bipasha, F. A. & Hossain, S. S. Synthesis of graphene. *Int. Nano Lett.* **6**, 65–83 (2016).
  127. Lee, C., Wei, X., Kysar, J. W. & Hone, J. Measurement of the Elastic Properties and Intrinsic Strength of Monolayer Graphene. *Science (80-. )*. **321**, 385–388 (2008).
  128. Geim, A. K. & Novoselov, K. S. *The Rise of Graphene. Nature Materials* **6**, (2007).
  129. Novoselov, K. S. *et al.* A roadmap for graphene. *Nature* **490**, 192–200 (2012).
  130. Sang, M., Shin, J., Kim, K. & Yu, K. J. Electronic and thermal properties of graphene and recent advances in graphene based electronics applications. *Nanomaterials* **9**, 1–33 (2019).
  131. Chua, C. K. & Pumera, M. Covalent chemistry on graphene. *Chem. Soc. Rev.* **42**, 3222–3233 (2013).
  132. Chen, D., Tang, L. & Li, J. Graphene-based materials in electrochemistry. *Chem. Soc. Rev.* **39**, 3157–3180 (2010).
  133. Allen, M. J., Tung, V. C. & Kaner, R. B. Honeycomb carbon: A review of graphene. *Chem. Rev.* **110**, 132–145 (2010).
  134. Muñoz, R. & Gómez-Aleixandre, C. Review of CVD Synthesis of Graphene. *Chem. Vap. Depos.* **19**, 297–322 (2013).
  135. Reina, A. *et al.* Large Area, Few-Layer Graphene Films on Arbitrary Substrates by Chemical Vapor Deposition. *Nano Lett.* **9**, 30–35 (2009).
  136. Zangwill, A. & Vvedensky, D. D. Novel Growth Mechanism of Epitaxial Graphene on Metals.

- Nano Lett.* **11**, 2092–2095 (2011).
137. Kageshima, H., Hibino, H., Nagase, M. & Yamaguchi, H. Theoretical Study of Epitaxial Graphene Growth on SiC(0001) Surfaces. *Appl. Phys. Express* **2**, 65502 (2009).
  138. Subrahmanyam, K. S., Panchakarla, L. S., Govindaraj, A. & Rao, C. N. R. Simple Method of Preparing Graphene Flakes by an Arc-Discharge Method. *J. Phys. Chem. C* **113**, 4257–4259 (2009).
  139. Li, N. *et al.* Large scale synthesis of N-doped multi-layered graphene sheets by simple arc-discharge method. *Carbon N. Y.* **48**, 255–259 (2010).
  140. Ray, S. C. Chapter 2 - Application and Uses of Graphene Oxide and Reduced Graphene Oxide. in *Micro and Nano Technologies* (ed. Ray, S. C. B. T.-A. of G. and G.-O. B. N.) 39–55 (William Andrew Publishing, 2015). doi:<https://doi.org/10.1016/B978-0-323-37521-4.00002-9>
  141. Partoens, B. & Peeters, F. M. From graphene to graphite: Electronic structure around the  $K$  point. *Phys. Rev. B* **74**, 75404 (2006).
  142. Zhang, G. *et al.* Tribological performances of highly dispersed graphene oxide derivatives in vegetable oil. *Tribol. Int.* **126**, 39–48 (2018).
  143. Wu, L., Xie, Z., Gu, L., Song, B. & Wang, L. Investigation of the tribological behavior of graphene oxide nanoplates as lubricant additives for ceramic/steel contact. *Tribol. Int.* **128**, 113–120 (2018).
  144. Mao, J., Zhao, J., Wang, W., He, Y. & Luo, J. Influence of the micromorphology of reduced graphene oxide sheets on lubrication properties as a lubrication additive. *Tribol. Int.* **119**, 614–621 (2018).
  145. Gupta, B., Kumar, N., Panda, K., Dash, S. & Tyagi, A. K. Energy efficient reduced graphene oxide additives: Mechanism of effective lubrication and antiwear properties. *Sci. Rep.* **6**, 1–10 (2016).
  146. Liu, C., Guo, Y. & Wang, D. PEI-RGO nanosheets as a nanoadditive for enhancing the tribological properties of water-based lubricants. *Tribol. Int.* **140**, 105851 (2019).
  147. Wang, X. *et al.* Experimental research on tribological properties of liquid phase exfoliated graphene as an additive in SAE 10W-30 lubricating oil. *Tribol. Int.* **135**, 29–37 (2019).
  148. Choudhary, S., Mungse, H. P. & Khatri, O. P. Dispersion of alkylated graphene in organic solvents and its potential for lubrication applications. *J. Mater. Chem.* **22**, 21032–21039 (2012).
  149. Lin, J., Wang, L. & Chen, G. Modification of graphene platelets and their tribological properties as a lubricant additive. *Tribol. Lett.* **41**, 209–215 (2011).
  150. Zin, V. *et al.* Tribological properties of engine oil with carbon nano-horns as nano-additives. *Tribol. Lett.* **55**, 45–53 (2014).
  151. Liu, L. *et al.* Recent advances in friction and lubrication of graphene and other 2D materials: Mechanisms and applications. *Friction* **7**, 199–216 (2019).
  152. Xiao, H. & Liu, S. 2D nanomaterials as lubricant additive: A review. *Mater. Des.* **135**, 319–332 (2017).
  153. Tang, W., Huang, Z. & Wang, B. Synthesis of ionic liquid functionalized graphene oxides and their tribological property under water lubrication. *Fullerenes Nanotub. Carbon Nanostructures* **26**, 175–183 (2018).
  154. Kogovšek, J. & Kalin, M. Lubrication performance of graphene-containing oil on steel and DLC-coated surfaces. *Tribol. Int.* **138**, 59–67 (2019).

155. Yin, X. *et al.* Graphene-induced reconstruction of the sliding interface assisting the improved lubricity of various tribo-couples. *Mater. Des.* **191**, 1–9 (2020).
156. Hu, Y. *et al.* One-pot pyrolysis preparation of carbon dots as eco-friendly nanoadditives of water-based lubricants. *Carbon N. Y.* **152**, 511–520 (2019).
157. Klemenz, A. *et al.* Atomic scale mechanisms of friction reduction and wear protection by graphene. *Nano Lett.* **14**, 7145–7152 (2014).
158. Chu, H. Y., Hsu, W. C. & Lin, J. F. Scuffing mechanism during oil-lubricated block-on-ring test with diamond nanoparticles as oil additive. *Wear* **268**, 1423–1433 (2010).
159. Lee, G. J., Park, J. J., Lee, M. K. & Rhee, C. K. Stable dispersion of nanodiamonds in oil and their tribological properties as lubricant additives. *Appl. Surf. Sci.* **415**, 24–27 (2017).
160. Restuccia, P. & Righi, M. C. Tribochemistry of graphene on iron and its possible role in lubrication of steel. *Carbon N. Y.* **106**, 118–124 (2016).
161. Marchetto, D. *et al.* Surface passivation by graphene in the lubrication of iron: A comparison with bronze. *Carbon N. Y.* **116**, 375–380 (2017).
162. Hamze, S., Cabaleiro, D. & Estellé, P. Graphene-based nanofluids: A comprehensive review about rheological behavior and dynamic viscosity. *J. Mol. Liq.* **325**, (2021).
163. Rasheed, A. K., Khalid, M., Rashmi, W., Gupta, T. C. S. M. & Chan, A. Graphene based nanofluids and nanolubricants - Review of recent developments. *Renew. Sustain. Energy Rev.* **63**, 346–362 (2016).
164. Gulzar, M. *et al.* Tribological performance of nanoparticles as lubricating oil additives. *J. Nanoparticle Res.* **18**, 1–25 (2016).
165. Shang, W. *et al.* Tuning of the hydrophilicity and hydrophobicity of nitrogen doped carbon dots: A facile approach towards high efficient lubricant nanoadditives. *J. Mol. Liq.* **266**, 65–74 (2018).
166. Chinas-Castillo, F. & Spikes, H. A. Mechanism of action of colloidal solid dispersions. *J. Tribol.* **125**, 552–557 (2003).
167. Chinas-Castillo, F. & Spikes, H. A. The behavior of colloidal solid particles in elastohydrodynamic contacts. *Tribol. Trans.* **43**, 387–394 (2000).
168. Chiñas-Castillo, F. & Spikes, H. A. Behaviour of colloiddally-dispersed solid particles in very thin film lubricated contacts. *Tribol. Ser.* **38**, 719–731 (2000).
169. Chinas-Castillo, F. & Spikes, H. A. Film Formation by Colloidal Overbased Detergents in Lubricated Contacts. *Tribol. Trans.* **43**, 357–366 (2000).
170. Dwyer-Joyce, R. S. & Heymcr, J. The Entrainment of Solid Particles into Rolling Elastohydrodynamic Contacts. *Tribol. Ser.* **31**, 135–140 (1996).
171. Ewen, J. P. *et al.* Nonequilibrium Molecular Dynamics Investigation of the Reduction in Friction and Wear by Carbon Nanoparticles Between Iron Surfaces. *Tribol. Lett.* **63**, 1–15 (2016).
172. Shafi, W. K. & Charoo, M. S. An overall review on the tribological, thermal and rheological properties of nanolubricants. *Tribol. - Mater. Surfaces Interfaces* **0**, 1–35 (2020).
173. Wang, W., Zhang, G. & Xie, G. Ultralow concentration of graphene oxide nanosheets as oil-based lubricant additives. *Appl. Surf. Sci.* **498**, 143683 (2019).
174. Martin, J. M. & Ohmae, N. *Colloidal Lubrication: General Principles.* (Wiley, 2008).
175. Mungse, H. P. & Khatri, O. P. Chemically functionalized reduced graphene oxide as a novel material for reduction of friction and wear. *J. Phys. Chem. C* **118**, 14394–14402 (2014).

176. Wang, H. Graphite Solid Lubrication Materials. in *Encyclopedia of Tribology* (eds. Wang, Q. J. & Chung, Y.-W.) 1550–1555 (Springer US, 2013). doi:10.1007/978-0-387-92897-5\_1261
177. Stachowiak, G. W. & Batchelor, A. W. *Engineering Tribology*. (2006). doi:https://doi.org/10.1016/B978-0-7506-7836-0.X5000-7
178. Clauss, F. J. *Solid Lubricants and Self-Lubricating Solids*. (Elsevier Science, 2012).
179. Bucholz, E. W., Phillpot, S. R. & Sinnott, S. B. Molecular dynamics investigation of the lubrication mechanism of carbon nano-onions. *Comput. Mater. Sci.* **54**, 91–96 (2012).
180. Hu, J. J., Jo, S. H., Ren, Z. F., Voevodin, A. A. & Zabinski, J. S. Tribological behavior and graphitization of carbon nanotubes grown on 440C stainless steel. *Tribol. Lett.* **19**, 119–125 (2005).
181. Chen, J. *et al.* Graphene layers produced from carbon nanotubes by friction. *Carbon N. Y.* **50**, 1934–1941 (2012).
182. Zhang, L., Pu, J., Wang, L. & Xue, Q. Frictional dependence of graphene and carbon nanotube in diamond-like carbon/ionic liquids hybrid films in vacuum. *Carbon N. Y.* **80**, 734–745 (2014).
183. Zhao, J., Mao, J., Li, Y., He, Y. & Luo, J. Friction-induced nano-structural evolution of graphene as a lubrication additive. *Appl. Surf. Sci.* **434**, 21–27 (2018).
184. Xu, L., Ma, T.-B., Hu, Y.-Z. & Wang, H. Vanishing stick–slip friction in few-layer graphenes: the thickness effect. *Nanotechnology* **22**, 285708 (2011).
185. Xu, L., Ma, T., Hu, Y. & Wang, H. Molecular dynamics simulation of the interlayer sliding behavior in few-layer graphene. *Carbon N. Y.* **50**, 1025–1032 (2012).
186. Lee, C. *et al.* Frictional characteristics of atomically thin sheets. *Science (80-. )*. **328**, 76–80 (2010).
187. Penkov, O., Kim, H. J., Kim, H. J. & Kim, D. E. Tribology of graphene: A review. *Int. J. Precis. Eng. Manuf.* **15**, 577–585 (2014).
188. Müser, M. H. Theoretical Studies of Superlubricity. in *Fundamentals of Friction and Wear on the Nanoscale* (eds. Gnecco, E. & Meyer, E.) 209–232 (Springer International Publishing, 2015). doi:10.1007/978-3-319-10560-4\_11
189. De Wijn, A. S., Fusco, C. & Fasolino, A. Stability of superlubric sliding on graphite. *Phys. Rev. E - Stat. Nonlinear, Soft Matter Phys.* **81**, 1–10 (2010).
190. Feng, X., Kwon, S., Park, J. Y. & Salmeron, M. Superlubric Sliding of Graphene Nanoflakes on Graphene. *ACS Nano* **7**, 1718–1724 (2013).
191. Kawai, S. *et al.* Superlubricity of graphene nanoribbons on gold surfaces. *Science (80-. )*. **351**, 957 LP – 961 (2016).
192. Zhai, W., Srikanth, N., Kong, L. B. & Zhou, K. Carbon nanomaterials in tribology. *Carbon N. Y.* **119**, 150–171 (2017).
193. Chen, X. & Li, J. Superlubricity of carbon nanostructures. *Carbon N. Y.* **158**, 1–23 (2020).
194. Berman, D., Deshmukh, S. A., Sankaranarayanan, S. K. R. S., Erdemir, A. & Sumant, A. V. Macroscale superlubricity enabled by graphene nanoscroll formation. *Science (80-. )*. **348**, 1118–1122 (2015).
195. Zhang, Z. *et al.* Macroscale Superlubricity Enabled by Graphene-Coated Surfaces. *Adv. Sci.* **7**, 1903239 (2020).
196. Li, J., Ge, X. & Luo, J. Random occurrence of macroscale superlubricity of graphite enabled by

- tribo-transfer of multilayer graphene nano flakes. *Carbon N. Y.* **138**, 154–160 (2018).
197. Ge, X. *et al.* Macroscale superlubricity under extreme pressure enabled by the combination of graphene-oxide nanosheets with ionic liquid. *Carbon N. Y.* **151**, 76–83 (2019).
  198. Ge, X., Li, J., Luo, R., Zhang, C. & Luo, J. Macroscale Superlubricity Enabled by the Synergy Effect of Graphene-Oxide Nanoflakes and Ethanediol. *ACS Appl. Mater. Interfaces* **10**, 40863–40870 (2018).
  199. Koukaras, E. N., Paterakis, G. & Trakakis, G. Tunable macroscale structural superlubricity in two-layer graphene via strain engineering. *Nat. Commun.* (2020). doi:10.1038/s41467-020-15446-y
  200. Hu, Y. *et al.* BLG-RGO: A novel nanoadditive for water-based lubricant. *Tribol. Int.* **135**, 277–286 (2019).
  201. Hu, Y. *et al.* PEGlated graphene as nanoadditive for enhancing the tribological properties of water-based lubricant. *Carbon N. Y.* **137**, 41–48 (2018).
  202. Tripathi, M. *et al.* Friction and Adhesion of Different Structural Defects of Graphene. *ACS Appl. Mater. Interfaces* **10**, 44614–44623 (2018).
  203. Long, F., Yasaei, P., Yao, W., Salehi-Khojin, A. & Shahbazian-Yassar, R. Anisotropic Friction of Wrinkled Graphene Grown by Chemical Vapor Deposition. *ACS Appl. Mater. Interfaces* **9**, 20922–20927 (2017).
  204. Vasić, B., Matković, A., Gajić, R. & Stanković, I. Wear properties of graphene edges probed by atomic force microscopy based lateral manipulation. *Carbon N. Y.* **107**, 723–732 (2016).
  205. Wang, J. *et al.* Theoretical study of superlow friction between two single-side hydrogenated graphene sheets. *Tribol. Lett.* **48**, 255–261 (2012).
  206. Wang, L. F., Ma, T. B., Hu, Y. Z. & Wang, H. Atomic-scale friction in graphene oxide: An interfacial interaction perspective from first-principles calculations. *Phys. Rev. B - Condens. Matter Mater. Phys.* **86**, 1–9 (2012).
  207. Min, C. *et al.* Fluorinated graphene oxide nanosheet: A highly efficient water-based lubricated additive. *Tribol. Int.* **140**, (2019).
  208. Ko, J. H. *et al.* Nanotribological properties of fluorinated, hydrogenated, and oxidized graphenes. *Tribol. Lett.* **50**, 137–144 (2013).
  209. Braun, O. M. Simple Model of Microscopic Rolling Friction. *Phys. Rev. Lett.* **95**, 126104 (2005).
  210. Sarno, M., Abdalgilil Mustafa, W. A., Senatore, A. & Scarpa, D. One-step “green” synthesis of dispersable carbon quantum dots/poly (methyl methacrylate) nanocomposites for tribological applications. *Tribol. Int.* **148**, 106311 (2020).
  211. Ye, M., Cai, T., Zhao, L., Liu, D. & Liu, S. Covalently attached strategy to modulate surface of carbon quantum dots: Towards effectively multifunctional lubricant additives in polar and apolar base fluids. *Tribol. Int.* **136**, 349–359 (2019).
  212. Zhang, W. *et al.* Soluble, exfoliated two-dimensional nanosheets as excellent aqueous lubricants. *ACS Appl. Mater. Interfaces* **8**, 32440–32449 (2016).
  213. Ivanov, M. & Shenderova, O. Nanodiamond-based nanolubricants for motor oils. *Curr. Opin. Solid State Mater. Sci.* **21**, 17–24 (2017).
  214. Shen, M., Luo, J. & Shizhu, W. The Tribological Properties of Oils Added with Diamond Nano-Particles. *Tribol. Trans.* **44**, 494–498 (2001).
  215. Bhushan, B., Gupta, B. K., Van Cleef, G. W., Capp, C. & Coe, J. V. Sublimed C60 films for

- tribology. *Appl. Phys. Lett.* **62**, 3253–3255 (1993).
216. Li, X., Xu, X., Zhou, Y., Lee, K. & Wang, A. Insights into friction dependence of carbon nanoparticles as oil-based lubricant additive at amorphous carbon interface. *Carbon N. Y.* **150**, 465–474 (2019).
  217. Lahouij, I. *et al.* Lubrication mechanisms of hollow-core inorganic fullerene-like nanoparticles: coupling experimental and computational works. *Nanotechnology* **23**, 375701 (2012).
  218. Hu, C., Bai, M., Lv, J., Kou, Z. & Li, X. Molecular dynamics simulation on the tribology properties of two hard nanoparticles (diamond and silicon dioxide) confined by two iron blocks. *Tribol. Int.* **90**, 297–305 (2015).
  219. Kang, J. W. & Hwang, H. J. Fullerene nano ball bearings: An atomistic study. *Nanotechnology* **15**, 614–621 (2004).
  220. Tevet, O. *et al.* Friction mechanism of individual multilayered nanoparticles. *Proc. Natl. Acad. Sci. U. S. A.* **108**, 19901–19906 (2011).
  221. Hu, J. J. & Zabinski, J. S. Nanotribology and lubrication mechanisms of inorganic fullerene-like MoS<sub>2</sub> nanoparticles investigated using lateral force microscopy (LFM). *Tribol. Lett.* **18**, 173–180 (2005).
  222. Lahouij, I., Dassenoy, F., de Knoop, L., Martin, J. & Vacher, B. In Situ TEM Observation of the Behavior of an Individual Fullerene-Like MoS<sub>2</sub> Nanoparticle in a Dynamic Contact. *Tribol. Lett.* **42**, 133–140 (2011).
  223. Liang, Q., Tsui, O. K. C., Xu, Y., Li, H. & Xiao, X. Effect of C<sub>60</sub> Molecular Rotation on Nanotribology. *Phys. Rev. Lett.* **90**, 4 (2003).
  224. Rapoport, L. *et al.* Inorganic fullerene-like material as additives to lubricants: Structure-function relationship. *Wear* **225–229**, 975–982 (1999).
  225. Rapoport, L. *et al.* Mechanism of friction of fullerenes. *Ind. Lubr. Tribol.* **54**, 171–176 (2002).
  226. Tannous, J., Dassenoy, F., Bruhács, A. & Tremel, W. Synthesis and Tribological Performance of Novel Mo<sub>x</sub>W<sub>1-x</sub>S<sub>2</sub> (0 ≤ x ≤ 1) Inorganic Fullerenes. *Tribol. Lett.* **37**, 83 (2009).
  227. Rosentsveig, R. *et al.* Fullerene-like MoS<sub>2</sub> Nanoparticles and Their Tribological Behavior. *Tribol. Lett.* **36**, 175–182 (2009).
  228. Lahouij, I., Dassenoy, F., Vacher, B. & Martin, J.-M. Real Time TEM Imaging of Compression and Shear of Single Fullerene-Like MoS<sub>2</sub> Nanoparticle. *Tribol. Lett.* **45**, 131–141 (2012).
  229. Joly-Pottuz, L. *et al.* Pressure-induced exfoliation of inorganic fullerene-like WS<sub>2</sub> particles in a Hertzian contact. *J. Appl. Phys.* **99**, 23524 (2006).
  230. Srolovitz, D. J., Safran, S. A., Homyonfer, M. & Tenne, R. Morphology of Nested Fullerenes. *Phys. Rev. Lett.* **74**, 1779–1782 (1995).
  231. Coffey, T. & Krim, J. C<sub>60</sub> molecular bearings and the phenomenon of nanomapping. *Phys. Rev. Lett.* **96**, 1–4 (2006).
  232. Zhao, W. & Duan, F. Friction properties of carbon nanoparticles (nanodiamond and nanoscroll) confined between DLC and a-SiO<sub>2</sub> surfaces. *Tribol. Int.* **145**, 106153 (2020).
  233. Ghaednia, H. & Jackson, R. L. The effect of nanoparticles on the real area of contact, friction, and wear. *J. Tribol.* **135**, (2013).
  234. Ewen, J. P., Heyes, D. M. & Dini, D. Advances in nonequilibrium molecular dynamics simulations of lubricants and additives. *Friction* **6**, 349–386 (2018).

235. Salah, N., Alshahrie, A., Abdel-wahab, M. S., Alharbi, N. D. & Khan, Z. H. Carbon nanotubes of oil fly ash integrated with ultrathin CuO nanosheets as effective lubricant additives. *Diam. Relat. Mater.* **78**, 97–104 (2017).
236. Salah, N., Abdel-Wahab, M. S., Alshahrie, A., Alharbi, N. D. & Khan, Z. H. Carbon nanotubes of oil fly ash as lubricant additives for different base oils and their tribology performance. *RSC Adv.* **7**, 40295–40302 (2017).
237. Heo, S. & Sinnott, S. B. Effect of molecular interactions on carbon nanotube friction. *J. Appl. Phys.* **102**, (2007).
238. Schall, J. D. & Brenner, D. W. Molecular dynamics simulations of carbon nanotube rolling and sliding on graphite. *Mol. Simul.* **25**, 73–79 (2000).
239. Buldum, A. & Lu, J. P. Atomic scale sliding and rolling of carbon nanotubes. *Phys. Rev. Lett.* **83**, 5050–5053 (1999).
240. Ni, B. & Sinnott, S. B. Tribological properties of carbon nanotube bundles predicted from atomistic simulations. *Surf. Sci.* **487**, 87–96 (2001).
241. Ni, B., Sinnott, S. B., Mikulski, P. T. & Harrison, J. A. Compression of Carbon Nanotubes Filled with C<sub>60</sub>, CH<sub>4</sub>, or Ne: Predictions from Molecular Dynamics Simulations. *Phys. Rev. Lett.* **88**, 205505 (2002).
242. Falvo, M. R., Steele, J., Taylor, R. M. & Superfine, R. Gearlike rolling motion mediated by commensurate contact: Carbon nanotubes on HOPG. *Phys. Rev. B - Condens. Matter Mater. Phys.* **62**, 665–667 (2000).
243. Falvo, M. R. *et al.* Nanometre-scale rolling and sliding of carbon nanotubes. *Nature* **397**, 236–238 (1999).
244. Ruoff, R. S., Tersoff, J., Lorents, D. C., Subramoney, S. & Chan, B. Radial deformation of carbon nanotubes by van der Waals forces. *Nature* **364**, 514–516 (1993).
245. Upadhyay, R. K. & Kumar, A. Boundary lubrication properties and contact mechanism of carbon/MoS<sub>2</sub> based nanolubricants under steel/steel contact. *Colloids Interface Sci. Commun.* **31**, 100186 (2019).
246. Czichos, H. Tribological Processes. in *Tribology: A systems approach to the science and technology of friction, lubrication and wear* (ed. Czichos, H. B. T.-T. S.) **1**, 45–175 (Elsevier, 1978).
247. Everett, D. H. & Koopal, L. K. Chemisorption and Physisorption. *IUPAC Manual of Symbols and Terminology for Physicochemical Quantities and Units - Appendix II* (2001). Available at: [https://old.iupac.org/reports/2001/colloid\\_2001/manual\\_of\\_s\\_and\\_t/node16.html](https://old.iupac.org/reports/2001/colloid_2001/manual_of_s_and_t/node16.html).
248. Friedrich, J. Interactions at Interface. in *Metal-Polymer Systems* 89–112 (John Wiley & Sons, Ltd, 2017).
249. Cui, M., Ren, S., Zhao, H., Wang, L. & Xue, Q. Novel nitrogen doped carbon dots for corrosion inhibition of carbon steel in 1 M HCl solution. *Appl. Surf. Sci.* **443**, 145–156 (2018).
250. Wang, B., Tang, W., Lu, H. & Huang, Z. Ionic liquid capped carbon dots as a high-performance friction-reducing and antiwear additive for poly(ethylene glycol). *J. Mater. Chem. A* **4**, 7257–7265 (2016).
251. Fan, X. *et al.* Study of the conductivity and tribological performance of ionic liquid and lithium greases. *Tribol. Lett.* **53**, 281–291 (2014).
252. Kajdas, C. Importance of anionic reactive intermediates for lubricant component reactions with friction surfaces. *Lubr. Sci.* **6**, 203–228 (1994).

253. Nakayama, K. & Hashimoto, H. Triboemission from various materials in atmosphere. *Wear* **147**, 335–343 (1991).
254. Oster, L., Yaskolko, V. & Haddad, J. Classification of Exoelectron Emission Mechanisms. *Phys. status solidi* **174**, 431–439 (1999).
255. Luo, Q. Tribofilms in Solid Lubricants. *Encycl. Tribol.* 3760–3767 (2013). doi:10.1007/978-0-387-92897-5\_1252
256. Biswas, S. K. Some mechanisms of tribofilm formation in metal/metal and ceramic/metal sliding interactions. *Wear* **245**, 178–189 (2000).
257. Luo, Q. Origin of Friction in Running-in Sliding Wear of Nitride Coatings. *Tribol. Lett.* **37**, 529–539 (2010).
258. Manyangadze, M. *et al.* Enhancing adsorption capacity of nano-adsorbents via surface modification: A review. *South African J. Chem. Eng.* **31**, 25–32 (2020).
259. Sastri, V. S. *Corrosion inhibitors: principles and applications*. (Wiley, 1998).
260. Cui, M., Ren, S., Xue, Q., Zhao, H. & Wang, L. Carbon dots as new eco-friendly and effective corrosion inhibitor. *J. Alloys Compd.* **726**, 680–692 (2017).
261. Mohammad, A., Hongxing, K., Ma, Q., Chung, Y. W. & Wang, Q. J. Relating Tribological Performance and Tribofilm Formation to the Adsorption Strength of Surface - Active Precursors. *Tribol. Lett.* **68**, 1–9 (2020).
262. Khanmohammadi, H., Wijanarko, W. & Espallargas, N. Ionic Liquids as Additives in Water-Based Lubricants: From Surface Adsorption to Tribofilm Formation. *Tribol. Lett.* **68**, 1–15 (2020).
263. Minami, I. Ionic liquids in tribology. *Molecules* **14**, 2286–2305 (2009).
264. Fan, X. & Wang, L. Ionic liquids gels with in situ modified multiwall carbon nanotubes towards high-performance lubricants. *Tribol. Int.* **88**, 179–188 (2015).
265. Vityaz, P. A., Zhornik, V. I., Kukareko, V. A. & Belotserkovsky, M. A. *Tribomechanical Modification of Friction Surface by Running-In in Lubricants with Nano-Sized Diamonds*. (Nova Science Publishers, Inc., 2010).
266. Cornelio, J. A. C., Cuervo, P. A., Hoyos-Palacio, L. M., Lara-Romero, J. & Toro, A. Tribological properties of carbon nanotubes as lubricant additive in oil and water for a wheel-rail system. *J. Mater. Res. Technol.* **5**, 68–76 (2016).
267. Chen, C. S., Chen, X. H., Xu, L. S., Yang, Z. & Li, W. H. Modification of multi-walled carbon nanotubes with fatty acid and their tribological properties as lubricant additive. *Carbon N. Y.* **43**, 1660–1666 (2005).
268. Cursaru, D. L., Andronescu, C., Pirvu, C. & Ripeanu, R. The efficiency of Co-based single-wall carbon nanotubes (SWNTs) as an AW/EP additive for mineral base oils. *Wear* **290–291**, 133–139 (2012).
269. Khalil, W., Mohamed, A., Bayoumi, M. & Osman, T. A. Tribological properties of dispersed carbon nanotubes in lubricant. *Fullerenes, Nanotub. Carbon Nanostructures* **24**, 479–485 (2016).
270. Joly-Pottuz, L. *et al.* Study of inorganic fullerenes and carbon nanotubes by in situ Raman tribometry. *Appl. Phys. Lett.* **91**, (2007).
271. Liu, S. W. *et al.* Robust microscale superlubricity under high contact pressure enabled by graphene-coated microsphere. *Nat. Commun.* **8**, (2017).

272. Kim, K. S. *et al.* Chemical vapor deposition-grown graphene: The thinnest solid lubricant. *ACS Nano* **5**, 5107–5114 (2011).
273. Yu, S. U. *et al.* Simultaneous visualization of graphene grain boundaries and wrinkles with structural information by gold deposition. *ACS Nano* **8**, 8662–8668 (2014).
274. Ni, Z., Wang, Y., Yu, T. & Shen, Z. Raman spectroscopy and imaging of graphene. *Nano Res.* **1**, 273–291 (2008).
275. Song, H., Wang, Z., Yang, J., Jia, X. & Zhang, Z. Facile synthesis of copper/polydopamine functionalized graphene oxide nanocomposites with enhanced tribological performance. *Chem. Eng. J.* **324**, 51–62 (2017).
276. Hunter, M. E. Rust Inhibitors. in *Encyclopedia of Lubricants and Lubrication* (ed. Mang, T.) 1681–1702 (Springer Berlin Heidelberg, 2014). doi:10.1007/978-3-642-22647-2\_184
277. Li, D. Y. Corrosive Wear. in *Encyclopedia of Tribology* (eds. Wang, Q. J. & Chung, Y.-W.) 590–596 (Springer US, 2013). doi:10.1007/978-0-387-92897-5\_866
278. Landolt, D. Electrochemical and materials aspects of tribocorrosion systems. *J. Phys. D. Appl. Phys.* **39**, 3121–3127 (2006).
279. Minami, I. Molecular science of lubricant additives. *Appl. Sci.* **7**, (2017).
280. Bunch, J. S. *et al.* Impermeable atomic membranes from graphene sheets. *Nano Lett.* **8**, 2458–2462 (2008).
281. Sun, P. Z. *et al.* Limits on gas impermeability of graphene. *Nature* **579**, 229–232 (2020).
282. Wu, L., Gu, L., Xie, Z., Zhang, C. & Song, B. Improved tribological properties of Si<sub>3</sub>N<sub>4</sub>/GCr15 sliding pairs with few layer graphene as oil additives. *Ceram. Int.* **43**, 14218–14224 (2017).
283. Chouhan, A., Mungse, H. P., Sharma, O. P., Singh, R. K. & Khatri, O. P. Chemically functionalized graphene for lubricant applications: Microscopic and spectroscopic studies of contact interfaces to probe the role of graphene for enhanced tribo-performance. *J. Colloid Interface Sci.* **513**, 666–676 (2018).
284. Paul, G., Hirani, H., Kuila, T. & Murmu, N. C. Nanolubricants dispersed with graphene and its derivatives: An assessment and review of the tribological performance. *Nanoscale* **11**, 3458–3483 (2019).
285. Xu, Y. *et al.* Synergistic lubricating behaviors of graphene and MoS<sub>2</sub> dispersed in esterified bio-oil for steel/steel contact. *Wear* **342–343**, 297–309 (2015).
286. Eswaraiyah, V., Sankaranarayanan, V. & Ramaprabhu, S. Graphene-based engine oil nanofluids for tribological applications. *ACS Appl. Mater. Interfaces* **3**, 4221–4227 (2011).
287. Mosleh, M. & Shirvani, K. A. In-situ nanopolishing by nanolubricants for enhanced elastohydrodynamic lubrication. *Wear* **301**, 137–143 (2013).
288. Kotia, A., Rajkhowa, P., Rao, G. S. & Ghosh, S. K. Thermophysical and tribological properties of nanolubricants: A review. *Heat Mass Transf.* **54**, 3493–3508 (2018).
289. Hu, C., Bai, M., Lv, J., Wang, P. & Li, X. Molecular dynamics simulation on the friction properties of nanofluids confined by idealized surfaces. *Tribol. Int.* **78**, 152–159 (2014).
290. Lv, J., Cui, W., Bai, M. & Li, X. Molecular dynamics simulation on flow behavior of nanofluids between flat plates under shear flow condition. *Microfluid. Nanofluidics* **10**, 475–480 (2011).
291. Cui, W. *et al.* On the flow characteristics of nanofluids by experimental approach and molecular dynamics simulation. *Exp. Therm. Fluid Sci.* **39**, 148–157 (2012).

292. Alirezaie, A., Saedodin, S., Esfe, M. H. & Rostamian, S. H. Investigation of rheological behavior of MWCNT (COOH-functionalized)/MgO - Engine oil hybrid nanofluids and modelling the results with artificial neural networks. *J. Mol. Liq.* **241**, 173–181 (2017).
293. Wang, B., Wang, X., Lou, W. & Hao, J. Rheological and tribological properties of ionic liquid-based nanofluids containing functionalized multi-walled carbon nanotubes. *J. Phys. Chem. C* **114**, 8749–8754 (2010).
294. Jabbari, F., Saedodin, S. & Rajabpour, A. Experimental Investigation and Molecular Dynamics Simulations of Viscosity of CNT-Water Nanofluid at Different Temperatures and Volume Fractions of Nanoparticles. *J. Chem. Eng. Data* **64**, 262–272 (2019).
295. Anton Paar. Internal structures of samples and shear-thinning behavior. Available at: <https://wiki.anton-paar.com/en/internal-structures-of-samples-and-shear-thinning-behavior/>.
296. Ansón-Casaos, A. *et al.* The viscosity of dilute carbon nanotube (1D) and graphene oxide (2D) nanofluids. *Phys. Chem. Chem. Phys.* **22**, 11474–11484 (2020).
297. Willenbacher, N. & Georgieva, K. Rheology of disperse systems. in *Product Design and Engineering* (eds. Bröckel, U., Meier, W. & Wagner, G.) 7–49 (WILEY-VCH Verlag, 2013). doi:<https://doi.org/10.1002/9783527654741.ch1>
298. Singh, H. & Bhowmick, H. Tribological behaviour of hybrid AMMC sliding against steel and cast iron under MWCNT-Oil lubrication. *Tribol. Int.* **127**, 509–519 (2018).
299. Balandin, A. A. Thermal properties of graphene and nanostructured carbon materials. *Nat. Mater.* **10**, 569–581 (2011).
300. Choi, S. U. S., Zhang, Z. G., Yu, W., Lockwood, F. E. & Grulke, E. A. Anomalous thermal conductivity enhancement in nanotube suspensions. *Appl. Phys. Lett.* **79**, 2252–2254 (2001).
301. Etefaghi, E., Ahmadi, H., Rashidi, A., Nouralishahi, A. & Mohtasebi, S. S. Preparation and thermal properties of oil-based nanofluid from multi-walled carbon nanotubes and engine oil as nano-lubricant. *Int. Commun. Heat Mass Transf.* **46**, 142–147 (2013).
302. Mingzheng, Z., Guodong, X., Jian, L., Lei, C. & Lijun, Z. Analysis of factors influencing thermal conductivity and viscosity in different kinds of surfactant solutions. *Exp. Therm. Fluid Sci.* **36**, 22–29 (2012).
303. Park, S. S. & Kim, N. J. Influence of the oxidation treatment and the average particle diameter of graphene for thermal conductivity enhancement. *J. Ind. Eng. Chem.* **20**, 1911–1915 (2014).
304. Paul, G., Shit, S., Hirani, H., Kuila, T. & Murmu, N. C. Tribological behavior of dodecylamine functionalized graphene nanosheets dispersed engine oil nanolubricants. *Tribol. Int.* **131**, 605–619 (2019).
305. Sarsam, W. S., Amiri, A., Kazi, S. N. & Badarudin, A. Stability and thermophysical properties of non-covalently functionalized graphene nanoplatelets nanofluids. *Energy Convers. Manag.* **116**, 101–111 (2016).
306. Huang, J., Tan, J., Fang, H., Gong, F. & Wang, J. Tribological and wear performances of graphene-oil nanofluid under industrial high-speed rotation. *Tribol. Int.* **135**, 112–120 (2019).
307. Xu, J. *et al.* Tribochemical Behaviors of Onion-like Carbon Films as High-Performance Solid Lubricants with Variable Interfacial Nanostructures. *ACS Appl. Mater. Interfaces* **11**, 25535–25546 (2019).
308. Sun, J. *et al.* Superlubricity Enabled by Pressure-Induced Friction Collapse. *J. Phys. Chem. Lett.* **9**, 2554–2559 (2018).
309. Georgakilas, V. *et al.* Functionalization of graphene: Covalent and non-covalent approaches,

- derivatives and applications. *Chem. Rev.* **112**, 6156–6214 (2012).
310. Eigler, S. & Hirsch, A. Chemistry with graphene and graphene oxide - Challenges for synthetic chemists. *Angew. Chemie - Int. Ed.* **53**, 7720–7738 (2014).
311. Zhang, J. *et al.* Solvent-free graphene liquids: Promising candidates for lubricants without the base oil. *J. Colloid Interface Sci.* **542**, 159–167 (2019).
312. Gong, K., Wu, X., Zhao, G. & Wang, X. Tribological properties of polymeric aryl phosphates grafted onto multi-walled carbon nanotubes as high-performances lubricant additive. *Tribol. Int.* **116**, 172–179 (2017).
313. Gan, C. *et al.* Hydroxyl-terminated ionic liquids functionalized graphene oxide with good dispersion and lubrication function. *Tribol. Int.* **148**, 106350 (2020).
314. Kristiansen, K., Zeng, H., Wang, P. & Israelachvili, J. N. Microtribology of aqueous carbon nanotube dispersions. *Adv. Funct. Mater.* **21**, 4555–4564 (2011).
315. Yu, B., Liu, Z., Zhou, F., Liu, W. & Liang, Y. A novel lubricant additive based on carbon nanotubes for ionic liquids. *Mater. Lett.* **62**, 2967–2969 (2008).
316. Bermúdez, M. D., Jiménez, A. E., Sanes, J. & Carrión, F. J. Ionic liquids as advanced lubricant fluids. *Molecules* **14**, 2888–2908 (2009).
317. Mu, Z., Zhou, F., Zhang, S., Liang, Y. & Liu, W. Effect of the functional groups in ionic liquid molecules on the friction and wear behavior of aluminum alloy in lubricated aluminum-on-steel contact. *Tribol. Int.* **38**, 725–731 (2005).
318. Yu, B. *et al.* Ionic liquid modified multi-walled carbon nanotubes as lubricant additive. *Tribol. Int.* **81**, 38–42 (2015).
319. Erdemir, A. *et al.* Carbon-based tribofilms from lubricating oils. *Nature* **536**, 67–71 (2016).
320. Min, C. *et al.* Graphene oxide/carboxyl-functionalized multi-walled carbon nanotube hybrids: Powerful additives for water-based lubrication. *RSC Adv.* **7**, 32574–32580 (2017).
321. Scharf, T. W. & Prasad, S. V. Solid lubricants: a review. *J. Mater. Sci.* **48**, 511–531 (2013).
322. Sliney, H. E. The Use of Silver in Self-Lubricating Coatings for Extreme Temperatures. *A S L E Trans.* **29**, 370–376 (1986).
323. Meng, Y., Su, F. & Chen, Y. Effective lubricant additive of nano-Ag/MWCNTs nanocomposite produced by supercritical CO<sub>2</sub> synthesis. *Tribol. Int.* **118**, 180–188 (2018).
324. Luo, T. *et al.* Laser irradiation-induced laminated graphene/MoS<sub>2</sub> composites with synergistically improved tribological properties. *Nanotechnology* **29**, (2018).
325. Spikes, H. A. Additive-Additive and Additive-Surface Interactions in Lubrication. *Lubr. Sci.* **2**, 3–23 (1989).
326. Olomolehin, Y., Kapadia, R. & Spikes, H. Antagonistic interaction of antiwear additives and carbon black. *Tribol. Lett.* **37**, 49–58 (2010).
327. Kontou, A., Southby, M., Morgan, N. & Spikes, H. A. Influence of Dispersant and ZDDP on Soot Wear. *Tribol. Lett.* **66**, 1–15 (2018).
328. Berbezier, I., Martin, J. M. & Kapsa, P. The role of carbon in lubricated mild wear. *Tribol. Int.* **19**, 115–122 (1986).
329. Song, W., Yan, J. & Ji, H. Tribological Study of the SOCNTs@MoS<sub>2</sub> Composite as a Lubricant Additive: Synergistic Effect. *Ind. Eng. Chem. Res.* **57**, 6878–6887 (2018).

330. Song, W., Yan, J. & Ji, H. Fabrication of GNS/MoS<sub>2</sub> composite with different morphology and its tribological performance as a lubricant additive. *Appl. Surf. Sci.* **469**, 226–235 (2019).
331. Yuan, X. & Wang, Y. Radial deformation of single-walled carbon nanotubes adhered to solid substrates and variations of energy: Atomistic simulations and continuum analysis. *Int. J. Solids Struct.* **144–145**, 145–159 (2018).
332. Kong, W. *et al.* Path towards graphene commercialization from lab to market. *Nat. Nanotechnol.* **14**, 927–938 (2019).
333. Technology readiness levels (TRL). *Horizon 2020 - Work Programme 2014-2015, Extract from Part 19 - Commission Decision C(2014)4995* (2014). Available at: [https://ec.europa.eu/research/participants/data/ref/h2020/wp/2014\\_2015/annexes/h2020-wp1415-annex-g-trl\\_en.pdf](https://ec.europa.eu/research/participants/data/ref/h2020/wp/2014_2015/annexes/h2020-wp1415-annex-g-trl_en.pdf). (Accessed: 28th March 2021)
334. Shen, D., Zhu, L., Wu, C. & Gu, S. State-of-the-art on the preparation, modification, and application of biomass-derived carbon quantum dots. *Ind. Eng. Chem. Res.* **59**, 22017–22039 (2020).
335. Chen, M. *et al.* Evolution of cellulose acetate to monolayer graphene. *Carbon N. Y.* **174**, 24–35 (2021).
336. Ding, Z., Li, F., Wen, J., Wang, X. & Sun, R. Gram-scale synthesis of single-crystalline graphene quantum dots derived from lignin biomass. *Green Chem.* **20**, 1383–1390 (2018).
337. Arvidsson, R., Boholm, M., Johansson, M. & de Montoya, M. L. “Just Carbon”: Ideas About Graphene Risks by Graphene Researchers and Innovation Advisors. *Nanoethics* **12**, 199–210 (2018).
338. Ou, L. *et al.* Toxicity of graphene-family nanoparticles: A general review of the origins and mechanisms. *Part. Fibre Toxicol.* **13**, (2016).
339. Zhang, X. *et al.* Seeking value from biomass materials: preparation of coffee bean shell-derived fluorescent carbon dots via molecular aggregation for antioxidation and bioimaging applications. *Mater. Chem. Front.* **2**, 1269–1275 (2018).
340. Wang, R. *et al.* Enhancing the antitumor effect of methotrexate in vitro and in vivo by a novel targeted single-walled carbon nanohorn-based drug delivery system. *RSC Adv.* **6**, 47272–47280 (2016).
341. Kobayashi, N., Izumi, H. & Morimoto, Y. Review of toxicity studies of carbon nanotubes. *J. Occup. Health* **59**, 394–407 (2017).
342. Xiao, Y.-Y. *et al.* Developmental Toxicity of Carbon Quantum Dots to the Embryos/Larvae of Rare Minnow (*Gobiocypris rarus*). *Biomed Res. Int.* **2016**, 4016402 (2016).
343. Lin, L., Peng, H. & Liu, Z. Synthesis challenges for graphene industry. *Nat. Mater.* **18**, 520–524 (2019).
344. Hou, P. X., Liu, C. & Cheng, H. M. Purification of carbon nanotubes. *Carbon N. Y.* **46**, 2003–2025 (2008).

